14. Symposium

# Tectonics, Structural Geology and Geology of Crystalline Rocks

# Tektonik, Strukturgeologie und Kristallingeologie

Kiel, 26. 3. - 1. 4. 2012

GEOMAR | Helmholtz-Zentrum für Ozeanforschung Kiel
Institut für Geowissenschaften | Universität Kiel

## Program
## Abstracts

## Programm
## Kurzfassungen

Michael Stipp, Jan Behrmann, Christian Berndt,
Volker Schenk, Klaus Ullemeyer

**Contents**

## Preface

The 14th Symposium on Tectonics, Structural Geology and Geology of Crystalline Rocks (TSK14) is the first TSK meeting to be held on the coast. Northern Germany is void of metamorphic and structural geology outcrops and study of their processes requires going underground into salt mines or driving as far as the Harz Mountains. This is precisely what we will do for the field trip. Nevertheless, marine research is much closer to the TSK topics than might be expected. The plate tectonics revolution in the end of the 60s of last century would not have been possible without research on the oceans. Many structural concepts for deformed rock associations found on the continents have their modern counterparts below the oceans. Today, marine research cruises contribute significantly to tectonic research using a multitude of geophysical methods, sampling of the ocean floor, and deep sea drilling. The collaborative research center (SFB) 574 "Volatiles and Fluids in Subduction Zones", a joint research venture between Christian-Albrechts-University Kiel and the GEOMAR Helmholtz Centre for Ocean Research Kiel, combines marine and onshore research on subduction zone processes in Central and South America. Among other topics the DFG-funded Excellence Cluster “The Future Ocean” is concerned with marine geohazards and georesources and, thus, tectonic studies. Related results in marine geophysics, tectonics, metamorphic and magmatic petrology will be presented during TSK14, as well as several results from other marine and onshore research projects. We also invite you to gather some deeper insights into our work and our research facilities.

The program of the symposium covers a wide range of current research in tectonics, geodynamics, structural geology and metamorphic petrology. We were overwhelmed by the large variety and the high quality of the submitted contributions. As the contributions did not go through a peer-review, the authors remain responsible for the content of their abstracts. There will be talks and posters on all of the six initially announced topics

1) Subduction zones and collisional orogens,
2) Rifting, spreading and transform faults,
3) Metamorphism, deformation and geochronology,
4) Fabrics, rheology and deformation mechanisms,
5) Brittle deformation, neotectonics and earthquake processes,
6) Pluton emplacement, volcano-tectonics und impact geology,

with many contributions covering two and more of them. The program of the plenary sessions from Wednesday, March 28th, to Friday, March 30th, 2012, has largely been organized around these topics. Abstracts are listed in alphabetical order of the first author and this abstract volume includes a mailing list of all the participants.

We are also happy about the strong interest in the three workshops and the field trip. We thank the workshop conveners and the field guides for their great preparatory work. Thanks also to the keynote speakers for accepting our invitations and presenting their research making this event even more interesting. Financial support through sponsorship by the Future Ocean Excellence Cluster (Kiel), ZEISS Germany, JEOL Germany, and K.U.M. (Kiel) is kindly acknowledged. Last but not least we would like to thank the organizers of the last TSK meetings in Frankfurt (2010), Karlsruhe (2008) and Göttingen (2006) for their advice and support while planning this symposium.

We are delighted about your participation and your contributions to posters, talks and discussions, and we hope that you will enjoy your time in Kiel and at the Baltic Sea.

Kiel, March 2012

Michael Stipp
Jan Behrmann
Christian Berndt
Volker Schenk
Klaus Ullemeyer

## Vorwort

Das 14. Symposium 'Tektonik-Strukturgeologie-Kristallingeologie' (TSK 14) ist das erste TSK-Treffen, das an der Küste stattfindet. Norddeutschland ist frei an metamorphen und strukturgeologischen Aufschlüssen, und diese Forschung erfordert Untertagearbeit in Salzbergwerken oder Fahrten zumindest bis zum Harz. Genau dies ist für die Exkursion vorgesehen. Ungeachtet dessen liegt die Meeresforschung näher an den TSK-Themen, als es vielleicht erwartet wird. Die plattentektonische Revolution am Ende der 60er Jahre des letzten Jahrhunderts wäre ohne Meeresforschung nicht möglich gewesen. Viele strukturelle Konzepte deformierter Gesteinsvergesellschaftungen auf den Kontinenten finden ihre modernen Gegenstücke unter den Ozeanen. Heute tragen marine Forschungsfahrten durch die Anwendung geophysikalischer Methoden, Probennahmen vom Meeresboden oder Tiefseebohrprojekte bedeutend zur tektonischen Forschung bei. Der Sonderforschungsbereich SFB 574 "Volatile und Fluide in Subduktionszonen", ein Forschungsprogramm der Christian-Albrechts-Universität Kiel und des GEOMAR Helmholtz Zentrums für Ozeanforschung Kiel, verbindet Forschung im Meer und an Land zur Untersuchung von Subduktionszonen- Prozessen in Zentral- und Mittelamerika. Der von der DFG geförderte Exzellenzcluster "Ozean der Zukunft" befasst sich neben anderen Themen mit marinen Geogefahren und Georessourcen und somit mit tektonischen Studien. Damit verbundene Ergebnisse der marinen Geophysik, Tektonik, metamorphen und magmatischen Petrologie als auch Ergebnisse weiterer Meeres- und Küstenforschungsprojekte werden auf der TSK14 vorgestellt. Wir laden Sie auch ein, einen tieferen Einblick in unsere Forschungstätigkeit und Forschungseinrichtungen zu gewinnen.

Das Programm des Symposiums umfasst eine weite Bandbreite aktueller Forschung in Tektonik, Geodynamik, Strukturgeologie und metamorpher Petrologie. Wir waren überwältigt von der großen Vielfalt und der hohen Qualität der eingereichten Beiträge. Da die Beiträge nicht begutachtet wurden, sind die Autoren allein für die Inhalte ihrer Kurzfassungen verantwortlich. Es wird Vorträge und Poster zu allen ursprünglich angekündigten Themenbereichen geben:

1) Subduktionszonen und Kollisionsorogene,
2) Rifting, Spreading und Transformstörungen,
3) Metamorphose, Deformation und Geochronologie,
4) Gefüge, Rheologie und Deformationsmechanismen,
5) Bruchhafte Deformation, Neotektonik und Erdbebenprozesse,
6) Platznahme von Plutonen, Vulkanotektonik und Impaktgeologie,

wobei viele Beiträge zwei und mehr von diesen abdecken. Das Programm der Plenarsitzungen von Mittwoch, 28. 3. bis Freitag, 30. 3. 2012 orientiert sich weitestgehend an diesen Themenbereichen. Die Kurzfassungen sind in alphabetischer Reihenfolge nach dem Erstautor aufgeführt, ein Adressverzeichnis aller Teilnehmer ist ebenfalls Bestandteil dieses Bandes.

Wir sind auch sehr erfreut über das große Interesse an den drei Workshops und der Exkursion und bedanken uns bei den Workshop-Leitern und den Exkursionsführern für ihre großartige Vorbereitung. Unser Dank gilt auch den eingeladenen Hauptrednern für ihre Bereitschaft, ihre Forschung vorzustellen und dadurch diese Veranstaltung noch interessanter zu gestalten. Über finanzielle Unterstützung durch den Exzellenz-Cluster "Der Ozean der Zukunft" (Kiel), ZEISS Deutschland, JEOL Deutschland und K.U.M. (Kiel) sind wir sehr erfreut. Nicht zuletzt möchten wir uns bei den Organisatoren der letzten TSK- Treffen in Frankfurt (2010), Karlsruhe (2008) und Göttingen (2006) für ihren Rat und ihre Unterstützung bei der Organisation dieses Symposium bedanken.

Wir freuen uns über Ihr Kommen und Ihre Poster-, Vortrags- und Diskussionsbeiträge und wünschen Ihnen einen angenehmen Aufenthalt in Kiel und an der Ostsee.

Kiel, im März 2012

Michael Stipp
Jan Behrmann
Christian Berndt
Volker Schenk
Klaus Ullemeyer

## PROGRAM

| | |
|---|---|
| **Monday, 26.3.2012** | |
| 9.00 – ca. 18.00 | **WORKSHOP "Deformation of polymineralic rocks in nature and experiment"** convened by Marco Herwegh, Rüdiger Kilian and Erik Rybacki |
| | |
| **Tuesday, 27.3.2012** | |
| 9.00 – ca. 18.00 | **WORKSHOP "Significance of long-term deformation and permeability of rock salt and clay for storage and waste disposal"** convened by Bernd Leiss, Janos Urai and Gernold Zulauf |
| 9.00 – ca. 18.00 | **WORKSHOP "Thermodynamic calculations with the Theriak/Domino software package"** convened by Thorsten Nagel |
| | |
| **Wednesday, 28.3.2012** | |
| 9.00 | **SALUTATION, OPENING OF THE SYMPOSIUM** |
| 9.20 | **Impact cratering on Earth and on Mars: defining the impact trajectories by structural analysis** Thomas Kenkmann |
| 9.50 | **The MEMIN research unit: hypervelocity impacts into geological materials** Michael H. Poelchau, Thomas Kenkmann, Klaus Thoma, Alex Deutsch, Tobias Hoerth and Frank Schäfer |
| 10.10 | **Porosity Reduction in the Sub-Surface of Experimentally Produced Impact Craters in Sandstone** Elmar Buhl, Michael H. Poelchau, Thomas Kenkmann, Georg Dresen and Klaus Thoma |
| 10.30 | **BREAK and POSTERS** |
| 11.00 | **Thermomechanical interaction of stoped blocks with magma – the role of volatile exsolution** Steffi Burchardt, Valentin R. Troll, Harro Schmeling, Hemin Koyi and Lara Blythe |
| 11.20 | **Magnetic fabric studies in flood basalts – how to get information on magma flow direction** Stefan Schöbel and Helga de Wall |
| 11.40 | **New Approaches in Rock Deformation and Recrystallisation Analysis at POWTEX Neutron Diffractometer, FRM II Germany** Jens M. Walter, Michael Stipp, Klaus Ullemeyer, Helmut Klein, Bernd Leiss, Bent T. Hansen and Werner F. Kuhs |

| | |
|---|---|
| 12.00 | **Deformation mechanisms active during catastrophic rock failure: preliminary results.**<br>Trullenque, G., Kenkmann, T. and Stein E. |
| 12.20 | **LUNCH BREAK** |
| 13.00 – 15.20 | **POSTER SESSION** |
| 15.20 | **Polyphase deformation in NW Namibia – tools to reconstruct regional tectonics**<br>Cees Passchier, Xavier Maeder and Rudolph Trouw |
| 15.50 | **Dislocation creep of dry quartz**<br>Rüdiger Kilian, Renée Heilbronner, Holger Stünitz, Andreas Kronenberg and Caleb Holyoke |
| 16.10 | **Mechanical behaviour of anhydrite rocks: results of field investigations and mineralogical-geochemical studies**<br>Michael Mertineit, Joachim Behlau, Jörg Hammer, Michael Schramm and Gernold Zulauf |
| 16.30 | **Experimental boudinage of anhydrite in rock-salt matrix: The impact of bulk finite strain geometry**<br>Gernold Zulauf, Janet Zulauf , Michael Mertineit and Jörg Hammer |
| 16.50 | **Metasomatic fault weakening at the Moresby Seamount detachment in the western Woodlark Basin (offshore Papua New Guinea)**<br>Romed Speckbacher, Jan H. Behrmann, Michael Stipp, Thorsten Nagel, Julia Mahlke and Colin W. Devey |
| 17.20 | **ICE BREAKER "MS Stadt Kiel"** |
| 20.00 | **Pier GEOMAR east shore** |
| 20.30 | **Pier GEOMAR west shore** |
| | |

## Thursday, 29.3.2012

| | |
|---|---|
| 9.00 | **Depth-dependent extension, two-stage breakup and depleted lithospheric counterflow at rifted margins**<br>Ritske S. Huismans |
| 9.30 | **New 3D seismic data and high-resolution bathymetry data give insight into active deformation in the Gulf of Cadiz**<br>Gareth J. Crutchley, Christian Berndt, Dirk Klaeschen and Doug G. Masson |
| 9.50 | **Erkundungsmaßnahmen zum tiefengeothermischen Potential der Leinetalgrabenstruktur**<br>Bernd Leiss, David C. Tanner, Axel Vollbrecht, Till Heinrichs, Gernot Arp und GGG |
| 10.10 | **Scales of deformation within a compressional flower structure modelled by varying the amount of fault-zone complexity**<br>David. C. Tanner, Steffen Prüfer, Dirk Kuhn and Charlotte M. Krawczyk |

| | |
|---|---|
| 10.30 | **BREAK and POSTERS** |
| 11.00 | **The Eastern Alps-Western Alps boundary: crustal scale sections from western Austria**<br>Bernhard Fügenschuh, Hugo Ortner, Hannah Pomella, Marcel Schulz and Michael Zerlauth |
| 11.20 | **The Giudicarie Fault System (Alps, Northern Italy): Evolution of a major Alpine fault system**<br>Hannah Pomella, Michael Stipp and Bernhard Fügenschuh |
| 11.40 | **HP-metamorphism in the Adula Nappe, Central Alps**<br>Sascha Sandmann and Thorsten J. Nagel |
| 12.00 | **Exhumation of fault blocks in the internal Sesia-Lanzo Zone and the Ivrea-Verbano Zone (Biella, Italy): Insights from FT-data, U/Pb ages and structural data**<br>Alfons Berger, Ivan Mercolli, Bernhard Fügenschuh and Notburga Kapferer |
| 12.20 | **LUNCH BREAK** |
| 13.00 – 15.20 | **POSTER SESSION** |
| 15.20 | **Tectonic enigmas revealed from petrological and geochemical studies of the Lesser- and Higher Himalaya in Sikkim, India**<br>Sumit Chakraborty |
| 15.50 | **Exhumation of subducted oceanic lithosphere at the South American convergent margin (Raspas Complex, Ecuador)**<br>Ralf Halama, Petra Herms, Timm John, Volker Schenk, Dieter Garbe-Schönberg and Folkmar Hauff |
| 16.10 | **Control of reaction kinetics on mantle serpentinization and double Benioff zones**<br>Karthik Iyer, Lars H. Rüpke, Ingo Grevemeyer and Jason Phipps Morgan |
| 16.30 | **What were the protoliths of the Middle Allochthon? Answers from zircon dating and geochemistry of metamorphosed sedimentary and magmatic rocks of the Ammarnäs Complex, central Scandinavian Caledonides**<br>Jens C. Grimmer, Fredrik A. Hellström, Axel Gerdes and Reinhard O. Greiling |
| 16.50 | **BREAK and POSTERS** |
| 17.20 | **Archean UHT metamorphism and Paleoproterozoic reworking at Uweinat in the East Sahara Ghost Craton**<br>Shreya Karmakar and Volker Schenk |
| 17.40 | **The granulite facies Ongole domain of the Eastern Ghats Belt, India – A Proterozoic island arc?**<br>Tapabrato Sarkar and Volker Schenk |
| 18.00 | **The role of extraction and out-of-sequence thrusting of nappes for the exhumation of (ultra)high-pressure rocks – A case study from Lago di Cignana (Western Alps, Italy)**<br>Frederik Kirst, Nikolaus Froitzheim, Thorsten Nagel, Bernd Leiss and Jan Pleuger |

| | |
|---|---|
| 18.20 | **A numerical study of conditions during thin-skinned thrust initiation and propagation: the example of the Jura mountains**<br>David Hindle and Melanie Lohrmann-Bromm |
| 19.30 | **SYMPOSIUM DINNER** |
| | |

## Friday, 30.3.2012

| | |
|---|---|
| 9.00 | **Numerical Modelling of Subduction and Collision Processes**<br>Taras V. Gerya |
| 9.30 | **Intra-oceanic subduction initiation caused by shear heating: What are the odds?**<br>Marcel Thielmann and Boris J.P. Kaus |
| 9.50 | **Bending-related faulting and mantle serpentinization at deep-sea trenches**<br>Ingo Grevemeyer |
| 10.10 | **Two plates many subduction zones: The Variscan orogeny reconsidered**<br>Uwe Kroner and Rolf L. Romer |
| 10.30 | **Extremely rapid exhumation from eclogite-facies conditions to the surface in the Rhodope mountains, Bulgaria**<br>Thorsten Nagel, Nikolaus Froitzheim, Silke Jahn-Awe, Maria Kirchenbaur and Neven Georgiev |
| 10.50 | **BREAK and POSTERS** |
| 11.20 | **Cosmogenic nuclides: applications in tectonic geomorphology**<br>Ralf Hetzel |
| 11.50 | **Quantifying vertical surface motion on different time-scales, example of Crete, Greece**<br>Stefanie Rieger, Nico Adam and Anke M. Friedrich |
| 12.10 | **Characterization of deeper crustal pseudotachylytes**<br>Uwe Altenberger, Giacomo Prosser, Antonella Grande and Christina Günter |
| 12.30 | **LUNCH BREAK** |
| 13.30 | **On the scale-invariance of fractures**<br>Michael Krumbholz; Steffi Burchardt; David C. Tanner; Christoph Hieronymus and Hemin Koyi |
| 13.50 | **Correlation of joints and fracture cements in Cretaceous carbonate rocks, Mt. Chianello, Italy**<br>Francesco Dati, Stefano Mazzoli, Stefano Vitale, Sofie Nollet and Christoph Hilgers |
| 14.10 | **Evidence for coseismic rupture in a low-strain intraplate rift (Lower Rhine Embayment, central Europe)**<br>Simon Kübler, Anke M. Friedrich and Manfred R. Strecker |

| | |
|---|---|
| 14.30 | **PLENARY DISCUSSION** |
| | **POSTER PRIZE**<br>**VOTE FOR THE NEXT TSK LOCATION** |
| ca. 15.30 | **ENDING OF THE SYMPOSIUM** |
| | |
| ca. 15.30 | **Departure for FIELD TRIP "Salt tectonics and Harz mountains' geology"**<br>Guides: C.H. Friedel, H. Blanke, H.J. Franzke, L. Stottmeister and D.C. Tanner |
| ca. 19.00 | Bad Helmstedt, overnight stay |
| | |
| **Saturday, 31.3.2012** | |
| 8.00 | **Salt tectonics**<br>Salt mine Morsleben, Deutsche Gesellschaft zum Bau und Betrieb von Endlagern (DBE) |
| | **Effects of salt tectonics on cover sediments**<br>Quartz sand mine Walbeck |
| | **Harz northern margin fault**<br>Teufelsbach, Blankenburg |
| ca. 18.00 | Blankenburg, overnight stay |
| | |
| **Sunday, 1.4.2012** | |
| 8.00 | **Calcmylonites in Devonian reef limestones**<br>Elbingerode, Rübeland |
| | **Crystalline basement units, Eckergneiss**<br>(depending on weather conditions) |
| | **Deformation structures in the Culm Fold zone**<br>Triangle zone/Okertal; Kellwassertal |
| ca. 21.00 | Kiel, GEOMAR |


Salonmotorschiff

# "Stadt Kiel"

Technisches Kulturdenkmal

www.salonmotorschiff-stadt-kiel.de

# POSTER CONTRIBUTIONS

| Index | Title and authors |
|---|---|
| **4.1** | **Measuring Structural Data with Smartphone Devices**<br>Peter Appel |
| **5.1** | **Brittle deformation during exhumation of eclogites and blueschist of the Bantimala Complex, Sulawesi: evidence for intra-slab shearing**<br>Rauno Baese and Volker Schenk |
| **2.1** | **Structural investigations of the spreading system north of the Rodriguez Triple Junction (Indian Ocean)**<br>Carolin Bartsch, Udo Barckhausen, Thomas Kuhn and Ulrich Schwarz-Schampera |
| **1.1** | **Large scale 3D geometry of deformation structures in the Aar massif and overlying Helvetic nappes (Central Alps, Switzerland) – A combined remote sensing and field work approach**<br>Roland Baumberger, Philip Wehrens and Marco Herwegh |
| **1.2** | **Strain in the Adula Nappe, Pennine Alps, Switzerland**<br>Jan H. Behrmann, Robert Keizer, Marcel Mizera and Peer Rahlf |
| **3.1** | **Evidence for Mesoproterozoic UHT metamorphism and two metamorphic events in the central Namaqualand Metamorphic Complex (Kakamas Terrane), South Africa**<br>Julia Bial, Volker Schenk, Steffen Büttner and Peter Appel |
| **4.2** | **The role of stress on chemical compaction of illite shale: An experimental study**<br>Rolf H. C. Bruijn, Bjarne S. G. Almqvist, Phil M. Benson and Ann M. Hirt |
| **4.3** | **AMS fabrics in a Permian laccolith from Tabarz (Thuringia, Germany) – a reconnaissance study**<br>Carlo Dietl |
| **1.3** | **Wavelength selection in 3D multilayer detachment folding**<br>Naiara Fernandez and Boris J.P. Kaus |
| **3.2** | **The Eckergneiss complex – state of the art and open questions**<br>Carl-Heinz Friedel and Kai Fischer |
| **1.4** | **The Vardar Ocean suture in the Rhodopes and the maximum-allochthony hypothesis for the Hellenides**<br>Nikolaus Froitzheim, Silke Jahn-Awe, Dirk Frei, Ashlea Wainwright, Roland Maas, Neven Georgiev, Thorsten J. Nagel and Jan Pleuger |
| **5.2** | **Segmentation of the 1960 and 2010 Chilean earthquakes controlled by a giant slope failure**<br>Jacob Geersen, David Völker, Jan Behrmann, Dirk Kläschen, Wilhelm Weinrebe, Sebastian Krastel and Christian Reichert |
| **1.5** | **A Silurian top-to-NW ductile shear zone in the Seve Nappe Complex (central Scandinavian Caledonides, Sweden): The top of a Scandian palaeo-extrusion wedge?**<br>Jens C. Grimmer, Johannes Glodny, Kirsten Drüppel, Agnes Kontny and Reinhard O. Greiling |

| | |
|---|---|
| **2.2** | **Strukturgeologisches 3D-Modell des östlichen Leinetalgrabenstörungssystems bei Bovenden/Südniedersachsen**<br>Johannes Großmann, Bernd Leiss und David C. Tanner |
| **6.1** | **The structure and evolution of magmatic complexes in fold-and-thrust belts – a case study of Cerro Negro, Neuquén Province, Argentina**<br>D. Gürer, O. Galland, H. A. Leanza, C. Sassier and P. R. Cobbold |
| **1.6** | **How does the Okhotsk plate deform? Insights from 3d numerical modelling**<br>David Hindle |
| **5.3** | **New Approach to Detect Possible Quaternary Tectonic Activity in the Alpine Foreland Basin, Southern Germany**<br>Markus Hoffmann and Anke M. Friedrich |
| **4.4** | **Mineralogisch-geochemische Charakterisierung des Staßfurt-Hauptsalzes (Knäuelsalz bis Kristallbrockensalz) im Salzstock Gorleben**<br>Hjördis Holler, Michael Schramm, Michael Mertineit und Jörg Hammer |
| **2.3** | **Influence of viscous channel thickness on the development of overlying brittle deformation patterns under extension: new insights from analogue modeling**<br>Ruth Keppler, Filipe Rosas and Thorsten Nagel |
| **2.4** | **The effect of preexisting joints on normal fault evolution – Insights from field work and analogue modeling**<br>Michael Kettermann, Heijn van Gent, Christoph Grützner and Janos Urai |
| **5.4** | **Recent stress directions in basement rocks of southern Sweden deduced from open microcracks – first results**<br>Michael Krumbholz and Axel Vollbrecht |
| **4.5** | **Texture analysis of mylonitic marbles from the Rhodope Metamorphic Core Complex (Greece) – A preliminary study in view of its kinematic evolution**<br>Rebecca Kühn, Bernd Leiss and Markos Tranos |
| **3.3** | **Alpine HP-metamorphism in orthogneisses from the Adula nappe (Lepontine Alps)?**<br>Robert Kurzawski, Thorsten Nagel, Sascha Sandmann and Jacek Kossak |
| **5.5** | **Joint patterns and vein formation in a fractured carbonate reservoir analogue, Eifel, Germany**<br>Dennis Laux, Tomas Fernandez-Steeger, Philippe Muchez and Christoph Hilgers |
| **4.6** | **Numerical investigation of stresses in sinking carbonate stringer in salt body**<br>Shiyuan Li, Steffen Abe and Janos Urai |
| **3.4** | **(U)HP metamorphism in the Makbal Complex, Tianshan Mountains (Kazakhstan & Kyrgyzstan): Different P-T evolutions of intimately interlayered ultra high- and high-pressure rocks**<br>Melanie Meyer and Reiner Klemd |
| **3.5** | **Isobaric evolution of staurolite-andalusite-cordierite-sillimanite schist in the Central Pyrenees – Early Variscan metamorphism of the Aston-Hospitalet domes**<br>Jochen E. Mezger and Jean-Luc Régnier |

| | |
|---|---|
| **2.5** | **Rifted structures of conjugated margins in the Tyrrhenian Sea**<br>Moeller, S., Berndt, C., Grevemeyer, I., Klaeschen, D. Ranero, C.R., Sallares, V. and Zittelini, N. |
| **4.7** | **Texturanalyse des Steinsalzgefügetyps "Kristallbrocken"**<br>Hans-Heinrich Müller, Bernd Leiss und Michael Schramm |
| **3.6** | **A slap for eoarchean slab melting**<br>Thorsten J. Nagel, J. Elis Hoffmann and Carsten Münker |
| **4.8** | **Mikrostrukturelle Charakterisierung von Karbonatgängen im Unteren Muschelkalk des Leinetalgrabens – erste Ergebnisse**<br>Christian Nikolajew, Axel Vollbrecht, Bernd Leiss und Alfons v.d. Kerkhof |
| **4.9** | **Spatial distribution of quartz recrystallization microstructures across the Aar massif**<br>Max Peters and Marco Herwegh |
| **5.6** | **Migration pathways in Upper Carboniferous unconventional reservoirs, Southern Ruhr Area, North Rhine-Westphalia, Germany**<br>Stefan Pietralla, Martin Salamon and Christoph Hilgers |
| **3.7** | **Disequilibrium textures in lower crustal rocks: Magmatic fabrics in the Eastern Segment, SW Sweden**<br>Bettina Richter and Uwe Altenberger |
| **4.10** | **Interpretative model of shearband boudins internal evolution in HT ductile shear zones**<br>Benedito C. Rodrigues, Mark Peternell, António Moura, Martin Schwindinger and Jorge Pamplona |
| **4.11** | **On the distribution and morphology of grain boundary fluids in natural rock salt**<br>Joyce Schmatz, Marc Sadler, Guillaume Desbois and Janos L.Urai |
| **6.2** | **Investigation of Nb-Ta-enriched Pegmatites in the Eastern Alps**<br>Tobias Schneider, Jürgen Konzett, Bernhard Fügenschuh and Frank Melcher |
| **4.12** | **Ultrasonic wave velocities during experimental deformation of silty clays from the Nankai accretionary prism**<br>Kai Schumann, Michael Stipp, Dirk Klaeschen and Jan Behrmann |
| **4.13** | **Synchrotron texture analysis of naturally and experimentally deformed water-rich sediments from the Nankai Trough offshore Japan**<br>Kai Schumann, Michael Stipp, Bernd Leiss and Jan H. Behrmann |
| **4.16** | **Deformation fabrics of quartz- and calcite-rich mylonites from the Moresby Seamount detachment, Woodlark Basin (offshore Papua New Guinea)**<br>Romed Speckbacher, Michael Stipp, Florian Heidelbach and Jan H. Behrmann |
| **4.14** | **Triaxial deformation experiments indicate strong sediments at the deformation front, and weak sediments at the rear of the Nankai accretionary prism**<br>Michael Stipp, Malte Rolfs, Yujin Kitamura and Jan H. Behrmann |
| **4.15** | **Experimental deformation of partially molten aplite in simple shear**<br>Michael Stipp, Jan Tullis and Alfons Berger |

| | |
|---|---|
| **5.7** | **Fluid-enabled inversion of half-grabens in unconsolidated Upper Pleistocene sands**<br>David C. Tanner, Christian Brandes and Jutta Winsemann |
| **4.17** | **Microfabrics and deformation mechanisms of hydrocarbon-bearing Gorleben rock salt**<br>Nicolas Thiemeyer, Maximilian Pusch, Jörg Hammer and Gernold Zulauf |
| **4.18** | **Evaluation of Crystallographic Preferred Orientations applying whole pattern deconvolution method**<br>Roman Vasin and Klaus Ullemeyer |
| **1.7** | **Heat flow in the Southern Chile Forearc controlled by large-scale tectonic processes**<br>Lucia Villar-Muñoz, Juan Diaz-Naveas and Jan H. Behrmann |
| **1.8** | **Terrane accretion at active continental margins: Numerical Modelling**<br>Katharina Vogt and Taras V. Gerya |
| **5.8** | **Tectonic control on submarine mass wasting off Central Chile**<br>David Völker and Jacob Geersen |
| **1.9** | **Structural Evolution in the Aar Massif (Central Alps): First attempts of linking the micron- to the kilometer-scale**<br>Philip Wehrens, Roland Baumberger and Marco Herwegh |
| **3.8** | **Petrological and structural observations along the Nestos Shear Zone in southern Bulgaria with emphasis on grandite-cpx-bearing rocks**<br>A. Katrin Wellnitz, Thorsten J. Nagel and Nikolaus Froitzheim |
| **2.6** | **Strukturgeologisches 3D-Modell des Nordcampusbereiches der Georg-August-Universität Göttingen – eine erste Näherung**<br>Henrike Werner, Bernd Leiss, Till Heinrichs und David C. Tanner |
| **4.19** | **Microfabrics and deformation mechanisms of experimentally deformed and recompacted Asse rock salt: The impact of grain boundary brine**<br>Janet Zulauf and Gernold Zulauf |

# ABSTRACTS

# Characterization of deeper crustal pseudotachylytes

Uwe Altenberger[1], Giacomo Prosser[2], Antonella Grande[3] and Christina Günter[1]

[1] *Institute of Earth and Environmental Sciences, University of Potsdam, Karl-Liebknecht-Str. 24, D-14476 Potsdam-Golm,*
[2]*Dipartimento di Scienze Geologiche, Universita` della Basilicata, Potenza, Italy,*
[3]*Istituto di Geoscienze e Georisorse-CNR, Pisa*

Fault-related pseudotachylytes provide unambiguous proof for ancient earthquakes. They are usually formed at upper crustal levels. However, evidence derived from both present seismicity and fossil earthquake sources indicate that the lower continental crust may also be a site where seismic events can be generated. In exhumed orogens it is important but difficult to recognize whether the pseudotachylyte formed in the upper, seismogenic crust or in the ductile middle to lower crust.

Field relations, micro-fabrics as well as newly formed phases from upper and deeper crustal samples are often very similar. Although pseudotachylytes of deeper origin could be affected by later metamorphic overprint, a comparison of pseudotachylytes of different regions reveals that a distinction is possible. We have analyzed pseudotachylytes from different rock types to ascertain their depth of crustal origin. Different protoliths were selected to test how lithology controls pseudotachylyte composition and textures.

The high-temperatures condition of all pseudotachylytes (>>1200°C) prevents the use of temperature-sensitive minerals for geothermometry. However, typical pressure-related phases, formed directly or subsequently to melt generation, can be used to estimate the depth of the paleo-seismic event.

In felsic migmatites and felsic granulites as well as in metabasites cauliflower-shaped or euhedral garnets directly crystallized from pseudotachylyte melts of near andesitic composition. Euhedral garnets are formed directly from melt or from cauliflower garnets during post-pseudotachylyte metamorphic overgrowth. Experimental studies indicate a minimum formation pressure of about 0.75 GPa. Quenched needle- to feather-shaped high-alumina orthopyroxene occurs in contact with newly crystallized plagioclase. The pyroxene crystallizes in garnet-free and garnet-bearing mafic veins. The simultaneous growth of orthopyroxene and almandine also suggests a deep origin of the pseudotachylyte melt. In contrast, upper crustal pseudotachylytes of similar protoliths contain no garnets or only garnet relicts. In addition, they are devoid of newly grown orthopyroxene. In conclusion, even though pseudotachylyte formation possibly includes disequilibrium processes, peculiar minerals and microstructures are indicative of crystallization at depth.

# Measuring Structural Data with Smartphone Devices

Peter Appel

*Institut für Geowissenschaften, Christian-Albrechts-Universität Kiel, 24098 Kiel, Germany*

Recent smartphones have bulid-in sensors which are used to measure the orientation and geoposition of the device with high precision: (1) an accelerometer provides the vector of the earth‘s gravity field for the coordinate frame of the device, (2) the magnetometer measures the earth‘s magnetic field and the GPS receiver chip provides the latitude and longitude coordinates for its location. I here present a smartphone software (a so-called app) that calculates from the data of these three sensors the angle of the dip and the direction of the dip and that turns the phone into a versatile and full-working geocompass that can be used in the field instead of a conventional compass.

The phone can directly be placed on the foliation plane and needs only rough adjustment in the direction of the dip. In the initial stages of the calculations, the software defines a vector **v** from the readings of the accelerometer X and Y values (vector components in the direction of the long and short sides of the device body). The dip direction is the angle between the projection of this vector **v** from the phone's coordinate system onto a horizontal plane and the azimutal vector that is obtained from the magnetometer. The angle of the dip is calculated from the Z component of the accelerometer (direction perpendicular to the device body) and the above mentioned vector **v**. Because the readings of the sensors are obtained at a high rate, a realtime stereographic projection for the current orientation of the device can be displayed. This feature helps to visualize the relationships between 2D projection diagrams and real-world (3D) orientation and has shown to be stimulating for students in structural geology classes or in the field.

All stored measurement data are shown in a Schmidt or Wulff net for quick data evaluation in the field. Additionally, a joint diagram shows the distribution of the strike values. The measurement data, together with GPS coordinates and additional metadata can be transfered to a computer either by email or via Wi-Fi network. The locations of the measurement points are shown in a Google Maps view. Furthermore, the app provides the option to choose whether you measure the dip direction relative to the magnetic or geographic north pole and whether you measure lineations or planes. The app is called „Lambert“ and will run on Apple iPhone devices. It is online available and can be downloaded from the iTunes App Store.

# Brittle deformation during exhumation of eclogites and blueschist of the Bantimala Complex, Sulawesi: evidence for intra-slab shearing

Rauno Baese[1] and Volker Schenk[1]

[1]*SFB 574 „Volatiles and fluids in subduction zones“, Christian Albrechts Universität Kiel, D-24118 Kiel*

The Bantimala Complex of SW Sulawesi (Indonesia) exposes HP and UHP metamorphic rocks, which derive from a subduction zone that was active during the Cretaceous. During this time the oceanic crust of the Ceno-Tethys was subducted beneath the Sundaland continent in the north (Parkinson et al., 1998). The complex is composed of tectonic slices that are interlayered and composed of either sediments (e.g. cherts) or metamorphic rocks (blueschists, eclogites, micaschists). Different metamorphic processes can be studied in these rocks as the prograde blueschist-eclogite transformation during subduction of the oceanic crust and the fluid-rock interaction processes that took place during uplift and retrogression.

The aim of this study is to unravel the formation of different kinds of breccias, which show evidence of brittle deformation during uplift. The deformation started at eclogite-facies conditions but continued through the blueschist facies up to the greenschist facies. Brecciated eclogites with rehydrated glaucophane-bearing material in the matrix between the clasts indicate a brittle deformation phase during uplift from eclogite-facies to blueschist-facies conditions. Whereas blueschist-facies clasts in a greenschist-facies matrix reflect lower grade conditions during deformation.

Thermobarometric calculations show that different blueschist and eclogite samples derive from different subduction depths within the slab. In addition, because some of the samples were formed under similar pressure conditions (2.6-2.7 GPa) but varying peak temperatures ($\Delta T$=150°C) and assuming that these rocks were formed during the same subduction process at nearly the same time, they seem to derive from different depths (original vertical) within the lithospheric slab.,.The breccias of the mafic rocks of the Bantimala Complex reflect an exhumation process that was driven by imbrication of different slices of the subducted slab.

The formation of the breccias during uplift and retrogression of the slab rocks and the observation of the displacement of the former stratigraphy within the slab argues for an exhumation of the HP/UHP rocks during compression. The HP/UHP rocks are not embedded and therefore were not carried by a low viscosity and low density matrix (e.g. serpentinite)., Therefore, exhumation was driven by intra-slab shearing and upward directed motion of single slices. This kind of exhumation is similar to that described by Angiboust et al. (2012) for ophiolites of the western Alps. As in the case of the Bantimala Complex even UHP rocks were exhumed, it becomes evident that this exhumation mechanism is effective even at great depth.

**References**

Parkinson,C.D., Miyazaki, K., Wakita, K., Barber, A.J. and Carlswell, D.A. (1998). The Island Arc. 7, 184-200.
Angiboust, S., Langdon, R., Agard, P., Waters, D. and Chopin, C. (2012). J. metamorphic Geol.. 30, 37-61.

# Structural investigations of the spreading system north of the Rodriguez Triple Junction (Indian Ocean)

Carolin Bartsch[1], Udo Barckhausen[1], Thomas Kuhn[1] and Ulrich Schwarz-Schampera[1]

[1]*Federal Institute for Geosciences and Natural Resources (BGR), Stilleweg 2, D-30655 Hannover*

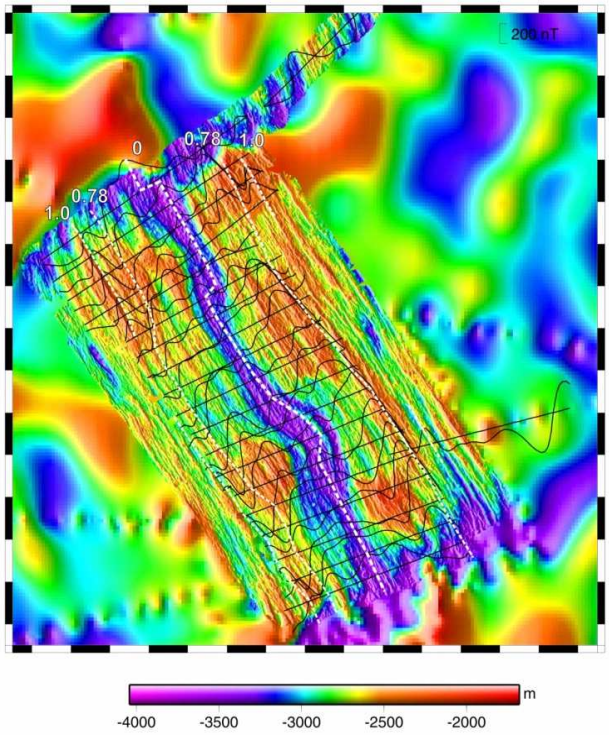


Fig. 1. Bathymetric map of one survey area (Segment 1) overlain by magnetic anomalies. Dashed lines and numbers are crustal ages in m.y.

The German industry depends on the import of base and precious metals for almost 100%. One important source for such metals are volcanic-hosted massive sulfide deposits (VMS) on land. However, these deposits once formed on the seafloor. Therefore, there is ongoing investigation and exploration whether modern seafloor massive sulfides (SMS) also could be mined for those metals. By order of the German Federal Ministry of Economics (BMWi) and in coordination with the International Seabed Authority (ISA), the BGR explores potential areas at the Rodriguez Triple Junction (RTJ) in the Indian Ocean. One goal is the identification of inactive SMS systems with the aid of modern exploration techniques. The Central Indian Ridge (CIR) separates the African and Indian plate. The CIR meets the Southwest Indian Ridge (SWIR) and the Southeast Indian Ridge (SEIR) at the RTJ. The poster shows the first results of the cruise INDEX 2011 with respect to bathymetry and magnetics. The active slow-spreading rift axis of the CIR strikes approximately North-South. The ridge was mapped over six segments and is characterized by five so-called non-transform discontinuities (NTD after Briais, 1995) and one transform fault, the Gemino transform fault. In segment 1 (Fig. 1) the rift valley is asymmetrical with steep slopes in the East and shallower slopes in the western part. It includes an overlapping spreading center (OSC) which is well expressed in the magnetic profiles and in the bathymetry. The recent axial valley shows an offset to the West at this location. A little further south in segment 1 the axial valley shows a more flexural and sigmoidal bend towards the East. Also the recent spreading center follows this direction change towards the East, which can be seen in the magnetic anomalies. This graben may have been abandoned very recently or might even still be active (Briais, 1995). One question which should be answered within the framework of a dissertation is the effect of an overlapping spreading center in terms of hydrothermal activity. Furthermore, spreading rate analyses at the Central Indian Ridge should be made with a comparison between the center of the magnetic anomaly and the bathymetric expression of the spreading center where they display a notable discrepancy. Future work will include a finite-element modeling to investigate the history and reason for uplift of the ridge flanks. With this modeling the question why such young crust segments show an obvious uplift may be answered.

**References**

Briais, A. (1995). Structural analysis of the Central Indian Ridge between 20°30'S and 25°30'S (Rodrigues Triple Junction). Marine Geophysics. Res. V. 17. P. 431-467.

# Large scale 3D geometry of deformation structures in the Aar massif and overlying Helvetic nappes (Central Alps, Switzerland) – A combined remote sensing and field work approach

Roland Baumberger, Philip Wehrens and Marco Herwegh

*University of Bern, Institute of Geological Sciences, Baltzerstrasse 1+3, CH-3012 Bern*

Allowing deep insight into the formation history of a rock complex, shear zones, faults and joint systems represent important sources of geological information. The granitic rocks of the Haslital valley (Switzerland) show very good outcrop conditions to study these mechanical anisotropies. Furthermore, they permit a quantitative characterisation of the above-mentioned deformation structures on the large-scale, in terms of their 3D orientation, 3D spatial distribution, kinematics and evolution in 3D.

A key problem while developing valid geological 3D models is the three-dimensional spatial distribution of geological structures, particularly with increasing distance from the surface. That is especially true in regions, where only little or even no "hard" underground data (e.g. bore holes, tunnel mappings and seismics) is available. In the study area, many subsurface data are available (e.g. cross sections, tunnel and pipeline mappings, bore holes etc.). Therefore, two methods dealing with the problems mentioned are developed: (1) A data acquisition, processing and visualisation method, (2) A methodology to improve the reliability of 3D models regarding the spatial trend of geological structures with increasing depth:

- Using aerial photographs and a high-resolution digital elevation model, a GIS-based remote-sensing structural map of large-scale structural elements (shear zones, faults) of the study area was elaborated. Based on that lineament map, (i) a shear zone map was derived and (ii) a geostastistical analysis was applied to identify sub regions applicable for serving as field areas to test the methodology presented above.

During fieldwork, the shear zone map was evaluated by verifying the occurrence and spatial distribution of the structures designated by remote sensing. Additionally, the geometry of the structures (e.g. 3D orientation, width, kinematics) was characterised and parameterised accordingly. These tasks were partially done using a GPS based Slate PC and the FieldMove$^{TM}$ software, in order to ease the subsequent data processing.

- Findings from the field work were visualised in 3D using the Move$^{TM}$ software suite. Applying its specific tools and incorporating own field data, the structure's near-surface 3D settings was modelled. In a second step, the combined use of surface and subsurface data helped to predict their trend with increasing distance from the surface, bypassing a height difference of partially more than 2000m.

Field work shows that the remote-sensing structural map fits very well with the field observations. Nevertheless, the shear zone map underwent an iterative refinement process, based on own observations in the field as well as on already existing maps. It now clearly describes the lithological subdivision of the study area.

The incorporation of the data into the 3D modelling software points towards the fact, that own large-scale data fits very well with small-scale structures provided by recent studies in the same area. Yet, their exact interplay in terms of orientation, kinematics and evolution is not clear. Additional analysis is needed in order to gain more detailed insight into the deformation history of the rocks in the study area.

# Strain in the Adula Nappe, Pennine Alps, Switzerland

Jan H. Behrmann[1], Robert Keizer[2], Marcel Mizera[2] and Peer Rahlf[2]

*[1]GEOMAR, Helmholtz-Zentrum für Ozeanforschung, Wischhofstr. 1-3, D-24148 Kiel, [2]Institut für Geowissenschaften, Christian-Albrechts-Universität Kiel, Ludewig-Meyn-Str. 10,*

The Adula Nappe in Western Grisons and North Ticino (Swiss Alps) is a structurally coherent fragment of continental crust that has been subducted to great (minimum 50 km) depth during Tertiary Alpine orogeny. The main body of the nappe is more than 40 km long in N-S direction, and, due to the 30° eastward dip of the Pennine stack of nappes, the E-W width of outcrop is between 10 and 20 km. In the central part the structural thickness of the nappe is approximately 3-5 km, and is the result of strong N-S oriented ductile stretching and subhorizontal flattening, expressed by a shallowly east-dipping penetrative foliation. The northern termination of the nappe is complicated by imbrication and folding, whereas the central and southern parts are characterized by interleaved and tightly folded paragneisses, foliated and folded marbles, numerous occurrences of boudinaged Alpine-age (Eocene) eclogites, and two thick continuous layers of augen gneisses with a N-S outcrop length of 20 km. Shear sense of ductile deformation is top-to-north throughout. Overprinting relationships suggest that ductile shearing was during the retrograde overprint after Alpine eclogitization, and hence must be related to exhumation of the high-pressure rocks.

In a field survey carried out in Summer 2011 we have used the Fry method of strain analysis to estimate the state of deformation in the augen gneisses. Principal axes of strain are oriented remarkably similar throughout the nappe, with average N-S stretching of about 100% (total range: 30-200%). Grand average of shortening normal to the foliation is about 50%, with maximum values up to more than 70%. The northern part of the investigated area (between Hinterrhein and San Bernardino Pass) shows strong partitioning into oblate and prolate strain geometries, while the central part (south of San Bernardino Pass) is characterized by plane strain. Most analyses from the southern part (south of Piz de Trescolmen and along Val Calanca) show deformation in the flattening field. Ductile deformation in the Calanca Gneiss was at high enough metamorphic grade to allow plastic stretching of Plagioclase along with the rock matrix (temperatures > 500°C): here the Lisle method (Lisle, 1977) was used in addition to analysis of position fabrics and yielded similar results. To check on the compatibility of strain between the packages of paragneiss and the augen gneisses, fold shapes were analyzed in the YZ section, normal to the stretching lineation and subparallel to the fold axes. Almost all folds have approximately similar geometry (class 2 folds in the sense of Ramsay, 1967). Where class 1C geometries were observed, the homogeneous overprinting strain was calculated using the method of Milnes (1971). YZ axial ratios range from 1.21 to 3.57. These values are comparable to those obtained from analyses using the Fry and Lisle methods on augen gneisses, indicating that the main body of the Adula Nappe deformed fairly homogeneously, leaving rock successions intact, and restricting fracture and boudinge to the most competent rock types, such as the eclogites.

We summarize by stating that ductile deformation during the exhumation stretched the Adula Nappe considerably, and reduced its tectonic thickness by about 50%. This means that the imbricated nappe originally occupied a cross sectional area of at least 25x10 km in the Eocene subduction channel, eventually choking it, and preventing the deep burial of the sedimentary fill of the Valais Trough located in the north and upward the subduction zone. What prompted the nappe to collapse and extend while moving back up the subduction channel is less clear. One possible cause may be plastic weakening while being heated by the overriding upper plate.

**References**

Lisle, R.J. (1977). Geol. Mijnbouw 56, 140-144.
Milnes, A.G. (1971). Eclogae Geol. Helv. 64, 335-342.
Ramsay, J.G. (1967). Folding and fracturing of rocks. McGraw Hill, New York, 568 pp.

# Exhumation of fault blocks in the internal Sesia-Lanzo Zone and the Ivrea-Verbano Zone (Biella, Italy): Insights from FT-data, U/Pb ages and structural data

Alfons Berger[1], Ivan Mercolli[2], Bernhard Fügenschuh[3] and Notburga Kapferer[2]

*[1]Institute for Geology and Geography, University of Copenhagen,DK-1350 Copenhagen [2] Institute for Geology, University of Bern, CH-3012 Bern, [3]Institute of Geology and Paleontology, University of Innsbruck, Innrain 52, A-6020 Innsbruck*

The combination of magmatic, structural and fission track (FT) data is used to unravel Oligocene/Miocene near surface tectonics in the internal Western Alps. This includes reburial of parts of the already exhumed Sesia-Lanzo Zone and their subsequent re-exhumation. The preservation of a paleo-surface allows a detailed reconstruction of the exhumation, burial and re-exhumation of different tectonic blocks. We define blocks on the base of FT data, paleomagnetic data and available fault data. Near-surface, rigid block rotation is responsible for the reburial of the Lower Oligocene paleosurface in part of the Sesia-Lanzo Zone (the Cervo Block) and for the conjugate uplift of deeper portions of the Ivrea-Verbano Zone (the Sessera-Ossola Block). This block rotation around the same horizontal axes produces in the currently exposed portions of the two blocks, quite different temperature/time paths. While the surface of the Cervo Block is buried, the lower part of the Sessera-Ossola Block is uplifted. The rotation is constrained between the age of emplacement of the Biella Volcanic Suite on top of the Sesia-Lanzo Zone and the intrusion of the Valle del Cervo Pluton. The Biella Volcanic Suite Valle del Cervo Pluton have been dated by single zircon grain U/Pb methods, and results in ages of 32.5 and 30.5 Ma, respectively. After this relative fast movements, the concerned blocks remained in (or underneath) the partial annealing zone of zircon until in Aquitanian times they were rapidly uplifted into the partial annealing zone of apatite. The further stage of exhumation out of the partial annealing zone of apatite extends over the entire Miocene.

In addition to the well-known post-collisional deformation in the axial- and external Western Alps, the internal units (i.e. the upper plate) hold an apparent stable position in terms of exhumation.

# Evidence for Mesoproterozoic UHT metamorphism and two metamorphic events in the central Namaqualand Metamorphic Complex (Kakamas Terrane), South Africa

Julia Bial[1], Volker Schenk[1], Steffen Büttner[2] and Peter Appel[1]

*[1]Institut für Geowissenschaften, Christian-Albrechts-Universität Kiel, 24118 Kiel, Germany, [2]Department of Geology, Rhodes University, Grahamstown, South Africa*

The Namaqualand Metamorphic Complex (NMC) of South Africa and Namibia is a classic low-pressure granulite-facies metamorphic terrane that surrounds the Kaapvaal craton to the south (Waters, 1989). Its formation is related to the Mesoproterozoic amalgamation of the supercontinent Rodinia and represents a segment of the global network of Grenville-aged belts (1.3-1.0 Ga). The evolution of the belt is characterized by two phases of granitoid magmatism (1210-1180 Ma and 1040-1020 Ma) (Robb et al., 1999; Clifford et al., 2004).

Robb et al. (1999) associates only the second of these phases of granitoid magmatism (1040-1020 Ma) with the regional low pressure amphibolite to granulite-facies metamorphism, reaching locally UHT conditions (>900°C) in the far southwest (e.g. Waters, 1989), whereas Clifford et al. (2004) suggests that both phases corresponds to a single metamorphic cycle reaching peak P-T conditions at 1210-1180 Ma. The lack of HP metamorphic rocks is characteristic of all the Mesoproterozoic belts of southern Africa.

We present new results on the P-T-t evolution of metapelites from the Namaqua basement in the central part of the belt, NW of the Pofadder lineament by analysis of reaction textures and U-Th-total Pb monazite geochronology. Both petrological and geochronological data sets suggest two metamorphic events separated by a phase of retrogression. During the first event UHT conditions have been locally attained as suggested by orthopyroxene-cordierite-K-feldspar-quartz symplectites forming pseudomorphs after osumilite. Garnet that coexisted with osumilite (Grt 1; $X_{Mg}$ = 0.268) is replaced by late-stage orthopyroxene-cordierite-plagioclase±biotite intergrowths. Within these pseudomorphs a second generation of poikilitic garnet (Grt 2; $X_{Mg}$ = 0.215) is growing enclosing all phases formed after Grt 1. Further evidence for UHT metamorphism provide textures suggesting the stability of spinel-quartz and corundum-quartz at the thermal peak. At a retrograde stage of the P-T path these assemblages formed thin garnet-sillimanite rims and/or garnet-coronas, and aluminous orthopyroxene (>7 wt% $Al_2O_3$)

A clockwise P-T path is indicated by sillimanite pseudomorphs after kyanite and relics of staurolite preserved as inclusions in garnet, occurring only in lower grade areas closer to the northern margin of the belt. Cordierite ± biotite coronas around garnet porphyroblasts provide evidence for late-stage decompression.

Two stages of monazite growths have been dated with the U-Th-total Pb method at 1189±14 Ma and 1004±14 Ma. These two ages are interpreted to correlate with the two metamorphic events deduced from reaction textures. The clockwise P-T path of the first metamorphism and the recognition of two distinct metamorphic events is at variance with former work on the Namaqualand Metamorphic Complex.

**References**

Clifford, T. N.; Barton, E. S.; Stern, R. A. & Duchesne, J.-C. (2004) U-Pb Zircon calendar for Namaquan (Grenville) crustal events in the granulite-facies terrane of the O`okiep Copper District of South Africa, *Journal of Petrology*, Vol. 45, 669-691

Robb, L.J.; Armstrong, R.A. and Waters, D.J. (1999) The history of granulite-facies metamorphism and crustal growth from single zircon U-Pb geochronology: Namaqualand, South Africa, Journal of Petrology, Vol. 40, 1747-1770

Waters, D. J. (1989) Metamorphic evidence for the heating and cooling path of Namaqualand granulites, *In: Evolution of Metamorphic Belts; Daly, J.S., Cliff, R.A., Yardley, B.W.D. (eds.); Geological Society Special Publication No.43*, 357-363

# The role of stress on chemical compaction of illite shale: An experimental study

Rolf H. C. Bruijn[1], Bjarne S. G. Almqvist[1], Phil M. Benson[1] and Ann M. Hirt[2]

[1] *Geological Institute, ETH Zurich, CH-8092 Zurich,* [2]*Institute of Geophysics, ETH Zurich, CH-8092, Zurich*

Physical properties of basin sediments are strongly affected by diagenesis. For the case of shale diagenesis, the mechanical processes that dominate in the upper 2-3 km of sedimentary columns have been simulated in the laboratory. In contrast, chemical processes that dominate in deeper basin domains are poorly constrained by laboratory studies. In addition, the effect of tectonic forces has received little attention in physical experiments.

We report on a series of compaction tests in which exposing the sample to well-controlled elevated temperature and pressure conditions relevant to deep basin-simulation activated chemical processes. We prepared our own synthetic samples by compacting illite shale powder into crystalline metapelite using a three-stage process, employing different stress fields to evaluate the effect of tectonic forces on compaction. In the first stage, dry powder (Maplewood Shale, New York, USA) was mechanically compacted in a hydraulic cold-press with a vertical load of 200 MPa. The second stage employed a hot isostatic press (HIP), set at 170 MPa confining pressure and 590 °C, to ensure powder lithification. In the final stage, further compaction was achieved by either repeating the HIP treatment or by performing confined deformation tests in a Paterson-type gas-medium apparatus. During the second HIP event, temperature and pressure were set at 490 °C and 172 MPa. Three different stress fields were applied in the Paterson apparatus: confined compression, confined torsion or isostatic stress. Deformation was enforced by applying a constant strain rate ranging from $7\times10^{-6}$ to $7\times10^{-4}$ $s^{-1}$. Experiments were performed at 300 MPa confining pressure and a fixed temperature of 500 °C, 650 °C, 700 °C or 750 °C. These conditions were chosen based on a thermodynamic forward simulation of mineral stability fields.

Compaction is quantified by connected porosity, anisotropy of magnetic susceptibility and mica texture strength. The synthetic metapelites range from 1.0 to 17.1 % in porosity, reflecting variation in experimental conditions. SEM investigation identifies chemical compaction as an increasing amount of authigenic phengite and biotite, coupled with a decrease in detrital illite and related sub-micron clay-micropores as a function of porosity. Ultrafine (< 2 μm) quartz and biotite form with a shape-preferred orientation, which gives rise to foliation. This microstructure development is ascribed to fluid-assisted mass transfer, which is controlled by permeability anisotropy. The presence of micro-folds and kinks in both isostatically compacted samples, and samples that were compacted by axial compression, is explained by exhausted pore closure. Pore closure is the dominant strain accommodation mechanism in all compressed samples. Magnetic fabric and crystallographic texture show a linear evolution with compaction, regardless of the applied stress field. We observe that differential stress accelerates chemical compaction, without modifying the evolution of fabric and the measured properties, and state that laboratory strain rates did not change the mechanisms of compaction. We conclude that tectonic forces have no effect on the development of magnetic properties and texture in chemically compacting pelites when strain is accommodated primarily by pore closing.

# Porosity Reduction in the Sub-Surface of Experimentally Produced Impact Craters in Sandstone

Elmar Buhl[1,2], Michael H. Poelchau[1], Thomas Kenkmann[1], Georg Dresen[2] and Klaus Thoma[3]

*[1]Institut für Geowissenschaften-Geologie, Albert-Ludwigs-Universität Freiburg, Germany, [2]GFZ German Research Centre for Geosciences, Potsdam, Germany, [3]Fraunhofer Institute for High-Speed Dynamics, EMI, Freiburg, Germany*

The impact crater formation in porous materials has shown to be strongly affected by the presence of pore fluids. To better understand the role of target porosity and pore space saturation during crater formation, the research unit MEMIN (Multidisciplinary Experimental and Modeling Impact Research Network) was founded in 2009 and is funded by the German Research Foundation (DFG). Within this framework hypervelocity (ca. 5 km/s) impact cratering experiments at into dry and saturated (ca. 90%) sandstone (Seeberger Sandstein, Bank 3) were performed at the two-stage acceleration facilities of the Fraunhofer Ernst-Mach-Institute (EMI) in Freiburg, Germany. For analysis of the crater sub-surface thin section were prepared and investigated by structural mapping. This revealed different modes of deformation with increasing distance from the crater floor. Also differences between the "dry" and the "wet" were found. To quantify damaged-induced changes in target porosity with respect to the calculated impact point source, quantitative image analysis software (ImageJ) was used on the basis of BSE micrographs (1.1 * 1.6 mm). Results of the porosity alteration with depth can be seen in the figure below.

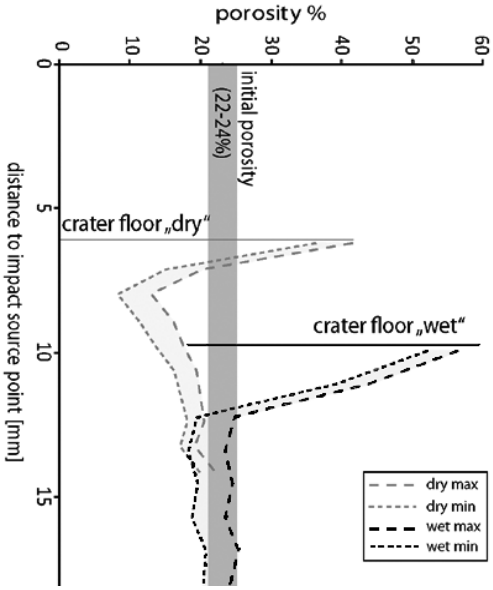


Porosity variation within the dry (gray) and the wet (black) target. Porosity is plotted against the distance to the impact point source.

We suggest that the presence of pore fluid reduced the pore collapse below the crater. Presumably the pore fluid reduced the shock impedance mismatch between grains and interstitial pores. It thus reduces and redistributes the stresses at grain-grain boundaries, which cause intragranular fracturation and thus compaction.

**References**

Kenkmann, T., Wünnemann, K., Deutsch, A., Poelchau, M. H., Schäfer, F. and Thoma, K. (2011). Meteoritics & Planetary Science 46 (6), 890–902.

Schäfer, F., Thoma, K., Behner, T., Nau, S., Kenkmann, T., Wünnemann, K. et al. (Eds.) (2006). Proceedings of the 1st International Conference on Impact Cratering in the Solar System. Noordwijk, May 8-12, 2006. European Space Research and Technology Centre - ESA.

# Thermomechanical interaction of stoped blocks with magma – the role of volatile exsolution

Steffi Burchardt[1], Valentin R. Troll[1], Harro Schmeling[2], Hemin Koyi[1] and Lara Blythe[1]

*[1]Solid Earth Geology, Department of Earth Sciences, Uppsala University, Villavägen 16, S-75236 Uppsala, [2]Faculty of Earth Sciences, J. W. Goethe Universität, Altenhöferallee 1, D-60438 Frankfurt am Main*

The interaction of country-rock fragments detached from the roofs and walls of crustal magma chambers through magmatic stoping is characterised by complex interactions of chemical, thermal, and mechanical processes. Evidence of the occurrence of magmatic stoping is abundant at walls and roofs of exposed plutons worldwide. However, the volumes of stoped blocks within plutons, as well as the amount of chemical contamination of the magma by xenolith assimilation, are out of all proportion to what the abundance of stoping-related structures suggest. Unravelling the fate of stoped blocks in magma chambers would shed light on processes such as the formation of continental crust, magma emplacement in the upper crust, enrichment of crustal components that ultimately form mineral deposits, explosivity of volcanoes etc.

Xenoliths erupted in volcanic areas in subduction zone, ocean-island, and continental intra-plate settings worldwide may provide an additional perspective on the fate of stoped blocks. These xenoliths frequently show signs of partial melting and volatile exsolution that together lead to the formation of vesicles and vesicle networks, leaving the xenoliths with a “frothy” texture and extremely low densities. We show examples of the texture and density of such xenoliths that originated from igneous, sedimentary, and metamorphic rocks.

Furthermore, we present 2D Finite Differences models of the thermomechanical processes triggered by volatile exsolution in xenoliths sinking within a magma chamber. The results show that the associated density decrease leads the xenolith to float (after an initial stage of sinking) instead of sink. Consequently, stoped blocks in crustal magma chambers may rise to the roof region of the magma chamber and eventually leave the system during an eruption. This may provide an explanation for the absence of large volumes of stoped blocks in magma chambers and the observation that volcanic rocks frequently exhibit stronger crustal contamination than their plutonic equivalents (cf. Meyer et al., 2009).

**References**

Meyer, R., Nicoll, G. R., Hertogen, J., Troll, V. R., Ellam, R. M. and Emeleus, C. H., 2009, Trace element and isotope constraints on crustal anatexis by upwelling mantle melts in the North Atlantic Igneous Province: an example from the Isle of Rum, NW Scotland. Geological Magazine v. 146, p. 382–399.

# Tectonic enigmas revealed from petrological and geochemical studies of the Lesser- and Higher Himalaya in Sikkim, India

Sumit Chakraborty

*Institut für Geologie, Mineralogie und Geophysik, Ruhr Universität Bochum, Bochum, Germany*

The eastern Himalayan state of Sikkim in India exposes an excellent and continuous sequence of Lesser- (LH) and Higher (HHC) Himalayan rocks that serves as a natural laboratory for petrological studies. We have carried out petrological and geochemical studies, including thermobarometry, geospeedometry and isotopic dating using different techniques (U-Pb in zircon and monazite as well as Lu-Hf dating of garnets) on the LH as well as the HHC rocks. These reveal three tectonic enigmas that will be posed in this talk.

It is found that if different thermodynamic techniques (e.g. individual thermobarometry, calculation of pseudosections) for calculation of pressure and temperature of metamorphism are used with proper attention to kinetic controls it is possible to obtain robust estimates (e.g. checks using interlayered sequences of rocks of different bulk compositions) of P and T from these rocks. The common practice of using only compositions from the rim, or from the core, of zoned metamorphic minerals (e.g. garnets) is not kinetically reasonable and yields incorrect metamorphic field gradients. We find that the LH represents a coherent and continuous inverted Barrovian sequence where P (at peak T) as well as T increases with metamorphic grade. This tight constraint on permissible tectonic models of metamorphism is consistent with numerical geodynamic models where melt triggered exhumation produces such sequences. However, the age of growth of garnet is different at different grades, with garnets at lower grades being younger (e.g. 13 my at sillimanite grade vs. 11 my at garnet grade). This poses a tectonic puzzle that needs to be resolved.

The amphibolites included in the LH as well as the HHC sequences appear to have all been metamorphosed at similar conditions (e.g. 9-12 kbar, 800 °C), but these conditions are different from those of the surrounding country rocks. This indicates that the amphibolites were metamorphosed earlier at a different tectonic setting (suppported by limited isotopic data) and were then subsequently emplaced within the metapelitic sequence. The mechanical mechanism of emplacement in their current setting within the metapelitic rocks remains somewhat enigmatic.

The HHC rocks were metamorphosed at about 800 °C and 10 kbar, isothermally decompressed to about 4 – 5 kbar and then cooled to below 600 °C extremely rapidly (several 100 °C/my), as shown by geospeedometry and dating of zircons and monazites. This demonstrates that it is possible to have extremely rapid cooling unrelated to exhumation and poses very important questions about the connection between cooling rates and exhumation. Moreover, the cooling rate as well as the geochronological data reveals unequivocally that there are at least two blocks within the HHC that were exhumed at different rates and at different times. Therefore, if a channel flow model is to apply to these rocks, one needs multiple channels. Alternately, models other than channel flow need to be considered to explain the HHC rocks.

# New 3D seismic data and high-resolution bathymetry data give insight into active deformation in the Gulf of Cadiz

Gareth J. Crutchley[1], Christian Berndt[1,2], Dirk Klaeschen[1] and Doug G. Masson[2]

*[1]GEOMAR | Helmholtz Centre for Ocean Research Kiel, Wischhofstrasse 1-3, D-24148 Kiel, Germany, [2]National Oceanography Centre, Southampton, European Way, Southampton SO14 3ZH, UK*

The nature of active deformation in the Gulf of Cadiz is important for developing a better understanding of the inter-plate tectonics and for revealing the source of the 1755 Great Lisbon earthquake. New, high-resolution 3D seismic data reveal a classic pull-apart basin that has formed on an east striking fault in the Southern Lobe of the Gulf of Cadiz accretionary wedge. Geometrical relationships between an array of faults and associated basins show evidence for both dextral and sinistral shear sense in the Southern Lobe. Strike-slip faulting within the lobe may provide a link between frontal accretion at the deformation front and extension and gravitational sliding processes occurring further upslope. Inception of the strikeslip faults appears to accommodate deformation driven by spatially variant accretion or gravitational spreading rates, or both. This implies that active deformation on strike-slip faults in the Southern Lobe is unrelated to the proposed modern inception of a transform plate boundary through the Gulf of Cadiz and underscores the importance of detailed bathymetric analysis in understanding tectonic processes.

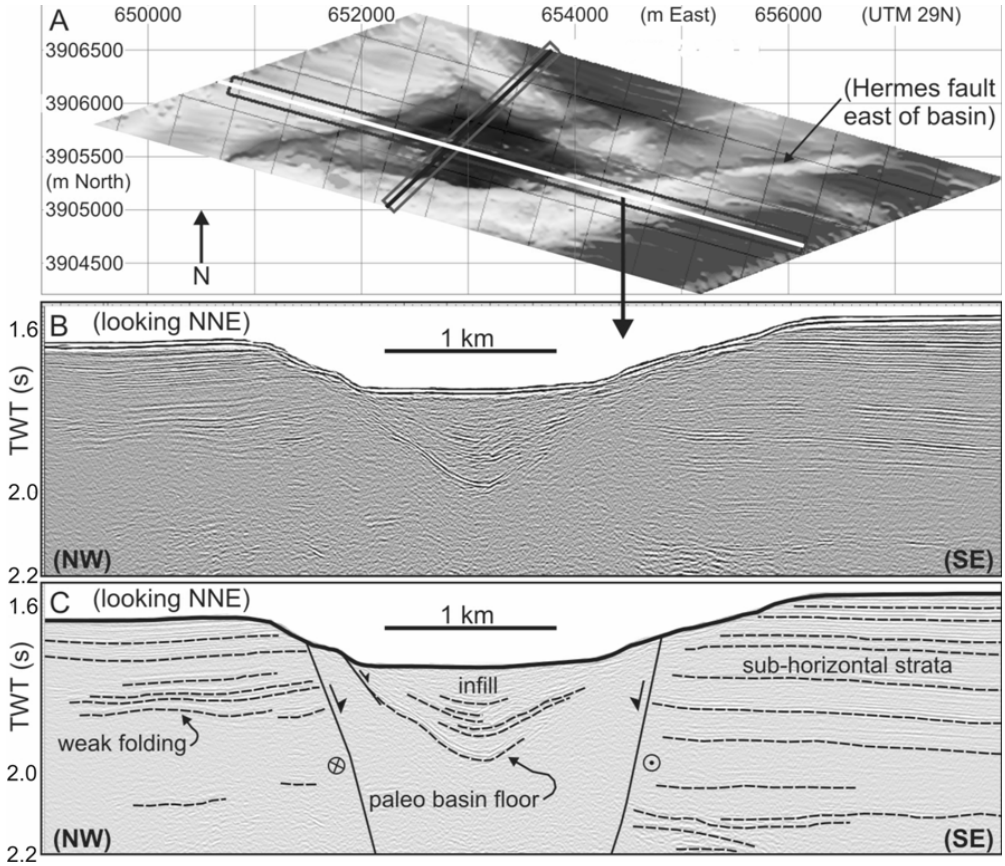


**A)** Seafloor surface of the seismic cube plotted in UTM Zone 29N coordinates. The white line (striking ESE) shows the location of the seismic section displayed in (B) and (C). **B)** ESE striking seismic section extracted from the seismic cube (vertical exaggeration at the seafloor is ~3.2.) **C)** Interpretation overlain on the seismic data.

# Correlation of joints and fracture cements in Cretaceous carbonate rocks, Mt. Chianello, Italy

Francesco Dati[1], Stefano Mazzoli[1], Stefano Vitale[1], Sofie Nollet[2] and Christoph Hilgers[2]

*[1]Department of Earth Sciences, University of Naples, Federico II, Largo S. Marcellino 10 - 80138 Napoli, Italy [2]Department of Reservoir-Petrology, RWTH-Aachen University, Wüllnerstrasse 2 - 52062 Aachen, Germany*

The study area is located in the southern Apennine, a NE-direct fold and thrust belt formed by two main parts: the Apennine accretionary wedge and the buried Apulian Platform Inversion Belt (Mazzoli et al.2008). The carbonate ridge of Mt. Chianello is part of Apennine Platform domain and comprises a 1200 m thick sequence of Cretaceous shallow water carbonates. This succession can be considered a good analogue for the fractured carbonate reservoir buried in the Val D´Agri area (Lucania region, southern Italy). In this study, we establish the deformation sequence of joint patterns in carbonate rocks and relate them to the regional deformation history. Results will be integrated in a study to the fracture cementation processes and stylolite.

The analyses succession has been deformed by early Miocene extensional tectonics related to the forebulge and foredeep stage, followed by compressional stage causes the formation of folds and thrusts, and finally by post-collisional Pliocene-Pleistocene strike-slip and final extensional tectonics (Vitale et al. 2012). The Cretaceous rocks are affected by pervasive sets of tensional joints associated to conjugate Miocene normal faults. Joints and veins form an orthogonal set striking NNE-SSW and WNW-ESE, both oriented normal to the bedding.

Petrographic analyses show that all the veins are characterized by blocky calcite and dolomite crystals and straight twins (type I and II). Early bedding-normal veins are associated to “background” joints because their orientations are coherent with the extension NW-SE (early extensional event). In cathodoluminescence, these vein cements show low luminescence levels, whereas the vein-wall interfaces resembles stylolites which are frequently more luminescent (next shortening stage). These syntaxial veins were cemented luminescent euhedral calcite overgrowths in the vein centre, followed a latest stage of anhedral quartz filling the pore space.

The wealth of microstructural observations matches well with the joint pattern, but also provides additional information on the deformation history and the evolution of pore space and fluid migration pathways.

**References**

Mazzoli, S., D‘Errico, M., Aldega, L., Corrado, S., Invernizzi ,C., Shiner, P., Zattin, M., 2008. Tectonic burial and ´young‘ (< 10 Ma) exhumation in the southern Apennines fold and thrust belt (Italy). Geology 36, 243-246.

Vitale, S., Dati, F., Mazzoli, S., Ciarcia, S., Guerriero, V., Iannace, A. 2012. Modes and timing of fracture network development in poly-deformed carbonate reservoir analogues, Mt. Chianello, southern Italy. Journal of Structural Geology. doi:10.1016/j.jsg.2012.01.005

# AMS fabrics in a Permian laccolith from Tabarz (Thuringia, Germany) – a reconnaissance study

Carlo Dietl[1]

[1]*Institut für Geowissenschaften, Goethe-Universität, Altenhöferallee 1, D-60438 Frankfurt am Main*

The Tabarz quarry exhibits Permian laccoliths of rhyolitic and lamprophyric composition which intrude siliciclastic rocks of the Oberhof Formation (Lower Permian) with a variegated composition from fine grained sandstones to breccia. One of these laccoliths was investigated for its magnetic fabric.

The magmatic body has an E-W extension of c. 100 m. In its center it is 20 m high. Its E' contact with the hosting sediments is faulted (steep normal fault, N trending). The western margin is intrusive. The outer part of the laccolith ($4/5^{th}$ of the intrusive body) consist of a very fine grained lamprophyre with spessartitic composition. The ground mass consists to 80 % of plagioclase + 15 % hornblende + 5 % ore minerals. Up to 10 % of the rock volume are taken by plagioclase phenocrysts of up to 2 mm size (+ some pyroxene crystals). The central part of the subvolcanic intrusion ($1/5^{th}$ of the laccolith) is occupied by a dark red to purple, very fine grained rhyolite with K-feldspar phenocrysts of up to 4 mm length (+ some sphene and hematite crystals). The ground mass of the rhyolite is rich in glass and opaque minerals (probably mainly hematite and magnetite). Most phenocrysts in both rock types have euhedral shapes. However, also anhedral individuals with rounded and irregular margins occur together with agglutinated feldspar crystals. Moreover, both lithologies are affected by slight hydrothermal alteration.

So far, five samples - taken along an W-E transect across the laccolith - were investigated for their magnetic susceptibility and fabric. Susceptibility is generally high ($10^{-2}$ - $10^{-3}$). This indicates that a ferrimagnetic mineral, probably magnetite, is the carrier of magnetic susceptibility However, the rhyolitic sample from the center of the intrusion has a susceptibility of only $10^{-3}$, in contrast to the lamprophyric samples from the outer parts of the intrusion. Anisotropy of all AMS fabrics is low (P' generally below 1.05) as it is typical for magmatic flow fabrics (Hrouda 1982). AMS ellipsoids from both the intrusion margins have prolate shape while those from the laccolith's center are oblate. Also the directional data of the AMS ellipsoids, i.e. the orientations of their main axes change in response to the sampling spots: the magnetic lineations (i.e. the long axis of the AMS ellipsoid) generally plunge moderately. However, one sample taken 50 m W of the laccolith's center displays a steep magnetic lineation. The same is true for the short axis of the AMS ellipsoids (i.e. the pole of the magnetic foliation): the magnetic foliation is generally steep, but within the center of the laccolith it dips moderately to the S.

The fact that the magnetic fabrics differ significantly across the laccolith is interpreted to be the result of magma flow within the intrusion. The flow fabric interpretation is supported by the low anisotropy of the AMS ellipsoids (Hrouda 1982). The pancake shaped AMS ellipsoids from the center of the intrusion might reflect flattening deformation during magma flow into the laccolith, while the cigar shaped AMS ellipsoids from the margins may be caused by channeled magma flow. Similar magmatic flow fabrics as those observed in the Tabarz laccolith were found by Zavada et al. (2009 a and b) in an experimentally produced dome (made from plaster of Paris) as well as within a trachytic lava dome.

**References**

Hrouda, F. (1982). Magnetic anisotropy of rocks and its application in geology and geophysics. Geophys. Surv.5, 37-82.

Zavada, P., Kratinova, Z., Kusbach, V., Schulmann, K. (2009). Internal fabric development in complex lava domes. Tectonophysics 466, 101-113.

Zavada, P., Schulmann, K., Lexa, O., Hrouda, F., Haloda, J., Tycova, P. (2009). The mechanism of flow and fabric development in mechanically anisotropic trachyte lava. J. Struct. Geol. 31, 1295-1307.

# Wavelength selection in 3D multilayer detachment folding

Naiara Fernandez and Boris J.P. Kaus

*Geophysics and Geodynamics, Institute of Geosciences, Johannes Gutenberg University Mainz, J.-J. –Becher-Weg 21, D-55128 Mainz, Germany*

Many fold-and-thrust belts are dominated by crustal scale folding that exhibits fairly regular fold spacing. For example, the Fars region in the Zagros Mountains shows a fold spacing with a normal distribution around a dominant wavelength of 14 Km ± 3 Km, yet having a wide variability of aspect ratios (length to wavelength ratios; Yamato et al., 2011). To which extend this is consistent with a crustal-scale folding instability or how the regional spacing of folding can be used to constrain regional rheological parameters are not fully resolved questions. To get insights into these problems we have investigated the dominant wavelength selection in a true multilayer system (Schmid and Podlachikov, 2006) with three different viscosities: lower salt layer ($\eta_s$), and overlying weak layers ($\eta_w$) and competent layers ($\eta_c$). Two different tools have been used for this study: a 2D semi-analytical solution and a 3D finite element numerical code (LaMEM).

Mechanical phase diagrams derived from the semi-analytical approach and based on two viscosity ratios ($R_1=\eta_c/\eta_s$ and $R_2=\eta_c/\eta_w$) can be used to distinguish different folding modes, some of which have not been described previously. The diagrams show the $R_1$ and $R_2$ combination values under which transition from gravity dependent to no gravity dependent domain occurs. The salt thickness to overlying overburden ratio ($H_s/H_o$) is another controlling parameter within the no gravity dependant domain, whereas within the gravity dependant domain, the salt thickness must be below a critical value for detachment folding mode to occur (mainly $H_s/H_o$ controlled folding mode). These results are in agreement with the folding modes defined for a two-layer system (Schmalholz, 2002).

Numerical simulations were performed to study the validity of the phase diagrams beyond the initial folding stages for which the semi-analytical method is applicable. The fold wavelength of the quasi-2D and 3D simulations is obtained using spectral analysis and its evolution and selection during deformation is tracked. The final wavelength that is in fact selected during strain is in agreement with the calculated phase diagrams and therefore, the observed fold spacing together with 3D numerical models and a semi-analytical theory can successfully be used to constrain the effective viscosity structure of the deformed layers.

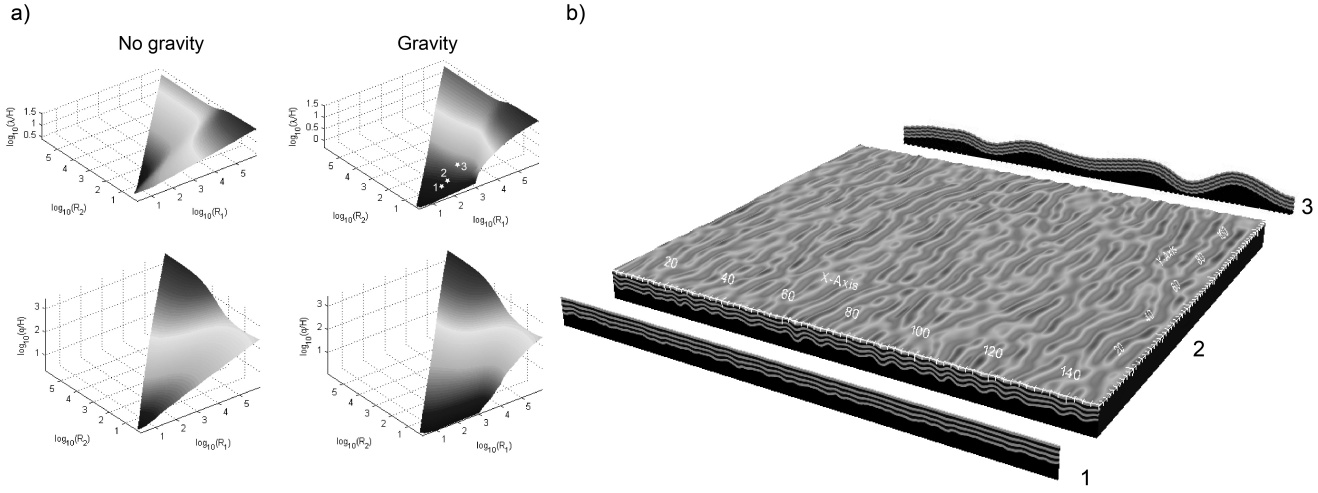


Figure 1. a) 3D phase diagrams of gravity influenced detachment folding. b) Result of different numerical models corresponding to numbered stars in the phase diagram.

**References**

Schmalholz, S.M., Podladchikov, Yu.Y. and Burg, J.-P. (2002). Journal of Geophysical Research Vol. 107 (B1), 2005, 16pp.
Schmid, D.W. and Podladchikov, Yu.Y. (2006). Philosophical Magazine 86:21. p. 3409-3423.
Yamato, P., Kaus, B.J.P., Mouthereau, F. and Castelltort, S. (2011). Geology Vol 39. No 9. p. 815-818.

# The Eckergneiss complex – state of the art and open questions

Carl-Heinz Friedel[1] and Kai Fischer[2]

*[1]Landesamt für Geologie und Bergwesen Sachsen-Anhalt D-06118 Halle/S., [2]Martin-Luther-Universität Halle-Wittenberg, Institut für Geowissenschaften D-06120 Halle/S.*

The ca 10 km$^2$ large Eckergneiss complex (EGC) is the largest crystalline complex of the mid-Europian part of the Rhenohercynian zone, which may provide important information about age, provenance and metamorphism of the crystalline basement of this zone.

The EGC is exposed in the NW part of the Harz Mountains (Germany). It forms an NE-SW striking tectonic slice of medium to high grade crystalline rocks within the very low-grade Paleozoic rocks of the Harz, and is bounded by large bodies of gabbro and granite that intruded at lowermost Permian age (295-280 Ma, e.g. Zech et al. 2010). The crystalline rocks dominantly consist of corderite (pinite) bearing gneiss, quartzite and mica schist, while metavolcanics (amphibolites) occur only subordinately. This and the composition of accessory detrital minerals indicate a protolithe of pelitic to psammitic composition developed at a passive continental margin (Martin-Gombojav 2003). U/Pb-SHRIMP dating of detrital zircons from quartzitic rocks of the EGC revealed dominantly Mesoproterozoic ages (900-1800Ma) which implies a SW-Baltica provenance of sedimentary educts and not Avalonian basement (Geisler et al. 2005). The youngest SHRIMP ages of 410 ± 10 Ma imply that sedimentation and metamorphism must have taken place between lower Devonian and lowermost Permian, thus a Cadomian age of metamorphism can be excluded.

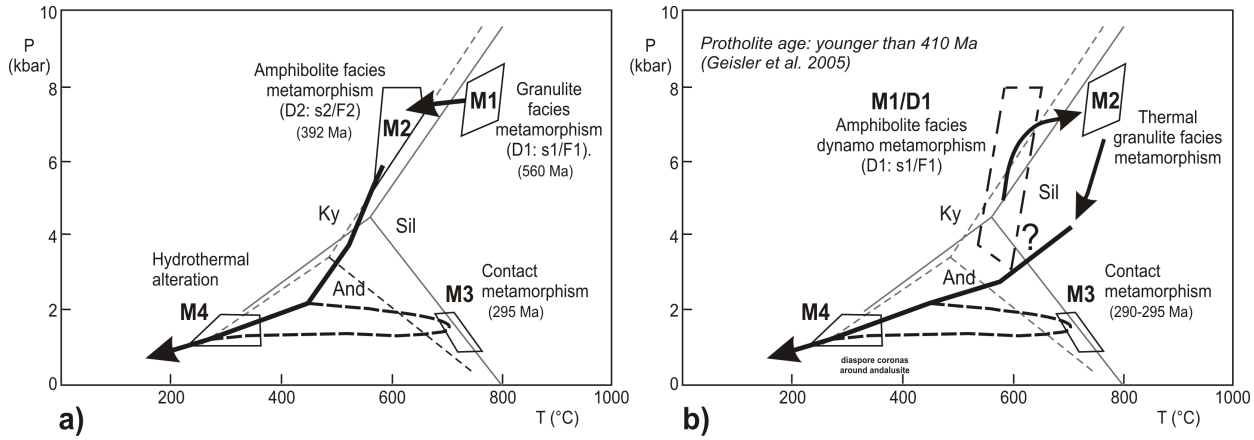


Figure 1: Different paths of metamorphic evolution of the EGC. a) After Franz et al. (1997), still assuming a Cadomian age of granulite facies metamorphism (M1). b) After Martin-Gombojav (2003); note, the P-T field of amphibolite grade metamorphism is not constrained by P-T data (from Fischer & Friedel 2009, modified).

The EGC was penetratively deformed (D) and metamorphosed under amphibolite and granulite facies conditions, respectively (M1, M2) before the rocks were overprinted by contact metamorphism and subsequent hydrothermal alteration (M3, M4 fig. 1). However, the tectono-metamorphic evolution (M1, M2) is still a matter of debate. Franz et al. (1997) obtained an anti-clockwise P-T path from granulitic (M1/D1) to amphibolitic conditions (M2/D2, fig. 1a). Contrary, Martin-Gombojav (2003) found textural evidences for a clockwise P-T evolution with a main stage of deformation and related amphibolite facies metamorphism (M1/D1), followed by a high-grade thermal overprint without deformation (M2, fig. 1b). This path is supported by strong recrystallization and a lack of texture, but well constrained P-T data are not yet available (Fischer & Friedel 2009). Another open question is related to the exact timing of metamorphic stages in order to recognize the history and mechanisms of exhumation of the EGC.

**References**

Geisler, Th., Vinx, R., Martin-Gombojav, N. and Pidgeon, R.T. (2005). Int. J. Earth Sci., 94, 369-384.
Franz, L., Schuster, K.A. and Strauss, K.W. (1997). Chem. Erde, 57, 105-135.
Fischer, K. and Friedel, C.-H. (2009). EDGG, 239, 43-48
Martin-Gombojav (2003). Unpubl. doctoral thesis, Univ. Hamburg, 173pp
Zech, J., Jeffries, T., Faust, D., Ullrich, B. and Linnemann, U. (2010). Geol Saxonica, 56, 9-24.

# The Vardar Ocean suture in the Rhodopes and the maximum-allochthony hypothesis for the Hellenides

Nikolaus Froitzheim[1], Silke Jahn-Awe[1], Dirk Frei[2], Ashlea Wainwright[1], Roland Maas[3], Neven Georgiev[4], Thorsten J. Nagel[1] and Jan Pleuger[5]

[1]*Steinmann-Institut, Universität Bonn, Poppelsdorfer Schloss, 53115 Bonn, Germany*
[2]*Department of Earth Sciences, Stellenbosch University, Private Bag X1, Matieland 7602, Stellenbosch, South Africa*
[3]*School of Earth Sciences, The University of Melbourne, Melbourne Victoria 3010, Australia*
[4]*Department of Geology and Paleontology, University St. Kliment Ohridski, 15 Tzar Osvoboditel Blv., 1000, Sofia, Bulgaria*
[5]*Geologisches Institut, ETH Zürich, Sonneggstrasse 5, CH-8092 Zürich, Switzerland*

The metamorphosed thrust stack of the Rhodopes, a key element of the Aegean-Hellenic orogenic system, comprises a level with ophiolites (Middle Allochthon) under- and overlain by continent-derived allochthons. The Upper Allochthon represents the European margin; the origin of the Lower Allochthon is controversial, either from a former microcontinent (Drama) or from the margin of Apulia. For ophiolites in the Middle Allochthon, ages between Proterozoic and Triassic have been discussed. U-Pb dating of zircon from a metamorphosed plagiogranite associated with metagabbro in one of the ophiolite slivers (Satovcha ophiolite) yielded a Late Jurassic age (160 ± 1 Ma), similar to the ages of the Guevgeli and other ophiolites in the eastern Vardar Zone bordering the Rhodopes to the SW. Trace element compositions and Sr and Nd isotope ratios show that the plagiogranite and the metagbbros are cogenetic and represent supra-subduction zone ophiolites. The trace element patterns closely resemble the ones of the Guevgueli ophiolites (Zachariadis, 2010), and the association with Late Jurassic arc-type granitoids is another feature that applies both to the Guevgueli ophiolites and the Rhodope Middle Allochthon. This suggests that the Middle Allochthon comprises the metamorphosed suture zone of the Vardar Ocean. In consequence, the Lower Allochthon most likely represents the Apulian margin and the Drama microcontinent did not exist. The “root” of the Vardar suture is at the NE boundary of the Rhodopes. Fragments of the floor thrust of the Internal Hellenides (Nestos-Olympos Thrust) have become spread out over a distance of 500 km, measured parallel to the thrusting direction, by rollback-related extension. The amount of SW-ward rollback of the Hellenic subduction zone in the last 45 to 40 Ma is also about 500 km, and the average rate of rollback 1.1 to 1.25 cm/a.

**References**

Zachariadis, P. T. (2007) Ophiolites of the eastern Vardar Zone, N. Greece (Ph. D. thesis): Mainz, Germany, Universität Mainz, 131 p.

# The Eastern Alps-Western Alps boundary: crustal scale sections from western Austria

Bernhard Fügenschuh[1], Hugo Ortner, Hannah Pomella[1], Marcel Schulz[2] and Michael Zerlauth[2]

*[1]Institut für Geologie, Universität Innsbruck, A-6020 Innsbruck, [2] alpS - Centre for climate change adaption technologies, 6020 Innsbruck*

Several crustal-scale cross-sections were constructed between the Rhine valley in the west and the Kleinwalser valley in the east in Vorarlberg. The construction was based on published data, surface geology, drillings as well as on reinterpreted seismic lines. The general geological architecture of the examined area can be described as a typical foreland fold-and-thrust belt, comprising the tectonic units of the Subalpine Molasse, (Ultra-)Helvetic, Penninic, and Austroalpine nappes. Along the south-dipping listric Alpine basal thrust these units overthrusted the autochthonous Molasse. The Subalpine Molasse is multiply stacked, forming a triangle-zone (MÜLLER et al. 1984). A well-defined seismic feature is the European basement together with its autochthonous cover, slightly dipping southward from about 3500m BSL to approx. 6500m BSL in the south. Furthermore a discontinuous double reflector, interpreted as the base of the Helvetic nappe complexes (approx. at 5000m BSL in the southernmost parts), could be identified.

The internal structure of the Helvetic nappe stack could hardly be resolved. The assumed hinterland dipping duplex-structure of the Helvetic nappes results from surface and borehole-data. However, there are at least two Helvetic nappes needed to fill the available space. The deeper one, termed “Hohenemser nappe” (WYSSLING 1985), is overlain by the superficially exposed “Säntis nappe”. In the southern part of the Säntis nappe (below the “Bregenzer Wald”) we suspect a Dogger basin (cut across by well VBG Au1) which is bordered by two steep lateral ramps, accompanied by tear faults in the hanging wall.

Based on our sections, the shortening within the Helvetic nappes has been calculated using the Cretaceous “Kieselkalk” and the Jurassic “Quinten Limestone”as a reference. The shortening amounts to approx. 50%, which is on the same order compared to estimates from eastern Switzerland (SCHMID et al. 1997, TRÜMPY 1969).

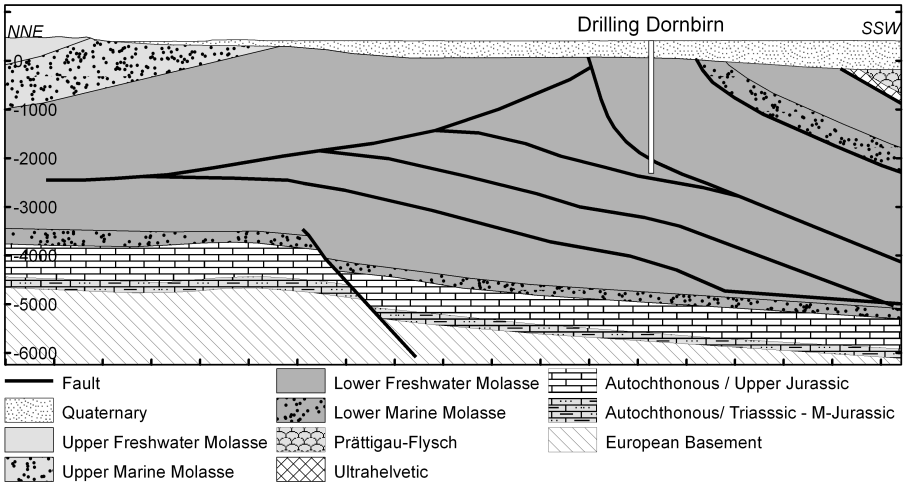


Detail of N-S section with triangle structure in the Lower Freshwater Molasse

**References**

Müller, M., Nieberding, F. and Wanninger, A. (1988). Geologische Rundschau, 77/3, 787-796.

Schmid, S.M., Pfiffner, O.A. and Schreurs, G. (1997). In Pfiffner, O.A. et al. (eds.). Deep Structure of the Alps, Results from NFP 20, 160-185.

Trümpy, R. (1969). Die helvetischen decken der Ostschweiz: Versuch einer palinspastischen Korrelation und Ansätze zu einer kinematischen Analyse. Eclogae geol. Helv. , 62/1, 105-138.

Wyssling, G. (1985). Palinspastische Abwicklung der helvetischen Decken von Vorarlberg und Allgäu. - Jb. Geol. B.-A., 127/4, 701-706.

# Segmentation of the 1960 and 2010 Chilean earthquakes controlled by a giant slope failure

Jacob Geersen[1], David Völker[1], Jan Behrmann[1,2], Dirk Kläschen[2], Wilhelm Weinrebe[1,2], Sebastian Krastel[2] and Christian Reichert[3]

*[1]Collaborative Research Center (SFB) 574; [2]Helmholtz-Zentrum für Ozeanforschung Kiel | GEOMAR, [3]Bundesanstalt für Geowissenschaften und Rohstoffe*

About 1000 km of the South Chilean margin were ruptured in 1960 by the Mw 9.5 Great Chile Earthquake. Early in 2010 the immediate area to the north was affected by the Mw 8.8 Maule Earthquake. In the area of the rupture boundary three giant Pleistocene submarine slope failures are observed in bathymetric and reflection seismic data. The slope failures each shifted volumes between 253 $km^3$ and 472 $km^3$ of slope sediments, compacted accretionary wedge material and continental framework rock from the continental slope into the trench. Seismic reflection data image an undisturbed well layered sedimentary trench fill and a continuous décollement in the areas where no slope failures are observed. However, at the exact locations of the slope failures, which coincide with the boundaries of the 1960 and 2010 ruptures, chaotic slide deposits compose the lower part of the trench-fill. At these locations no continuous décollement has developed. We speculate that the underthrusting of the highly inhomogeneous slide deposits prevents the development of a continuous décollement and thus the buildup of a thin (few millimeters) slip zone that is continuous in space as necessary for earthquake rupture propagation. Thus the 1960 Great Chile – 2010 Maule earthquake rupture boundary seems to be controlled by the underthrusting of products of giant submarine slope failures which impeded further propagation of earthquake rupture during both events. Our results emphasize that upper plate mass wasting, if it impacts on the internal structure and composition of the subduction channel rocks, can play a key role in defining seismotectonic segmentation at convergent plate boundaries.

# Numerical Modelling of Subduction and Collision Processes

Taras V. Gerya

*Geophysical Fluid Dynamics Group, Institute of Geophysics, Department of Geosciences, Swiss Federal Institute of Technology (ETH-Zurich), Sonneggstrasse 5, CH-8092 Zurich ( Switzerland)*

Despite four decades of development of plate tectonic theory and practice a number of first order questions concerning nucleation, dynamics and demise of convergent plate boundaries remain unresolved. Indeed, serious restrictions for answering these questions are related to natural space-time limitations of human ability to directly observe very slow and deep plate tectonic and mantle processes. Consequently, numerical analysis of these processes is used more and more actively to complement observations with quantitative numerical modelling results. The following unresolved outstanding problems of plate tectonics will be discussed in this lecture: (A) initiation of subduction, (B) crustal growth in subduction zones, (C) the fate of subduction, continental collision, arc/continent assembly, continental subduction and slab detachment.

***(A) Initiation of subduction:*** The gravitational instability of an old oceanic plate is believed to be the main reason for subduction. However, the bending and shear resistance of the lithosphere prevent subduction from arising spontaneously. Many hypotheses have been proposed to obviate this restriction but no undisputable examples of the ongoing initiation are yet known. The major obstacle in the possibility to directly investigate subduction initiation is the uncertainty about localities where subduction starts now. As suggested by 2D numerical experiments spontaneous subduction initiation at a passive margin is a long-term process with a "hidden" phase of initial movements that are not expressed in diagnostic subduction features such as trench and magmatic arc. The main challenge is, therefore, to identify possible subduction initiation localities in the world by evaluating numerically probability of subduction initiation at existing passive margins and oceanic plate boundaries (based on a local lithospheric/mantle structure and acting tectonic forces). Further progress will also crucially depend on applying high-resolution 3D modelling that take into account actual plate geometries.

***(B) Crustal growth in subduction zones:*** Volcanic arcs are thought to be the main sites of production of continental crust, particularly in post-Archaean times. Crustal growth rate estimates in magmatic arcs are widely variable and partly controversial. Numerical modelling studies of long-term evolution and associated crustal growth in magmatic arcs are yet relatively limited. The predicted rate of crust formation positively correlates with the rate of trench retreat and is close to the lower edge of the observed range of rates in arcs. Computed spatial and temporal pattern of melt/crust production rate in 2D and 3D appeared to be strongly controlled by the thermal-chemical plumes rising from slabs which are comparable to the spatial periodicity and the life extent of volcanic clusters in nature. Recent natural observations and high-pressure melting experiments with subducted rock melanges indicate that silicic melts that are documented in arcs can be formed inside the plumes. In the future intraoceanic and oceanic-continental subduction should be modelled in 3D and results should be compared with key magmatic arcs worldwide.

***(C) Continental collision, arc/continent assembly, continental subduction, slab detachment:*** Continent-continent and arc-continent collisions are inevitable consequences of plate tectonics. Collision processes often culminate subduction episodes causing the fate of subduction, orogenesis, arc/continent assembly, continental subduction and subducted slab detachment. In the last two decades 2D numerical simulations have been widely used to investigate continent-continent collision and significant progress has been achieved in our understanding of this tectonic regime. In contrast, numerical modelling of arc/continent assembly is limited by 2D simulation of episodic accretion of small continental terranes based on mechanical model with kinematic lower boundary condition. Applicability of 2D models to natural collisional orogens is restricted as orogen-parallel movements (that can easily take several hundred kilometers) cannot be described. However, only a few 3D numerical modelling studies of continental collision have been published so far been limited by relatively coarse resolution and simple lithospheric geometries. Further progress in our understanding of collisional processes is crucially dependent on performing realistic high-resolution modelling in 3D.

# Bending-related faulting and mantle serpentinization at deep-sea trenches

Ingo Grevemeyer[1]

[1]*GEOMAR | Helmholtz Zentrum für Ozeanforschung Kiel, Wischhofstraße 1-3, D-24148 Kiel*

The understanding of the Earth's water cycle is inherently linked to the subduction of water at deep sea trenches. The transfer of water into the deep Earth's interior is related to the alteration and hydration of the incoming lithosphere. The release of water from subducting lithospheres affects the composition of the mantle wedge, enhances partial melting and triggers intermediate-depth earthquakes. Water is transferred with the incoming plate into the subduction zone as water trapped in sediments and open void spaces in the igneous crust and as chemically bound water in hydrous minerals in sediments and oceanic crust (Jarrad, 2003). However, if water reaches upper mantle rocks, significant amounts can be transferred into the deep subduction zone as water-bearing mineral serpentine (Peacock, 2004). Serpentinites have nearly the same chemical composition as mantle peridotite except that they contain approximately 13 wt% water in mineral structures.

Seismic refraction and wide-angle data were collected at a number of active continental margins in the trench-outer rise to investigate the impact of bending related normal faulting on the seismic properties of the oceanic lithosphere prior to subduction. Surveys provided data from offshore of Nicaragua (Grevemeyer et al., 2007; Ivandic et al., 2008), Chile (Contreras-Reyes et al., 2008), and Tonga (Contreras-Reyes et al., 2011). At all settings tomographic joint inversion of seismic refraction and wide-angle reflection data yielded anomalously low seismic P-wave velocities in the crust and uppermost mantle seaward of the trench axis. Crustal velocities are reduced by 0.2-0.8 km/s compared to normal mature oceanic crust. Seismic velocities of the uppermost mantle are 7.4-7.8 km/s and hence 5-12% lower than the typical velocity of mantle peridotite. These systematic changes in P-wave velocity from the outer rise towards the trench axis indicate an evolutionary process in the subducting slab consistent with percolation of seawater through the faulted and fractured lithosphere and serpentinization of mantle peridotites. The observed velocity reduction suggests that mantle serpentinization reaches 12-25%. Thus, processes occurring in the trench-outer rise affect indeed the Earth's water cycle and indicate that significant amount of waters are transferred into the subducting lithosphere and hence carried to the deep Earth interior.

**References**

Contreras-Reyes, E., Grevemeyer, I., Flueh, E.R., and Reichert, C. (2008), Upper lithospheric structure of the subduction zone offshore of southern Arauco peninsula, Chile, at 38°S, J. Geophys. Res., 113, B07303, doi:10.1029/2007JB005569.

Contreras-Reyes, E., Grevemeyer, I., Watts, A.B., Flueh, E.R., Peirce, C., Moeller, S., and Papenberg, C. (2011). Deep seismic structure of the Tonga subduction zone: Implications for mantle hydration, tectonic erosion, and arc magmatism, J. Geophys. Res., 116, doi:10.1029/2011JB008434.

Grevemeyer**,** I., Ranero, C.R., Flueh, E., Kläschen, D., Bialas, J. (2007). Passive and active seismological study of bending-related faulting and mantle serpentinization at the Middle America trench. Earth Planet. Sci. Lett. 258, 528-542.

Ivandic, M., Grevemeyer, I., Berhorst, A., Flueh, E.R. and McIntosh, K. (2008), Impact of bending related faulting on the seismic properties of the incoming oceanic plate offshore of Nicaragua, *J*. Geophys. Res., 113, B05410, doi:10.1029/2007JB005291.

Jarrad, R.D. (2003). Subduction fluxes of water, carbon dioxid, chlorine, and potassium. Geochemistry, Geophysics, Geosystems 4: doi: 10.1029/2002GC000392.

Peacock, S.M. (2004). Insight into the hydrogeology and alteration of oceanic lithosphere based on subduction zones and arc volcanisms. In: Davis E.E, Elderfield, H. (Eds.), Hydrogeology of Oceanic Lithosphere. Cambridge University Press, pp. 659-676.

# A Silurian top-to-NW ductile shear zone in the Seve Nappe Complex (central Scandinavian Caledonides, Sweden): The top of a Scandian palaeo-extrusion wedge?

Jens C. Grimmer[1], Johannes Glodny[2], Kirsten Drüppel[1], Agnes Kontny[1] and Reinhard O. Greiling[1]

[1]*Institut für Angewandte Geowissenschaften, Karlsruher Institut für Technologie (KIT), D-76131 Karlsruhe,*
[2]*Deutsches GeoForschungsZentrum (GFZ), D-14473 Potsdam*

The central Scandinavian Caledonides comprise a fold-and-thrust belt emplaced onto the Fennoscandian Shield during Silurian times during top-to-ESE tectonic transport. The degree of metamorphism generally increases from E to W from the external sub-greenschist facies nappes in the E to higher grade metamorphic nappes in the W. Large-scale late- to post-orogenic WSW-directed extension to transtension during early Devonian times and related exhumation of high-grade metamorphic rocks are well known for the westernmost more internal parts of the Scandinavian Caledonides (e.g. Braathen et al. 2002). In the more external parts of the Scandinavian Caledonides the Slipsiken shear zone near Klimpfjäll (southern Västerbotten, Sweden) separates the medium to high-grade Seve Nappe Complex (SNC) in the footwall from the greenschist grade Köli Nappe Complex (KNC) in the hanging wall, hence displaying normal fault geometry. For this ductile shear zone, development due to Devonian extension was tentatively suggested (e.g. Braathen et al. 2002). We provide structural, geochronological, petrological, and geochemical data to test possible early Devonian ductile extension along this shear zone.

The Slipsiken shear zone comprises ca. 1 km of mylonitic garnet-micaschists with intercalations of minor gneisses, amphibolites, and ultramafic rocks. P-T pseudosection calculation in the NCKFMASH system reveals P-T conditions of *c.* 600-650°C, 10-11 kbar for the observed peak-metamorphic mineral assemblage (garnet - biotite - white mica - K-feldspar - plagioclase) of the garnet-micaschists. Similar temperatures are constrained by conventional garnet-biotite thermometry. Stretching lineations trend SE-NW with a top-to-NW normal sense of shear, which is derived from rotated clasts and S-C-fabrics as observed elsewhere along the SNC-KNC boundary (e.g. Trouw 1973; Greiling et al. 1998). The micaschists show increasing degrees of anisotropy of the magnetic susceptibility with increasing degrees of mylonitization due to inferred synkinematic magnetite growth (Kontny et al. 2012). Multimineral Rb-Sr-data for a mylonite sample yield a well-constrained isochron age of 431 ± 9 Ma.

The lack of both, significant retrograde mineral reactions and of cataclastic overprint indicates that ductile shearing ceased at lower crustal levels and further exhumation most likely was transferred to other structures, or accomplished by other processes. Initiation of nappe stacking is up to now poorly constrained in this part of the Caledonides. We hypothesize that normal shear on top of the Seve Nappe Complex was coeval with thrusting at the base, thus forming an extrusion wedge as proposed by Ring and Glodny (2010) for other orogenic belts. In any case, the combined top-to-NW kinematics and geochronological data clearly rule out Devonian extensional shear along the Slipsiken shear zone and mark instead Silurian large-scale top-to-NW ductile shear, possibly related to the exhumation of high-grade metamorphic rocks in the course of Scandian nappe stacking. Scandian top-to-ESE vergent thrusts may have been active at about the same time, as described also for other parts of the Central Scandinavian Caledonides (Gee et al. 2010). The regional early Devonian extensional paleostress field most likely finds its expression in commonly observed distinct epidote-quartz coated, NW- to N-striking joints.

**References**

Braathen, A. et al. (2002) Norwegian J. Geol. 82, 225-241.
Gee, D. et al. (2010) GFF 132, 29-44.
Greiling, R.O., Garfunkel, Z., Zachrisson, E. (1998) GFF 120, 181-190.
Kontny, A. et al. (2012) Int. J. Earth Sci. doi: 10.1007/s00531-011-0713-8
Ring, U., and Glodny, J. (2010) J. Geol. Soc. London 167, 225-228.
Trouw, R.A.J. (1973) Sveriges Geologiska Undersökning C 689, 155 pp.

# What were the protoliths of the Middle Allochthon? Answers from zircon dating and geochemistry of metamorphosed sedimentary and magmatic rocks of the Ammarnäs Complex, central Scandinavian Caledonides

Jens C. Grimmer[1], Fredrik A. Hellström[2], Axel Gerdes[3] and Reinhard O. Greiling[1]

*[1]Institut für Angewandte Geowissenschaften, Karlsruher Institut für Technologie (KIT), D-76131 Karlsruhe, [2]Geological Survey of Sweden, S-75128 Uppsala, [3]Institut für Geowissenschaften, Goethe-Universität Frankfurt, D-60438 Frankfurt*

The central Scandinavian Caledonides comprise a fold-and-thrust belt emplaced onto the Fennoscandian Shield during Silurian top-to-(E)SE tectonic transport. The nappes are subdivided into the Lower, Middle, Upper and Uppermost Allochthons with the Lower and Middle Allochthons representing the former margin of Fennoscandia. The Ammarnäs Complex is a distinct nappe complex in the Middle Allochthon of the central Scandinavian Caledonides. It consists of several hundred metres thick uniform meta-greywacke successions of greenschist metamorphic grade containing kilometre-scale allochthonous lenses of pre-Caledonian crystalline basement rocks.

The crystalline basement rocks are alkali-calcic and dominated by gabbros, monzo-gabbros, monzonites, and quartz-monzodiorites and other subordinate rocks reflecting together a high-K suite. In comparison with MORB the rocks are enriched in LREE and depleted in HFSE. Ductile deformed feldspars in mylonitic gneisses indicate at least lower amphibolite facies metamorphic overprint. In situ U-Pb-Th SIMS analyses of zircons from two rock samples were performed at the NORDSIM facility at the Museum of Natural History in Stockholm: An orthogneiss of quartz-monzodioritic protolith composition yielded a weighted average $^{207}Pb/^{206}Pb$ zircon age of 1799±10 Ma and a metasyenite sample yielded a weighted average $^{207}Pb/^{206}Pb$ zircon age of 1786±7 Ma. One zircon analysis of the orthogneiss yielded a concordia age of 967±20 Ma. Our geochemical and geochronological data suggest that the basement rocks of the Ammarnäs Complex represent fragments of the early 1.81−1.76 Ga igneous phase of the Transscandinavian Igneous Belt (=TIB 1) with a possible, but poorly understood Sveconorwegian overprint. Similar protolith ages with a poorly constrained Sveconorwegian overprint are documented from allochthonous crystalline basement rocks in the Middle Allochthon about 100 km south of the Ammarnäs Complex (Greiling et al. 2002).

In contrast to the crystalline basement rocks, the meta-greywacke succession were metamorphosed under greenschist facies conditions. Lithoclasts and geochemical data indicate that the greywackes were mainly derived from granitic-granodioritic rocks. LA-ICP-MS dating of zircons yields 7% Neoproterozoic, 52% Mesoproterozoic, and 41% Palaeoproterozoic $^{207}Pb/^{206}Pb$-ages with two prominent age peaks at 1.64 Ga and 1.5 Ga, and a broad distribution of Sveconorwegian (1140−900 Ma) and `pre-Sveconorwegian´ (1340−1140 Ma) ages (Grimmer et al. 2011).

Recent studies from various places in the Middle Allochthon yielded similar detrital zircon age distributions (Kirkland et al. 2011, Be'eri-Shlevin et al. 2011, Bingen et al. 2011). We interpret the Ammarnäs Complex as a Neoproterozoic basin fragment, which accumulated detritus from the Sveconorwegian orogen and the TIB. Neoproterozoic basins covered large areas between Baltica and Laurentia in the North Atlantic Region (NAR; Kirkland et al. 2011). The sedimentary rocks of these basins and parts of their crystalline basement now constitute major parts of the Middle Allochthon in the Scandinavian Caledonides. We tentatively interpret the amphibolite-grade metamorphism, our geochronological data, and those of Greiling et al. (2002) as late- to post-Sveconorwegian magmatic-metamorphic overprint of the westernmost TIB-rocks predating deposition of the greywacke succession between 730 and 630 Ma.

**References**

Be'eri-Shlevin, Y. et al. (2011) Prec. Res. 187, 141−160.
Bingen, B., Belousova, E.A., Griffin, W.L. (2011) Prec. Res. 189, 347−367.
Cawood, P.A. et al. (2010) Geology 38, 99−102.
Greiling, R.O., Stephens, M.B., Persson, P.-O. (2002). Sveriges geologiska undersökning C 834, pp. 31–42.
Grimmer, J.C., Greiling, R.O., Gerdes, A. (2011) Terra Nova 23, 270−279.
Kirkland, C.L., Bingen, B., Whitehouse, M.J., Beyer, E., Griffin, W.L. (2011) Prec. Res. 186, 127−146.

# Strukturgeologisches 3D-Modell des östlichen Leinetalgrabenstörungssystems bei Bovenden/Südniedersachsen

Johannes Großmann[1], Bernd Leiss[1] and David C. Tanner[2]

*[1]Geowissenschaftliches Zentrum der Universität Göttingen, D-37077 Göttingen, [2]Leibniz-Institut für Angewandte Geophysik, D-30655 Hannover*

Zum Verständnis der kinematischen Entwicklung der Leinetalgrabenstruktur in der Region Göttingen/Südniedersachsen und im Rahmen der dortigen Erkundungsmaßnahmen zum tiefengeothermischen Energiepotential spielt die Kenntnis der Geometrie und der Raumlage der Störungssysteme eine Schlüsselrolle – insbesondere in Hinblick auf den Stockwerksbau (a) variszisches Grundgebirge, (b) Zechsteinsalze und (c) mesozoisches Deckgebirge.
Auf der Basis von Kartierungen, aktuellen detaillierten Profilaufnahmen sowie Bohrkleinauswertungen flacher Geothermiebohrungen wurde das östliche N-S streichende Störungssystem mit Grabenschulterbereich und dem mit ca. 20° zur Störung hin einfallende Grabeninnere im Bereich Bovenden für das Deckgebirge modelliert. Über die Simulation der Schollenbewegungen und unterschiedlicher geometrischer Annahmen der grabenrandparallelen Aufwölbungsstruktur im Grabeninneren können u.a. die Fragen diskutiert werden, ob es sich hierbei um eine Rollover-Struktur oder um Inversionstektonik handelt (wie z.B. von Tanner et al. 2010 postuliert) und ob die Zechsteinsalzlage als Abscherhorizont fungierte und damit das Störungssystem tatsächlich den angenommenen listrischen Verlauf hat. Eine erste ergänzende Profilmessung der natürlichen elektromagnetischen Strahlung scheint die Annahme eines Störungsbündels bzw. einer Störungszone zu bestätigen.

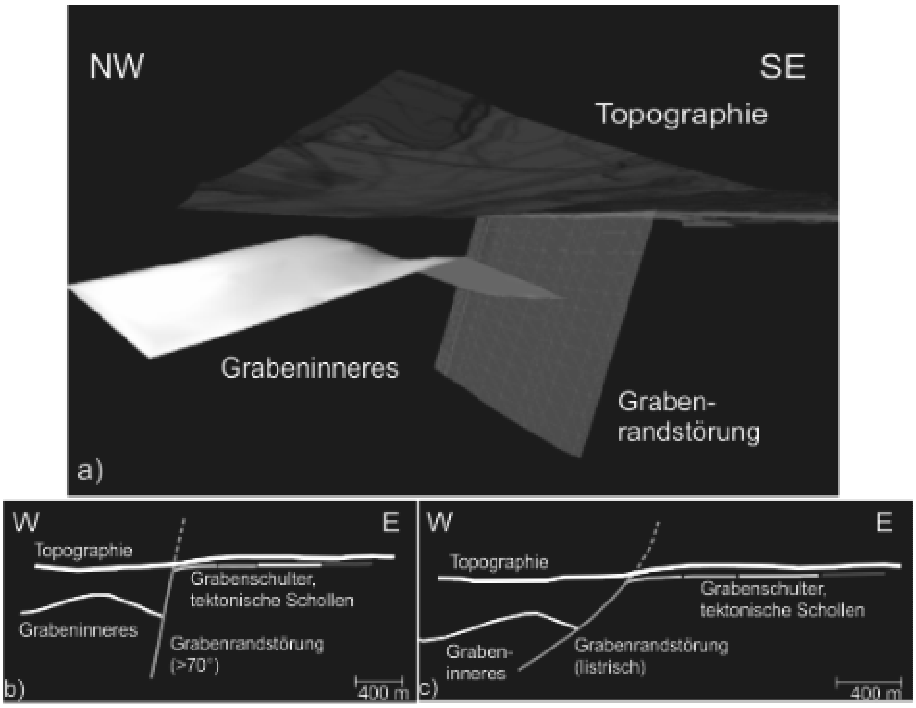


Abb. 1: Strukturmodell des östlichen Leinetalgrabenstörungssystems bei Bovenden/Südniedersachsen. a) 3D-Geometrie des Grabeninneren und der Grabenrandstörung des Leinetalgrabens bei Bovenden (Grabeninneres und Grabenschulter repräsentiert durch die Basis des Unteren Muschelkalks). b) & c) 2D-Schnitte der 3D-Darstellung von a) mit steilem (b) und flachem listrischen Einfallen der Grabenrandstörung (c).

**Referenzen**

Tanner, D.C, Leiss, B., Vollbrecht, A. und die GGG (2010). ZDGG, 161/4, 369-377.

# The structure and evolution of magmatic complexes in fold-and-thrust belts – a case study of Cerro Negro, Neuquén Province, Argentina

D. Gürer[1,2], O. Galland[1], H. A. Leanza[3], C. Sassier[4] and P. R. Cobbold[5]

[1] Physics of Geological Processes, University of Oslo, P.O. Box 1048, Blindern, Oslo, Norway (Derya.Guerer@gmail.com),
[2] Steinmann Institut für Geologie, Mineralogie und Paläontologie, Rheinische Friedrich-Wilhelms-Universität Bonn, Poppelsdorfer Schloss, 53115 Bonn, Germany,
[3] SEGEMAR & CONICET, Av. Julio A. Roca 651, 10◦ piso, 1322 Buenos Aires, Argentina,
[4] Department of Geosciences, University of Oslo, P.O. Box 1047, Blindern, 0316 Oslo, Norway,
[5] Géosciences-Rennes (UMR6118), CNRS et Université de Rennes 1, 35042 Rennes, France

In contrast to the classical concept of magma ascent in extensional settings, recent studies show that volcanism also occurs in compressional settings. The nature of the interplay between magmatism and tectonics in fold-and-thrust belts however, remains a major question, notably in active margins. The mechanisms of magma transport in such settings and whether magmatism affects tectonic deformation need to be addressed.

Therefore, we carried out detailed structural mapping and sampling of an intrusive complex: the Cerro Negro of Tricao Malal, Neuquén Province, Argentina. This intrusive system belongs to a magmatic province that intruded into the intensely deformed Agrio fold-and-thrust belt, located between 37°S and 38°S in the Argentinean foothills of the Andes. The fold-and-thrust belt has resulted from intense E-W shortening, and contains tight folds and thrusts, trending N-S. The intrusive complex crops out as a network of sills and dykes around a main intrusion, all of which are of andesitic composition.

The plumbing system of Cerro Negro is well exposed so that the structural relations between the intrusions and the tectonic structures can be studied. We have identified at least two generations of intrusions: two thick sills that predate or are coeval with deformation, and numerous sub-vertical dykes that strike N-S, i.e. perpendicular to the shortening.

We observed that the main intrusive body and the dykes have formed in a central anticline, the dykes being close to the hinge. Furthermore, the dykes crosscut folded sills, postdating all visible deformation. From the structural and temporal relationships between the anticline and the dykes, we infer that local stresses controlled the formation of the dykes during outer-arc stretching. This illustrates how tectonic deformation may control magma emplacement. Conversely, the traces of the main tectonic structures curve around the intrusive complex, suggesting that the latter influenced the tectonic deformation.

# Exhumation of subducted oceanic lithosphere at the South American convergent margin (Raspas Complex, Ecuador)

Ralf Halama[1], Petra Herms[1], Timm John[2], Volker Schenk[1], Dieter Garbe-Schönberg[1] and Folkmar Hauff[3]

*[1]SFB 574 and Institut für Geowissenschaften, Universität Kiel, D-24098 Kiel, [2]Institut für Mineralogie, Universität Münster, 48149 Münster, [3]GEOMAR, Wischhofstr. 1-3, 24148 Kiel*

High-pressure low-temperature (HP-LT) metamorphic rocks provide important information on the evolution of convergent margins and fossil subduction zones. In contrast to continental rocks, burial and exhumation of oceanic rocks have received relatively little attention. A global survey revealed that exhumed oceanic crust has typically experienced peak pressure conditions of <2.3 GPa, corresponding to depths of about 70 km, and is systematically associated with serpentinites that are relatively buoyant compared to dry mantle and provide the driving force for exhumation (Agard et al., 2009).

In the Andes of South America, HP-LT metamorphic rocks are conspicuously rare, demonstrating that exhumation of oceanic crust is almost impossible in this setting despite ongoing subduction for more than 150 million years. This has been attributed to fast subduction, which does not favor hydration of the mantle and causes dehydration to take place at greater depths (Agard et al., 2009). The Raspas metamorphic complex in southwest Ecuador is one of the few occurrences of HP-LT rocks at the South American convergent margin and one of the few HP ophiolites that contain the whole lithological sequence of a typical subducting slab (Feininger, 1980).

Most of the Raspas eclogites have trace element geochemical signatures similar to mid-ocean ridge basalts (MORB; John et al., 2010). These MORB-type eclogites exhibit Sr and O isotopic compositional differences on outcrop scale and Sr-Nd isotopic trends typical for seafloor alteration, interpreted to be inherited from variably altered oceanic crust (Halama et al., 2011). The serpentinized peridotites show major and minor elemental trends that reflect high degrees of melt depletion, consistent with trends observed for oceanic slab mantle. Some of the serpentinized peridotites have positive Eu anomalies and geochemically resemble oceanic serpentinites. The geochemical data provide evidence that the mafic and ultramafic rocks of the Raspas complex are of oceanic origin and experienced seafloor alteration.

Peak metamorphic conditions for eclogites and garnet-chloritoid-kyanite metapelites are overlapping at about 1.8-2.0 GPa and 550-600 °C (Gabriele et al., 2003; John et al., 2010). Serpentinized peridotites have experienced similar peak metamorphic temperatures because some samples are chlorite-tremolite harzburgites that exhibit pseudo-spinifex textures of orthopyroxene blades which formed due to deserpentinization at >600 °C. Hence, the Raspas Complex is one of the few locations worldwide where HP deserpentinization, thought to be a key factor for convergent margin magmatism, can be observed.

**References**

Agard, P., Yamato, P., Jolivet, L and Burov, E. (2009). Earth Sci. Rev. 92, 53-79.
Feininger, T. (1980). J. Petrol. 21, 107-140.
Gabriele, P., Ballèvre, M., Jaillard, E. and Hernandez, J. (2003). Eur. J. Mineral. 15, 977-989.
Halama, R., John, T., Herms, P., Hauff, F. and Schenk, V. (2011). Chem. Geol. 281, 151-166.
John, T. Scherer, E.E., Schenk, V., Herms, P., Halama, R. and Garbe-Schönberg, D. (2010). Contrib. Mineral. Petrol. 159, 265-284.

# Cosmogenic nuclides: applications in tectonic geomorphology

Ralf Hetzel

*Institut für Geologie & Paläontologie, Westfälische Wilhelms-Universität Münster, Corrensstr. 24, D-48149 Münster*

The permanent bombardment of the Earth by high-energy cosmic-ray particles generates cosmogenic nuclides such as $^{10}$Be, $^{26}$Al, $^{36}$Cl in near-surface rocks. The analysis of these nuclides allows dating a wide variety of landforms as well as determining erosion rates at the outcrop and catchment scale. With two field examples from the Andes and Tibet, I demonstrate how cosmogenic nuclides can be used to quantify the slip rates of active faults and to decipher the growth of fault-bounded mountain ranges.

The eastern margin of the Andean Precordillera is characterized by a high level of seismicity and several destructive earthquakes have occurred in this region during the last few hundred years. Using $^{10}$Be exposure dating of tectonically offset terraces and fault scarp profiles we quantified slip rates and coseismic displacements for two thrust faults: the Peñas and Cal faults near Mendoza (Schmidt et al. 2011a,b). At the Peñas fault, a terrace that is vertically offset by ~11 m has a $^{10}$Be age of ~12 ka. When combined with the fault dip of 25°, this age and the vertical displacement yield a Holocene shortening rate of ~2.0 mm/a, which is more than half of the current, GPS-based shortening rate in the Precordillera. At the Cal thrust fault farther south, the ages and offsets measured on three terrace levels indicate that slip on this fault has accelerated in the late Holocene (Schmidt et al. 2011b). At both thrust faults, the smallest vertical scarp offsets (0.8-1.0 m) are interpreted as coseismic displacements, which suggests that these faults are capable of producing magnitude $M_w$ ~6.9 earthquakes. This is corroborated by an earthquake on the Cal fault that destroyed Mendoza in 1861. As the Cal fault extends into the downtown area of Mendoza, this fault poses a serious seismic hazard to the one million inhabitants of the city (Salomon et al., in review).

Tibet, the world's largest plateau, continues to grow laterally at its northeastern rim, where initial mountain-building and plateau-forming processes can be studied (e.g. Hetzel et al., 2002; 2004). In this region, elongate mountains that are similar in shape but differ in length and local relief represent different growth stages of fault-bounded mountain ranges (Hetzel et al., 2004). One of these ranges – the 70-km-long Yumu Shan – is an isolated range bounded by an active NW-SE striking thrust fault. Fault scarps at the mountain front, wind gaps, and hanging paleo-catchments indicate that the Yumu Shan continues to grow laterally and vertically. Scarp profiles and $^{10}$Be exposure ages of deformed alluvial fans and fluvial terraces yield rock uplift rates of ~800 and ~500 mm/ka for the central and eastern parts of the range, respectively (Palumbo et al., 2009). Since the rock uplift rate in the central part of the Yumu Shan is higher than catchment-wide $^{10}$Be erosion rates of ~180 to ~280 mm ka$^{-1}$ (Palumbo et al., 2010), the mountain range has not yet reached an erosional steady-state and continues to grow. In contrast, mountain ranges in the higher and more interior parts of Tibet erode at rates up to ~800 mm/ka. Hence, this region has presumably attained an erosional steady state, in which rock uplift is balanced by erosion (Palumbo et al., 2011).

**References**

Hetzel, R., Tao, M., Niedermann, S., Strecker, M.R., Ivy-Ochs, S., Kubik, P.W. (2004). *Terra Nova* 16, 157-162.
Hetzel, R., Niedermann, S., Tao, M., Kubik, P.W., Ivy-Ochs, S., Gao, B., Strecker, M.R. (2002). *Nature* 417, 428-432.
Palumbo, L., Hetzel, R., Tao, M., Li, X. (2011). *Terra Nova* 23, 42-48.
Palumbo, L., Hetzel, R., Tao, M., Li, X. (2010). *Geomorphology* 117, 130-142.
Palumbo, L., Hetzel, R., Tao, M., Li, X., Guo, J. (2009). *Tectonics* 28, TC4017.
Salomon, E., Schmidt, S., Hetzel, R., Mingorance, F., Hampel, A. (in review). *Bull. Seismol. Soc. Am.*
Schmidt, S., Hetzel, R., Kuhlmann, J., Mingorance, F., Ramos V.A. (2011a). *EPSL* 302, 60-70.
Schmidt, S., Hetzel, R., Mingorance, F. and Ramos, V.A. (2011b). *Tectonics* 30, TC5011.

# How does the Okhotsk plate deform? Insights from 3d numerical modelling

David Hindle[1]

[1]*Institut für Geowissenschaften, Friedrich Schiller Universität Jena, D-07749 Jena*

The Okhotsk (Okh) plate is one of the last frontiers in tectonics. Sandwiched between the giant Eurasian (Eur) and North American (NAm) plates, the Eur-Okh-NAm triple junction lies almost coincident with the Eur-NAm pole of rotation. This causes increasing amounts of convergence to be presumably absorbed across Okh the further south one goes. North of the triple junction, the Eur-NAm plate boundary is formed by the Arctic spreading centres and ultimately the North Atlantic ridge.

How exactly Okh behaves in response to Eur-NAm convergence remains somewhat mysterious. There are several hypotheses (Hindle et al. 2006, 2009, 2011), but so far no clear evidence favouring any one of them.

This study uses 3 dimensional, distinct element, numerical modelling of the convergence process to try to understand the likely behaviour of Okh at the present day. The study uses the present day geometry of Okh, to delineate the lateral boundaries of the region, as well as inverting topography to give an approximation of crustal thickness, assuming Airy isostasy. The model has a layered, frictional rheology, and bounding fault frictions can also be varied to reflect different hypotheses about how slip is accommodated across the region. The model rheology is strain rate independent, and thus, instantaneous Airy isostatic equilibrium is the basal/surface boundary condition applied in the vertical direction.


Simulation geometry for Okhtosk plate – showing location of the region and also the 3d approach using a spherical radially oriented gravity vector, acting against a buoyant aesthenosphere/mantle lithosphere.

**References**

Hindle, D. et al. (2006). Geophysical Research Letters, 33, L02306, doi:10.1029/2005GL024814.
Hindle, D. et al. (2009). In D. B. Stone, K. Fujita, et al. (eds.). Stephan Mueller Spec. Pub. Ser. 4, 147-156.
Hindle, D. and Mackey K. (2011). Journal of Geophysical Research, 116, B02301 doi:10.1029/2010JB007409

# A numerical study of conditions during thin-skinned thrust initiation and propagation: the example of the Jura mountains

David Hindle[1] and Melanie Lohrmann-Bromm[1]

[1]*Institut für Geowissenschaften, Friedrich Schiller Universität Jena, D-07749 Jena*

Although the role of thin-skinned tectonics in the evolution of the Swiss, Jura-Molasse fold-thrust system is now well-established, a number of questions remain open regarding the detailed dynamics of their growth and emplacement.

The system represents the most external and latest deformation of the western Alps, forming between ~12 - 2.5 Ma. The Jura-Molasse consists of an "inverted", Tertiary Alpine foreland basin sequence, lying above Mesozoic, Tethyan margin sediments, mostly carbonates and marls, which are detached from the underlying, mostly Permo-Carboniferous "basement" by thick (up to 200m) accumulations of halite within Triassic evaporites. The geometry of the system was broadly wedge shaped, with a depocentre original depth to detachment of ~6.5km (Burkhard and Sommaruga, 1998) falling to less than 1km at the basin rim. It has recently been proposed (Hindle, 2008; Willett and Schlunegger, 2010) that this geometry, itself the result of flexural bending of the European lithosphere in response to loading by alpine orogeny, is the key to the mixture of stable sliding and active shortening that affected the Jura-Molasse over its history. At the largest scale, this may well be true, leading to a non-deforming, stable-sliding Molasse Basin region due to the steeper angle of its flexed basement, and a strongly shortened Jura mountains, external to this, lying over a lower dipping basement.

However, the detail of thrust formation, and sequencing is still ignored in these explanations. In fact, within the Jura chain itself, there are 3 distinct morpho-tectonic zones, the "Haute-Chaine" (easternmost, and a true, fold-thrust belt), the "Plateau Jura", a zone with little shortening and generally flat lying Mesozoic sequences, and most external, the "Faisceaux Jura", which are generally characterised as being narrow zones of intense deformation, but with a different structural style to the Haute Chaine. Quite how these zones can evolve has up until now remained unclear.

We present a numerical modelling study using a disinct element technique, into the mechanics of thrusting and sliding in the system. We use the restored geometry of the Jura-Molasse from Burkhard and Sommaruga (1998) and apply 25km shortening to it. Our model consists of a "weak" (friction angle ~5°-15°) Triassic detachment layer, a "strong" (friction angle ~25°-35°) Jurassic sequence, and an overlying "unconsolidated" but frictional Molasse. We find that the combination of weakness of the basal detachment and strength of the Jurassic (presumably Malm) layer is critical in determining the total number of anticlines formed, the degree of backthrusting, and the presence or absence of out-of-sequence evolution of structures, as well as the actual length/ amplitude of overthrusts/folds. The stable-sliding Molasse region by contrast appears, as predicted, to be little-affected by small changes in basal properties or material strength, and instead is controlled by the initial basin geometry prior to thrusting.

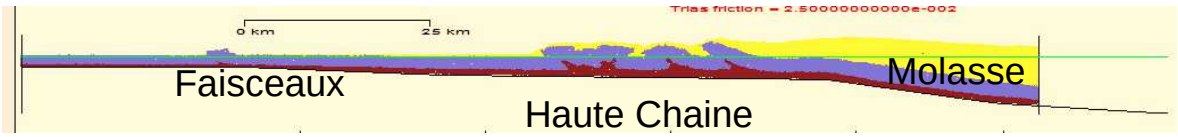


Simulation result with ~20km shortening. Haute Chaine, Plateau and Faisceaux units clearly developed. Note also backthrusting and stable-sliding Molasse.

**References**

Hindle, D. (2008). Swiss Journal of Geosciences, 101, 305-310.
Burkhard, M., Sommaruga, A. (1998). In Mascle A. et al. (eds.). Spec. Publ. Geol. Soc. London 134, 279-298.
Willett, S., Schlunegger, F. (2010). Basin Research, 22, 623-629.

# New Approach to Detect Possible Quaternary Tectonic Activity in the Alpine Foreland Basin, Southern Germany

Markus Hoffmann[1] and Anke M. Friedrich[1]

[1] *Department für Geo- und Umweltwissenschaften, Ludwig-Maximilians-Universität München, Luisenstraße 37, 80333 München, Germany*

The geomorphology of tectonically active regions is a recorder of climatic and geodynamic processes on different scales in space and time. One example of a complex landscape that is influenced by both, tectonic and climatic processes, is the northern Alpine foreland basin. In this basin lithospheric subsidence occurred throughout the Tertiary, but appears to have ended a few million years ago. Given a current geodetic velocity field of less than 1 - 2 mm/yr between the Eurasian plate and the Adriatic plate and a likely Euler pole location in the central or western Alps, active lithospheric deformation would be expected in the western and eastern Alps and their foreland basins, respectively. Thus, the goal of our project is to quantify the amount of deformation along the southern boundary of the Eurasian plate, despite the more dominant climatically induced geomorphic response.

In order to reconstruct the Quaternary tectonic and geomorphic record of the foreland basin region, we determined the tectonic boundary conditions on a regional scale. This first step of our analysis is mainly based on a synthesis of published subsurface fault traces inferred from published seismic reflection transects and boreholes. The seismic data cover depths ranging from 500 m to about 3,5 km below the surface, in Tertiary sediments. Hence, the end of tectonic deformation has been inferred to coincide with the upper bound of the seismic data. No data are available in younger deposits above 500 m. Therefore, it is presently unclear whether tectonic activity continued beyond the Pliocene. The Tertiary Hills region in the NE portion of the foreland basin is characterized by asymmetric hill slopes that are generally attributed to Pleistocene aeolian loess deposition and reworked river networks. However, as some of the basement-faults are located directly below the asymmetric hills, we currently cannot rule out a tectonic origin of this landscape.

Previous workers had attributed the pronounced asymmetry to climatic variations that caused asymmetric river network developments and therefore predetermined asymmetric surface pattern. From these observations we developed three approaches to test our hypothesis: (1) regional analyses of high-resolution topographic and subsurface data, (2) regional geomorphic investigation on river profiles, and (3) local shallow geophysical prospection. Our preliminary field mapping, river profile and DEM analyses and geophysical investigations are generally consistent with the interpretation referring to climatic processes as driving factor, but we propose that the observed geomorphology is also influenced by the structural framework of the basement faults and enables us to detect possibly results of local tectonic activity after the late Miocene. The detailed analyses is in progress and shows promising correlations between surface morphology effects that may have been caused by tectonic activity – providing an alternative interpretation of the observed morphology.

# Mineralogisch-geochemische Charakterisierung des Staßfurt-Hauptsalzes (Knäuelsalz bis Kristallbrockensalz) im Salzstock Gorleben

Hjördis Holler, Michael Schramm, Michael Mertineit and Jörg Hammer

*Bundesanstalt für Geowissenschaften und Rohstoffe, Stilleweg 2, 30655 Hannover*

Seit 1979 wird der Salzstock Gorleben als potentielles Endlager für wärmeentwickelnde Abfälle untersucht (Bornemann et al. 2008). Um Aussagen über die Langzeitsicherheit und die Eignung des Salzstocks als Endlager treffen zu können, sind u.a. umfangreiche Kenntnisse zur mineralogisch-geochemischen Zusammensetzung sowie zur Genese der Salzgesteine und besonders des als Wirtsgestein für die Endlagerung vorgesehenen Hauptsalzes erforderlich. Exemplarisch wurden an Proben des Hauptsalzes der Bohrung 02YER20 RB254 mineralogisch-geochemische, petrographische und rasterelektronen-mikroskopische Untersuchungen durchgeführt.

Mit Hilfe der ICP-OES wurden die Haupt- und Spurenkomponenten (Na, K, Ca, Mg, Cl, $SO_4$, Sr, Br) bestimmt und in Verbindung mit der XRD der quantitative Mineralbestand ermittelt. Der hieraus abgeleitete Bromidgehalt der Halite ist ein wichtiges Hilfsmittel zur genetischen Interpretation von Evaporiten (z.B. Braitsch 1962). Prinzipiell wird bei fortschreitender Meerwassereindunstung in charakteristischer Weise verstärkt $Br^-$ anstelle des $Cl^-$ in das Kristallgitter neu gebildeter Halite eingebaut. Anhand der Änderungen im Bromidgehalt kann festgestellt werden, ob eine ungestört progressiv fortschreitende Eindunstung, bzw. eine natürliche Abfolge der Schichten erhalten geblieben ist, metamorphe Prozesse stattgefunden haben oder ob eine Verfaltung bzw. Verschuppung der Schichten vorliegt. Zusätzlich wurde ein feinstratigraphisches Profil der Bohrung 02YER20 RB254 erstellt, um in Verbindung mit makroskopischen Untersuchungen und petrographischen Untersuchungen die Internstrukturen im Hauptsalz in diesem Bereich des Salzstocks zu erkunden.

Die Analysen ergaben, dass der Anhydrit-Gehalt vom liegenden und mittleren Teil des Hauptsalzes (Knäuel- und Streifensalz) zum Hangenden (Kristallbrockensalz) hin von durchschnittlich 5 auf 2 Gew.-% abnimmt. Im Gegensatz dazu steigt der Bromidgehalt vom Liegenden über den mittleren Teil zum Hangenden von 66,7 über 79,7 auf 136,9 µg/g Halit. Die Bromidwerte zeigen den Verlauf einer überwiegend progressiv fortschreitenden Eindunstung. Bei der Untersuchung der Dünnschliffe mit dem REM konnten neben den Mineralen Halit, Anhydrit und Polyhalit folgende akzessorische Minerale identifiziert werden: Albit, Baryt, Cölestin, Hämatit, Ilmenit Kalifeldspat, Kaolinit, Sylvin, Pyrit, Xenotim und Zirkon sowie gerundete und idiomorphe Quarze. In fast allen Dünnschliffen wurde mit Karbonat vergesellschafteter Anhydrit beobachtet. Eine mögliche Erklärung dafür ist, dass durch Transgression frisches, an Karbonat gesättigtes Meerwasser auf mit Anhydrit und Halit gesättigtes Meerwasser getroffen ist.

**References**

Bornemann, O., Behlau, J., Fischbeck, R., Hammer, J., Jaritz, W., Keller, S., Mingerzahn, G., Schramm, M. (2008): Standortbeschreibung Gorleben Teil 3: Ergebnisse der über- und untertägigen Erkundung des Salinars. Geologisches Jahrbuch, C73, 211 Seiten, 50 Abbildungen, 7 Tabellen, 7 Beilagen (5 Anlagen, 2. Tab.), Hannover.

Braitsch, O. (1962): Mineralogie und Petrographie in Einzeldarstellungen, Band 3, Kapitel: Entstehung und Stoffbestand der Salzlagerstätten. 232 S.; Springer; Berlin.

# Depth-dependent extension, two-stage breakup and depleted lithospheric counterflow at rifted margins

Ritske S. Huismans

*Dep. Earth Science, Bergen University, Bergen, Norway*

Uniform lithospheric extension predicts basic properties of non-volcanic rifted margins but fails to explain other important characteristics. Significant discrepancies are observed at ‘type I’ margins (such as the Iberia–Newfoundland conjugates), where large tracts of continental mantle lithosphere are exposed at the sea floor, and ‘type II’ margins (such as some ultrawide central South Atlantic margins), where thin continental crust spans wide regions below which continental lower crust and mantle lithosphere have apparently been removed. Neither corresponds to uniform extension. Instead, either crust or mantle lithosphere has been preferentially removed. Using dynamical models, we demonstrate that these margins are opposite end members: in type I, depth-dependent extension results in crustal-necking breakup before mantle-lithosphere breakup and in type II, the converse is true. These two-layer, two-stage breakup behaviours explain the discrepancies and have implications for the styles of the associated sedimentary basins. Laterally flowing lower-mantle lithosphere may underplate both type I and type II margins, thereby contributing to their anomalous characteristics.

# Control of reaction kinetics on mantle serpentinization and double Benioff zones

Karthik Iyer[1], Lars H. Rüpke[1,2], Ingo Grevemeyer[2] and Jason Phipps Morgan[3]

*[1]The Future Ocean, GEOMAR, Wischhofstraße 1-3, D-24148 Kiel, Germany, [2]SFB-574, GEOMAR, Wischhofstraße 1-3, D-24148 Kiel, Germany, [3]Department of Earth and Atmospheric Sciences, Cornell University, Ithaca NY 14853, USA*

The subduction of partially serpentinized oceanic mantle may potentially be the key geologic process leading to the regassing of Earth's mantle and also has important consequences for subduction zone processes such as element cycling, slab deformation, and intermediate-depth seismicity. Little is known about the quantity of water that is retained in the slab during mantle serpentinization (Billen, 2009). Recent studies using thermodynamical and/or experimental models of subduction zone processes have assumed that the mantle is uniformly serpentinized to a depth determined from the equilibrium stability of serpentine minerals in P-T space (e.g. Hacker et al., 2003). This approach yields an incomplete picture of the pattern of serpentinization that may occur during bending-related faulting; an initial state that is essential for quantifying subsequent dehydration processes. In order to provide further constraints on the pattern of hydration and the amount of water trapped in the subducting mantle, we build a 2-D reactive-flow model incorporating the kinetic rate-dependence of serpentinization based on experimental results (Martin and Fyfe, 1970). After simulating hydration processes at the trench outer-rise, we find that the water content in serpentinized mantle strongly depends on the age of the subducting lithosphere and subduction rate, with values ranging between $1.8 \times 10^5$ and $4.0 \times 10^6$ $kgm^{-2}$ reactive water uptake into the subducting mantle column. Serpentinization also results in a reduction in surface heat flux towards the trench caused by advective downflow of seawater into the reaction region. Observed heat flow reductions are larger than the reduction due to the minimum-water downflow needed for partial serpentinization, predicting that active hydrothermal vents and chemosynthetic communities should also be associated with bend-fault serpentinization. Model results agree with previous studies that the lower plane of double Benioff zones can be generated due to dehydration of serpentinized mantle at depth. The depth-dependent pattern of serpentinization including reaction kinetics predicts a separation between the two Benioff planes consistent with seismic observations (Brudzinski et al., 2007).

**References**

Billen, M.I., 2009. Tectonics: Soaking slabs. Nature Geosci, 2(11): 744-746.

Brudzinski, M.R., Thurber, C.H., Hacker, B.R. and Engdahl, E.R., 2007. Global Prevalence of Double Benioff Zones. Science, 316(5830): 1472-1474.

Hacker, B.R., Abers, G.A. and Peacock, S.M., 2003. Subduction factory - 1. Theoretical mineralogy, densities, seismic wave speeds, and H2O contents. Journal of Geophysical Research-Solid Earth, 108(B1): 26.

Martin, B. and Fyfe, W.S., 1970. Some experimental and theoretical observations on the kinetics of hydration reactions with particular reference to serpentinization. Chemical Geology, 6: 185-202.

# Archean UHT metamorphism and Paleoproterozoic reworking at Uweinat in the East Sahara Ghost Craton

Shreya Karmakar[1] and Volker Schenk[1]

[1] *Institute for Geosciences, University Kiel, 24118 Kiel, Germany*

The enigmatic East Sahara Ghost Craton lies in the northeastern part of Africa. It occupies the area between the Arabian-Nubian Shield in the East and the Tuareg Shield in the West and the Congo Craton in the South. Its northern margin is obscured under Phanerozoic cover. In its present status, it is neither a craton nor an orogenic belt in the classical meanings of the term (Bates and Jackson, 1980).

Previous geochronological and isotopic data indicate the existence of a craton prior to the Neoproterozoic orogenic events, possibly since the Archean. But the craton is thought to have decratonized during Neoproterozoic time (Black and Liegeois, 1993; Liegeois et al., 1994) or suffered repeated intense thermal events during Paleoproterozoic time (Bea et al. 2011). This decratonization is also supported by seismic tomography studies of Africa, which indicate the presence of a cratonic root below the Sahara Ghost Craton only to depths of about 150 km, while roots below the West African, Congo and Kalahari Cratons extend down to a depth of 250 km (Begg et al. 2009). The root beneath the Ghost Craton was separated from the crust possibly after thickening as a result of Neoproterozoic collisional events.

The Uweinat region is dominated by high-grade migmatitic gneisses and granulites of metapelitic, charno-enderbitic and mafic compositions, unconformably overlain by undeformed Phanerozoic sediments. All these metamorphic rocks are intruded by post tectonic granitoids and alkali-syenites; the latter forms ring complexes (Abdelsalam et al. 2002). Ultra-high-temperature metapelites from a locality between Jebel Uweinat and Jebel Kamil, occur in association with fuchsite-quartzite and BIFs, which are, in some places, interbanded with charnockitic gneisses. The metapelites are highly heterogeneous locally in their mineral assemblage and show a variety of multiphase reaction textures. The sequence of reactions, as deduced from inclusions in porphyroblasts, symplectites and corona assemblages, together with petrogenetic grid considerations record a P-T evolution with the following distinct stages: (1) Equilibration of initial ultra high T assemblages (Spr-Qz) in the deep crust (10-12 kbar) followed by near isobaric cooling. During cooling, sillimanite was transformed to kyanite. This resulted in the assemblage Grt+Sil/Ky+Opx+Spr co-existing with melt. (2) Subsequently, as a result of decompression, to 6-8 kbar, at ca. 1000°C (with some initial heating), a sequence of symplectite assemblages (Opx+Sil+Spr+Crd / Opx+Spr+Crd / Opx+Crd / Crd+Spl) developed at the expense of garnet, orthopyroxene and sillimanite. This stage of near isothermal decompression implies a rapid ascent of the metapelites to mid crustal depths. (3) Regrowth of garnet at the expense of symplectite assemblages and development of late biotite, sapphirine and orthopyroxene due to back-reaction of melt with residual garnet and symplectite minerals indicate a stage of near isobaric cooling. The second and third stages of the evolution are also supported by textures from the mafic granulites. Complete to partial replacement of garnet porphyroblasts by orthopyroxene and plagioclase symplectites, and clinopyroxene relicts within orthopyroxene represent the stage of near isothermal decompression, while the regrowth of garnet around the symplectite orthopyroxene grains represent the stage of isobaric cooling.

BSE Images and U-Th-total Pb dating of monazite grains reveal that the grains, occurring as inclusions within garnet, are compositionally homogeneous and have an apparent age of 2.6 ± 0.1 Ga. The grains occurring outside garnet, in the symplectite or matrix, show complex compositional zoning and are younger 1.9 ± 0.1 Ga, but sometimes with a core giving the older age. This indicates that the early part of the evolutionary history (1) occurred during Archean time at 2.6 ± 0.1 Ga; while the isothermal decompression of the granulites occurred during late Paleoproterozoic time at 1.9 ± 0.1 Ga. The assumed Pan-African decratonization is not reflected in the metamorphic history of the crust at Uweinat.

**References**

Abdelsalam, M.G., Gao, S.S., Liegeois, J.P. (2011). Journal of African Earth Sciences 60, 328-336.

Abdelsalam, M.G., Liegeois, J.P., Stern, R.J. (2002). Journal of African Earth Sciences 34, 119-136.

Bea, F., Montero, P., Abu Anbar, M., Talavera, C. (2011). Precambrian Research 189, 32-346.

Black, R., Liegeois, J.P. (1993). Journal of the Geological Society of London 150, 89–98.

Liegeois, J.P., Black, R., Navez, J., Latouche, L. (1994). Precambrian Research 67, 59–88.

Begg, G.C., Griffin, W.L., Natapov, L.M., O'Reilly, S.Y., Grand, S., O'Neill, C.J., Hronsky, J.M.A., Poudjom Djomani, Y., Swain, C.J., Deen, T., Bowden, P. (2009). Geosphere 5, 23–50.

# Impact cratering on Earth and on Mars: defining the impact trajectories by structural analysis

Thomas Kenkmann[1]

[1]*Institut für Geowissenschaften – Geologie, Albert-Ludwigs-Universität Freiburg, Albertstrasse 23-B, 79104 Freiburg, Germany, thomas.kenkmann@geologie.uni-freiburg.de*

Impact crater formation is a highly dynamic and complex geological phenomenon, and methods of structural geology are capable of giving insights into the details of the deformation processes that occur during crater formation from the nano to kilo-meter scale.

The impact process can be subdivided into three stages: (i) contact and compression, (ii) excavation (iii) modification. The initial hypervelocity impact of a body with a planetary surface generates a shock wave at the impactor-target interface. As a result, the impactor and a similar volume of target rocks are compressed to very high density, which raises the pressure and temperature of these materials. The amplitude of the excursion decays with distance travelled by the shock wave. Behind the shock wave, a rarefaction wave generated by reflection of the shock wave at the free surface (i.e., the rear of the projectile and the air-target interface), releases the compressed material from its high-pressure state. Shock wave compression is irreversible, whereas decompression is reversible; hence, the passage of the shock wave results in a net increase in temperature and particle velocity in the rocks. The residual velocity component in the target rocks after unloading from shock pressure is the most important aspect that distinguishes hypervelocity impacts from the low velocity impact of a projectile. It induces a material flow, the so-called excavation flow. This is directed outwards, away from the point of impact, which leads to the actual opening of a deep bowl-shaped cavity. Eventually, the excavation flow is halted and the cavity stops growing, when insufficient kinetic energy remains to displace the target against its own weight (gravity-dominated cratering) or against the cohesive strength of the target material (strength-dominated cratering). The resulting cavity at the end of the excavation stage is called the transient cavity and is typically 10-20 times the size of the projectile in diameter. The cross-sectional shape of the transient crater is often assumed to be a paraboloid with a depth-diameter ratio of roughly 1/3. While the excavation flow describes the motion of target material away from the impact center the modification flow is the reverse of this and acts to close the transient cavity. Gravity and buoyancy are the principal forces that drive the collapse of the transient cavity. Depending on the degree of modification, the final crater is classified into either a simple or complex morphology.

This contribution focuses on processes related to crater modification: Impact-induced deformations often exhibit a radial symmetry. Effects of impact obliquity on transient cavity modification and the associated sub-surface structure have long been neglected, or even ruled out, and have been investigated only recently. The geometry of the ejecta blanket was regarded as the only indicator to decipher azimuth and angle for an oblique impact. However, recently, the deep internal structure of the eroded crater floor and central uplift was tested as a tool to derive the impact vector. These terrestrial studies were combined with high-resolution remote sensing studies of Martian impact craters. It could be shown that the strike of upturned bedrock layers in central uplifts is on average perpendicular to the impact trajectory. Some statistical noise and bias can occur due to strata folding. The usefulness of strike orientation as an indicator for defining impact trajectories is validated and confirmed by the presence of asymmetric ejecta blankets and crater ellipticity. An uprange dip of strata is pre-dominant if layers are not in an upright position. This uprange dip is a consequence of stacking of tilted bedrock that experienced a top-downrange shearing. The main faults in central uplifts of oblique impact craters trend both parallel to the impact trajectory and perpendicular to it. Faults parallel to the trajectory are predominantly strike-slip faults, whereas those perpendicular to the trajectory are reverse or normal faults that accommodate the propagation of the central uplift center from uprange in downrange direction by imbricated stacking of inclined layers.

# Influence of viscous channel thickness on the development of overlying brittle deformation patterns under extension: new insights from analogue modeling

Ruth Keppler [1,3], Filipe Rosas [2] and Thorsten Nagel [1]

*[1] Universität Bonn, Steinmann-Institut, Poppelsdorfer Schloss, D-53115 Bonn, [2] Universidade de Lisboa, Faculdade de Ciências, Departamento de Geologia, Campo Grande, Ed. C6, 1749-016 Lisboa, Portugal, [3]Institut für Geowissenschaften, Universität Kiel, D-14098 Kiel*

The geometry of continental rifts is controlled by different factors, such as the rheological stratigraphy of the crust and the thickness of its layers. The influence of a ductile, mid-crustal layer on the extensional deformation pattern of the overlying brittle crust has been examined in previous analogue experiments (Brun et al. 1994, Tirel et al. 2006). These previous studies, however, only focus on the influence of the varying viscosity of this ductile layer, the strain rate and the amount of extension.

Through sand-silicone analogue experiments (see figure) we studied the influence of the varying thickness of a mid-crustal ductile layer on the extensional fault pattern in the upper brittle crust. Our models show that thinning of a lower ductile silicone layer (representing middle crust) is an effective way of delocalizing deformation in an overlying brittle sand layer (representing upper crust).

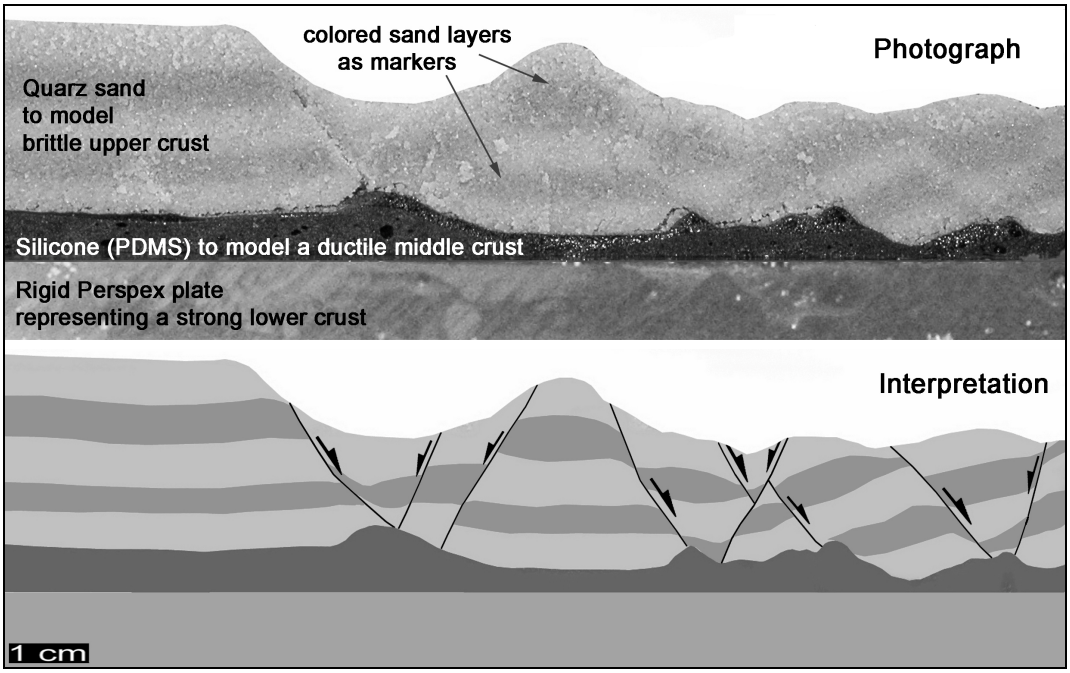


Figure shows photograph and interpretation of an experiment with a thin silicone layer after 36% of extension. Black lines show faults and fault movement.

The experiments involving thin viscous layers, hence distributed brittle fault patterns effectively simulate continental rifting of relatively cold, slow straining crust, including a brittle upper crust (sand), a thin ductile middle crust (silicone) and a strong lower crust (Perspex bottom of the experiment). Our experiments demonstrate that a distributed brittle deformation during extension can be achieved without gravitational collapse of a thermally modified continental crust.

**References**

Brun J.-P., Sokoutis, D. and Van Den Driessche, J. (1994). Analogue modeling of detachment fault systems and core complexes. Geology. 22, 319-322.

Tirel, C., Brun, J.-P., Sokoutis, D. (2006). Extension of thickened and hot lithospheres: Inferences from laboratory modeling. TECTONICS. 25, 1-13.

# The effect of preexisting joints on normal fault evolution – Insights from field work and analogue modeling

Michael Kettermann[1], Heijn van Gent[2], Christoph Grützner[3] and Janos Urai[1]

*[1]Structural Geology, Tectonics and Geomechanics, RWTH-Aachen University, Germany, [2]Shell Global Solutions, Rijswijk, the Netherlands, [3]Neotectonics and Natural Hazards, RWTH-Aachen University, Germany*

Huge hydrocarbon reservoirs worldwide are bound to brittle lithologies that are affected by interacting fracture networks. For a better prediction of reservoir qualities a basic investigation of such interactions is important. In this context, the present work aims for an understanding of the effect of preexisting joint sets on normal fault geometries. Methods used for this work include a field study, remote sensing and analogue modeling.

The Grabens Area of the Needles fault zone in the Canyonlands National Park, Utah/USA was chosen as field prototype. This arcuate array of young grabens (estimated to be younger than 100 ka) extends over several kilometers along the Colorado River in Permian brittle lithologies with distinct preexisting joint sets. The graben-bounding normal faults formed due to gravity-driven extension above Pennsylvanian evaporites. The well-preserved outcrops and the stratigraphic similarity to producing reservoirs make this region a perfect field analogue.

The work in this area included more than 70 ground penetrating radar (GPR) surveys along and across graben floors. Remote sensing of this area consisted of geographic information system (GIS)-based mapping of over 20,000 joints and 500 faults from high resolution orthoimagery as well as calculations of drainage pattern and dip directions from digital elevation models.

For the analogue modeling cohesive and very fine-grained hemihydrate powder was used as an analog for brittle lithologies. To create cohesionless open joints within the sensitive powder, sheets of paper were attached on strings inside the deformation box. The powder was then sieved in, embedding the sheets almost entirely. Finally the paper was carefully removed by using the strings, leaving thin open voids. In this work the angle between the strike of the joint-set and a defined basement-fault was incrementally changed between 0° and 25°. Analytic methods include high resolution time-lapse photography and particle imaging velocimetry (PIV) to analyze the spatial deformation patterns.

The GIS analysis revealed a correlation between joint and fault orientation. Sinkholes, mapped in airborne imagery and in the field, indicated steep-dipping dilational faulting close to the surface. This is consistent with the observation that graben walls coincide with original joint surfaces without slickenlines or toolmarks. Additional measurements of heave and throw at some outcrops allowed estimating fault dips at depth. The GPR surveys worked well for the upper 10 m of sediment and the interpreted profiles implied an ongoing horizontal extension as well as in some cases changing rates of displacement or sedimentation. The analogue models finally confirmed the findings that faults localize along the preexisting joints at the surface, requiring a change in fault geometry at depth. The models came up with very similar structures and features as observed in the field and airborne imagery. Hence, it could be shown that preexisting joint-sets do affect normal fault geometries distinctly.

**References**

Kettermann, M. (2011). The effect of preexisting joints on normal fault evolution – Insights from field work and analogue modeling. MSc thesis, RWTH-Aachen

# Dislocation creep of dry quartz

Kilian Rüdiger[1], Heilbronner Renée[1], Stünitz Holger[2], Andreas Kronenberg[3] and Caleb Holyoke[3]

*[1]Geological Institute, Basel University, Basel, Switzerland, [2]Department of Geology, Tromsø University, Tromsø, Norway, [3]Center for Tectonophysics, Texas A&M University, College Station, TX, USA*

Small scale shear zones formed during heterogeneous, amphibolite facies condition in the Truzzo granite in the Penninic Tambo nappe. Magmatic quartz grains recrystallized dynamically by subgrain rotation and grain boundary migration. The presence of a monoclinic shape fabric and a crystallographic preferred orientation are typical for deformation by dislocation creep. Dynamically recrystallized mean grain sizes vary between 200 and 750 µm which indicate deformation at at relatively low differential stresses (5 - 30 MPa).

Fourier-Transform-Infrared (FTIR) spectroscopy reveals water contents mostly below 200 H/10$^6$Si in the interior of recrystallized grains (in the form of discrete OH peaks and very little broad band absorption). This water content is in the range of values reported for dry Brazil quartz. Primary magmatic quartz grains contain fluid-inclusion-rich areas with a broad absorption band and higher water concentrations. Recrystallized grains are dry, except for postkinematic inclusion trails. These measurements present the first data on strictly intracrystalline water contents of dynamically recrystallized quartz in nature.

Dry quartz is extremely strong and does not deform by dislocation creep in deformation experiments at the low differential stress levels that would correspond to natural deformation. In contrast, deformation experiments on wet polycrystalline quartz have produced flow laws that can be extrapolated to natural conditions, which yield satisfying results.

This is in contrast with our data of the dry quartz deforming by dislocation creep at relatively low differential stresses at natural strain rates. Contrary to the conventional concept of recovery, our data and observations imply that quartz would be hardening as a consequence of grain boundary migration because fluid inclusions are expelled. The drainage of fluid inclusions and microstructures in the feldspar-mica matrix indicate that water during deformation was at least present in the grain boundary region.

FTIR measurements of natural deformed quartz reported in literature include grain boundaries and usually yield concentration of up to several 1000s H/10$^6$Si. Therefore it is concluded that either introduction of water into the deforming grains must have been transient or that the intragranular water concentrations, which are rheologically effective in the naturally deformed Truzzo granite, are much lower than those previously reported in the literature.

# The role of extraction and out-of-sequence thrusting of nappes for the exhumation of (ultra)high-pressure rocks - A case study from Lago di Cignana (Western Alps, Italy)

Frederik Kirst[1], Nikolaus Froitzheim[1], Thorsten Nagel[1], Bernd Leiss[2] and Jan Pleuger[3]

*[1]Steinmann-Institut, Universität Bonn, Poppelsdorfer Schloss, D-53115 Bonn, [2]Geowissenschaftliches Zentrum, Universität Göttingen, Goldschmidtstr. 3, D-37707 Göttingen, [3]Geologisches Institut, ETH Zürich, Sonneggstr.5, CH-8092*

In the Pennine Alps of Switzerland and Italy a stack of ocean- and continent-derived nappes from the Piemont-Ligurian paleogeographic domain is exposed. These are from bottom to top the eclogite-facies Zermatt-Saas zone, the greenschist- to blueschist-facies Combin zone and the polymetamorphic Dent Blanche nappe. Between the Zermatt-Saas zone and the Combin zone a pressure gap of 1.4 to 2.0 GPa exists. The Combin Fault, the contact between these two units, has been interpreted either as a large top-to-the-SE normal fault accommodating exhumation of the underlying (ultra)high-pressure rocks (Reddy et al., 1999) or as a major top-to-the-NW thrust (Ring, 1995). However, structural work in the Lago di Cignana area (Valtournenche, Italy) where a complete cross-section through this nappe stack is exposed shows that the Combin Fault is in fact a mixed extraction fault (Froitzheim et al., 2006).

The first deformation phase was probably characterized by top-to-the-NW shearing associated with burial of the units but structures related to this event are hardly preserved, except an internal foliation in Zermatt-Saas garnets. During subsequent nappe emplacement the Combin zone was thrust towards the NW over the Sesia/Dent Blanche block in the southeast and the Zermatt-Saas zone in the northwest leading to penetrative greenschist-facies deformation within the Combin zone with NW-SE striking stretching lineations. (U)HP-rocks of the Zermatt-Saas zone display E-W striking stretching lineations and top-to-the-(S)E shear bands which developed under high-pressure conditions and are interpreted to have formed during extraction of the overlying mantle wedge of the Sesia/Dent Blanche block to the (S)E. At the trailing edge of the extracting wedge the Zermatt-Saas and Combin zones came into direct contact. Ongoing NW-directed movement of the Combin zone, as supported by x-ray texture analyses of quartz mylonites from the base of the Combin zone, led to development of a top-to-the-NW greenschist-facies shear zone in the uppermost part of the Zermatt-Saas zone just above (U)HP-rocks. Subsequently, the Sesia/Dent Blanche nappe was thrust out-of-sequence towards the NW over the Combin zone. Mylonites from the basal contact of the Dent Blanche nappe, the Dent Blanche Basal Thrust, display diverse microstructures which are the result of this top-to-the-NW shearing event.

The proposed tectonic model and sequence of thrusting is able to explain the large pressure gap between the Zermatt-Saas and Combin zones and to provide a consistent tectonic scenario for the exhumation of Zermatt-Saas (U)HP-rocks. Structural work in the Lago di Cignana area suggests that the Combin fault represents a mixed extraction fault which developed as a result of extraction of the Sesia/Dent Blanche mantle wedge to the (S)E. Afterwards, the Sesia/Dent Blanche nappe was thrust out-of-sequence over the Zermatt-Saas and Combin zones leading to its present-day structural position on top of the nappe stack.

**References**

Froitzheim, N., Pleuger, J. and Nagel, T.J. (2006). J. Struct. Geol. 28, 1388-1395.
Reddy, S.M., Wheeler, J. and Cliff, R.A. (1999). J. Met. Geol. 17, 573-589.
Ring, U. (1995). Geol. Rundsch. 84, 843-859.

# Two plates many subduction zones: The Variscan orogeny reconsidered

Uwe Kroner[1] and Rolf L. Romer[2]

[1] *TU Bergakademie Freiberg, Department of Geology, B. v. Cotta Str. 2, D-09596 Freiberg,*
[2] *Deutsches GeoForschungsZentrum GFZ, Telegrafenberg, D-14473 Potsdam, Germany*

The Variscides of Central Europe are the result of the convergence of the plates of Gondwana and Laurussia in the Paleozoic. This orogen is characterized by the juxtaposition of blocks of continental crust that are little affected by the Variscan orogeny separated by high strain zones containing the record of subduction-related processes. Traditionally the high strain zones are interpreted as former active plate boundaries between one or more postulated microplates sandwiched between the two major plates. Contrastingly, paleo-bio-geographic constraints in combination with geochemical and isotopic fingerprints of the protoliths implicate that the Variscides are the result of the exclusive interaction of the two plates of Gondwana and Laurussia.

Here we combine the two-plate approach with a three stage geodynamic scenario comprising an oceanic subduction stage followed by intracontinental accretion-subduction processes and finally by orogenwide transpressional tectonics. This model gives a consistent explanation for the spatial arrangement of the continental blocks essentially unaffected by Variscan orogenic processes, the intracontinental subduction zones, and the sequence of deformational, magmatic, and metamorphic events. Furthermore, it explains the coexistence of marine basins close to orogenic domains with contemporenous (U)HP metamorphism in the internal sections of the orogen.

The present lobate shape of the Variscan orogen is the result of oblique convergence between the decoupled Iberian and Saxothuringian subplates and Laurussia during the transpressional stage of the orogeny.

# On the scale-invariance of fractures

Michael Krumbholz[1,2]; Steffi Burchardt[1,2]; David C. Tanner[3]; Christoph Hieronymus[1] and Hemin Koyi[1]

[1] *Department of Earth Sciences, Uppsala University, Villavägen 16, 75236 Uppsala, Sweden*
[2] *Geoscience Centre Göttingen, Georg-August Universität, Goldschmidtstraße 1-3, 37077 Göttingen, Germany*
[3] *Leibniz Institute of Applied Geophysics, Stilleweg 2, Hannover, Germany*

Studying the statistical distribution of fracture dimensions, as well as their spatial distribution, is of great importance in many fields of applied geology, e.g. to determine the quality of fractured reservoirs for geothermal energy or CO2 sequestration. Commonly, the study of fracture systems is restricted to small areas and a limited range of scales due to the size of the accessible outcrops or samples, but also by the resolution of the measuring method. In addition, fractures and fracture systems can frequently be studied only in two dimensions, i.e. only fracture trace lengths are measured.

Fracture properties (i.e. length and width) are commonly assumed to be scale-invariant within a certain range, i.e. they follow a power-law distribution. Therefore, knowing the fractal dimension of the size distribution of a given property within a fracture population, allows conclusions to be drawn from an accessible scale to another, inaccessible scale.

We studied fracture trace lengths and patterns at hand-specimen-, outcrop-, and map scale, which cover a large area of the Transscandinavian Igneous Belt. The dataset comprises 11 fracture maps that contain 8641 fracture trace lengths.

In addition to the power-law distribution, we tested the fracture trace lengths for a number of other statistical distributions (log-normal, exponential, Rayleigh, Chi-square, and Weibull). First, we transferred the probability density functions of each dataset to cumulative frequency distribution functions to avoid arbitrariness in bin sizes. With a non-linear, least-square fit we calculated the parameter(s) of the distribution function. The goodness-of-fit was evaluated using three methods: (1) the residual sum of squares, (2) the Kolmogorov-Smirnov statistics, and (3) p-values using 10,000 synthetic datasets. To determine the fractal dimension of the fracture pattern we used the standard box-counting method.

The statistical tests showed that each individual dataset is best described by a log-normal distribution. However, scaling up the different datasets to a common cumulative frequency distribution indicates that the fracture trace lengths follow a power law with a fractal dimension of about 1.8 over about 8 orders of magnitude. The variation between the log-normal distribution observed at hand-specimen, outcrop, and map scale and the power law for a combination of all scales may result from censoring effects due to (1) the shape of individual fractures, (2) their probability of intersecting the outcrop surface, as well as (3), the level of intersection of fracture and outcrop surface.

Analyses with the box-counting method show that the fracture patterns are not scale-invariant. The box-counting dimension increases with increasing scale because it is a measure of the complexity and maturity of a fracture system, which increases with scale. Consequently, the complexity of fracture pattern is scale-variant.

# Recent stress directions in basement rocks of southern Sweden deduced from open microcracks – first results

Michael Krumbholz[1,2] and Axel Vollbrecht[2]

*[1]Department of Earth Sciences, Uppsala University, Villavägen 16, 25236 Uppsala, Sweden, [2]Geoscience Center of the Georg-August University Göttingen, Goldschmidtstr. 3, 37077 Göttingen, Germany*

Microcracks in rocks are indicators for crustal stresses. Due to the fact that the tensile strength of minerals is lower than their shear strength the majority of microcracks should be of Mode 1 (extensional) type (e.g. Kranz, 1983). These microcracks should, regardless of driving forces and crack mechanisms (e.g. Vollbrecht et al., 1998), propagate perpendicular to the minimum principal compressive stress direction (σ3). Thus, the frequently developed steeply dipping cracks should be oriented normal to the least horizontal normal stress (σh) and parallel to the maximum horizontal normal stress (σH), respectively. Consequently, open microcracks that generally represent the latest generation of microcracks should reflect the (sub)-recent maximum horizontal stress direction.

We determined the strike direction of open microcracks in granitic and metasedimentary rocks from 5 localities distributed over an area of about 160 $km^2$ in the Precambrian basement of southern Sweden. The orientation of microcracks was determined separately for quartz and feldspar grains on polished horizontal slices of oriented samples.

For the whole area, microcracks display a pronounced preferred NW-SE strike. The deduced direction of σH (136°) correlates with published data of in-situ stress measurements and focal plane solutions in the area. Microcracks in samples taken close to large-scale faults, that are expected to have been recently active due to isostatic uplift, show no deviations from this common stress direction, holding either for small-scale fault-related stress reorientations only or indicating that local stress relieve was completely accommodated along pre-existing, open macrofractures.

**References**

Kranz, R.L. (1983). Tectonophysics 100, 449-480.

Vollbrecht, A., Duerrast, H., Schild, M., Szagun, U. and Siegesmund, S. (1998). Euroconference on Earth Stress and Industry – The World Stress Map and Beyond, Sept. 3-6, 1998, Heidelberg, Germany, Abstracts, p. 44.

# Evidence for coseismic rupture in a low-strain intraplate rift (Lower Rhine Embayment, central Europe)

Simon Kübler[1], Anke M. Friedrich[1] and Manfred R. Strecker[2]

[1]*Department für Geo- und Umweltwissenschaften, Geologie, LMU München, Luisenstraße 35, 80335 München,*
[2]*Institut für Erd- und Umweltwissenschaften, Universität Potsdam, Karl-Liebknecht-Str. 24-25, 14476 Potsdam-Golm*

The spatio-temporal recurrence pattern of destructive earthquakes represents one of the most enigmatic problems in intraplate earthquake geology. Low-strain intraplate rifts such as the European Cenozoic rift system (ECRS) are subject to considerable seismic hazards, because fault activity is highly disparate in space and time and our knowledge about the recurrence of large earthquakes is still rudimentary. Particularly in the Lower Rhine Embayment, the NW branch of the ECRS, it has been debated whether earthquakes can be large enough at all to cause surface rupture or if displacement along fault scarps is rather accomplished by steady, aseismic creep.

We present new results of a trench study that reveals seismogenic ground rupturing associated with the ML 6.2 ± 0.2 Düren earthquake, Germany's largest historical earthquake. This is the first evidence of coseismic ground rupturing in this part of Europe on centennial time scales. At the trench site, the fault is covered by <5 m-thick Holocene fluvial gravel and flood deposits overlaying Devonian shale. We mapped a surface offset of ~1 m and a ~10 m wide zone of localized deformation expressed by abundant fractures with aligned and broken clasts affecting the entire gravel. Mapping of 237 fractured clasts and the long-axis orientation of ~10.000 clasts defines a deformation zone coinciding with the surface offset and two offset markers within the gravel layers.

We interpret these features as the result of coseismic deformation at the near-surface end of the rupture. We rule out alternative processes which may lead to fracturing of pebbles such as freeze-thaw weathering or sediment loading effects, since both the gravel fabric and fracture planes coincide well with the fault orientation. We preclude slow deformation due to aseismic creep as governing process to cause rupturing of pebbles this close to the surface, as this would require an overburden stress of several hundreds of meters according to modelling results (e. g. Eidelmann, 1992). With a significantly smaller overburden, as in this study, a high differential acceleration force, such as a shock wave produced by an earthquake rupture or a seismic wave would be needed to overcome the pebble's shear resistance. Preliminary radiocarbon data bracket the youngest event horizon to Latest Holocene age.

In conclusion, we identified coseismic deformation at the trench site, because special conditions produced a number of features not usually observed in other fault exposures. The thin sedimentary cover (<5 m) above basement rocks and the high groundwater table, which may reduce the shear strength of the pebbles, may have played an important role in producing this deformation pattern. our study emphasizes that ground rupturing earthquakes can be produced by normal faults in the European rift system. This fact has to be taken into consideration for future attempts to improve earthquake hazard assessments of the region.

**References**

Eidelmann, A., Z. Reches, Fractured pebbles - a new stress indicator. *Geology* **20**, 307 (1992).

# Texture analysis of mylonitic marbles from the Rhodope Metamorphic Core Complex (Greece) – A preliminary study in view of its kinematic evolution

Rebecca Kühn[1], Bernd Leiss[1] and Markos Tranos[2]

*[1]Geowissenschaftliches Zentrum der Universität Göttingen, D-37077 Göttingen, [2]Department of Geology of the Aristotle University of Thessaloniki, GR-54124 Thessaloniki*

The Rhodope Metamorphic Core Complex (RMCC) located in Northern Greece is the most prominent feature of the Hellenic hinterland. It is the screen exposure of the Pangeon Unit (PU) of the Rhodope Massif underneath the Serbomacedonian Massif along the Strymon Line (or Strymon Valley detachment) and underneath the higher metamorphic Sidironero Unit (SU) of the Rhodope Massif along the Nestos shear zone.

The PU consists of massive marbles, which upwardly intercalate with several horizons of schists, whereas the SU mainly consists of migmatic gneisses, amphibolites, orthogneisses, mafic and scarce ultramafic rocks. The exposed rocks of the Pangeon Unit indicate intense shearing towards SW and appear in NE–SW–trending narrow strips due to the tertiary NE–SW trending isoclinal, recumbent D1-folds and the similarly trending NE–SW large open buckle D2-folds.

The formation of the RMCC is attributed to the tertiary orogenic or late-orogenic processes. However, the time-related precise onset and mechanism under which the RMCC has been formed and developed remains as an unsolved problem. The brittle deformation suggests that the post-orogenic extension generally began in the Late Miocene by following a late Oligocene transpressional regime driven by the late collision between Apulia and Eurasia plates. In contrast, the ductile deformation suggests that the orogen collapse after the collisional stacking was responsible for the formation of the RMCC.

This contradiction inferred from the brittle and ductile structures of the region forces us to figure out if a quantitative fabric analysis with the focus on the crystallographic preferred orientations (textures) of the PU-marbles can contribute to a better understanding of the kinematic development of the RMCC. For this reason, five representative mylonitic marble samples from the PU have been sampled in the Lekani Mts. along a 25-km-long sampling section oriented normal to the Strymon Line and the Nestos shear zone, as well as normal to the large megafolds. X-ray texture analyses were applied with a diffractometer setup especially designed for rock samples (e.g. large measurable sample volumes).

Microstructure analyses revealed grain sizes ranging from about 0.04 mm to 1 mm. Three samples show a heterogeneous distribution with alternating fine and coarse-grained layers. Four samples display an oblate and one sample a prolate grain shape, all samples with the long axes parallel to the mylonitic foliation. In all samples grain boundaries are interlobate, sutured or amoebeous. Twinning occurs most pronounced in three samples. Some samples show small amounts of quartz and mica.

All samples show two different and distinctly developed texture types with different orientations in respect to the mylonitic foliation. Type A is defined by an axial symmetric c-axes point maximum which can be oriented nearly parallel to the foliation normal or tilted with or against the mineral lineation. Texture type B shows c-axes as a well-developed girdle distribution around the mineral lineation with a maximum normal to the mylonitic foliation.

The differently developed calcite texture types and their varying directional relationship in respect to the mylonitic foliation as well as the differently developed microstructures demonstrate in this first study, that local kinematic characteristics are preserved in the marbles of the Lekani Mts. and that a more systematic study can significantly contribute to the analysis of the deformation history of the Rhodope Core Complex.

# Alpine HP-metamorphism in orthogneisses from the Adula nappe (Lepontine Alps)?

Robert Kurzawski, Thorsten Nagel, Sascha Sandmann and Jacek Kossak

*Steinmann Institut für Geologie, Mineralogie und Paläontologie. Universität Bonn. Poppelsdorfer Schloss, 53115 Bonn*

The Adula Nappe in the Central Alps represents the former most distal portion of the European continental margin, which got subducted in the Eocene and reached eclogite-facies conditions.

So far, HP conditions have been identified in eclogites, garnet peridotites which occur as lenses in metapelitic bands. All these units are intensely deformed together with layers of various orthogneisses without obvious HP-indicators. It is unclear whether (1) orthogneisses completely reequilibrated after exhumation from HP-conditions, (2) got subducted but did not equilibrate at depth, or (3) never experienced such conditions and rather got juxtaposed against the unambiguous HP-shists during exhumation in the subduction channel. Recent studies suggest that the Adula Nappe has been subducted and exhumated as a coherent block during the alpine orogenic cycle (e.g. Herwartz et al. 2011).

We search for evidence of HP conditions in orthogneisses from the central Adula Nappe (Alp de Ganan, Fig. A). In the study area, orthogneisses occur as 1 to hundreds of meters thick layers welded together with garnet-phengite schists enclosing perfectly fresh eclogites. White mica inclusions in K-feldspar porphyroclasts from augengneisses show enriched Si contents up to 3.5 Si cations p.f.u. in contrast to distinctly lower contents in matrix crystals. Additionally, large matrix grains show zonation with increasing Si-content towards the core (Fig. B). Such phengitic mica is generally accepted to represent HP-conditions and may be used for geobarometry. These first petrological hints support our working hypothesis that orthogneisses have experienced HP-conditions together with the eclogite bearing metapelitic successions. We propose that the Adula Nappe has been subducted and exhumated as a coherent block.

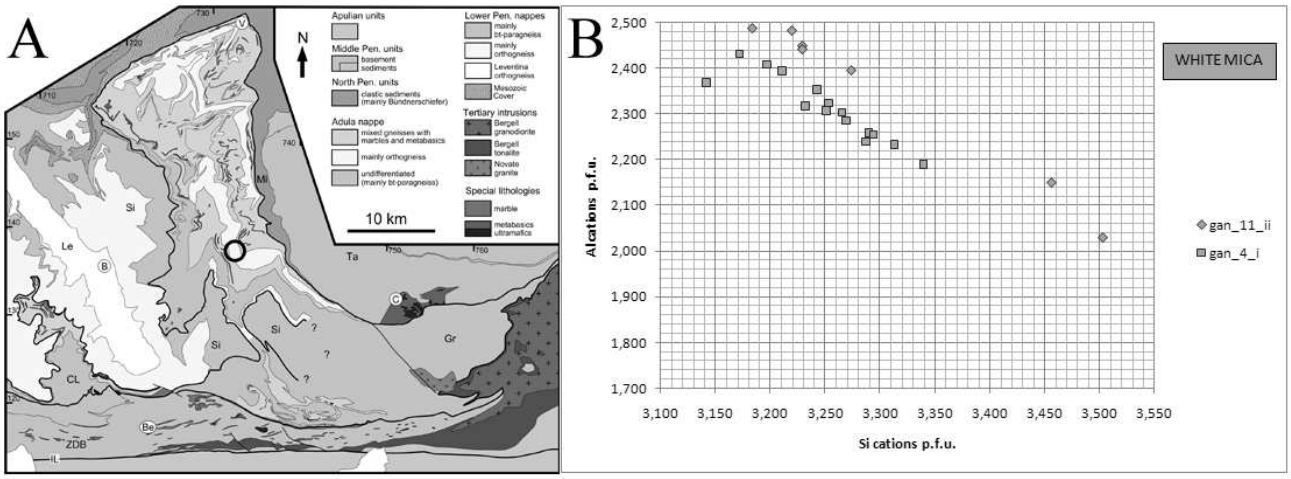


A: Tectonic overview map of the Adula Nappe (circle indicates the location of the working area). B: Al vs. Si content p.f.u. in phengite from two augengneiss samples. Diamonds represent single matrix grains with low Si content and inclusions in K-feldspar with high Si. Squares show a zoning pattern of one big mica crystal. The Si-content increases towards the core.

**References**

Herwartz, D., Nagel, T.J., Muenker, C., Scherer, E.E. and Froitzheim, N. (2011). Nature Geoscience 4, 178-183.

# Joint patterns and vein formation in a fractured carbonate reservoir analogue, Eifel, Germany

Dennis Laux[1], Tomas Fernandez-Steeger[2], Philippe Muchez[3] and Christoph Hilgers[1]

*[1]Energy- & Mineral Resources Group, Department of Reservoir-Petrology, RWTH Aachen University, Wüllnerstrasse 2, 52056 Aachen, Germany, [2]Department of Engineering Geology and Hydrogeology, Lochnerstrasse 4-20, 52056 Aachen, Germany, [3]Division of Geology, K.U. Leuven, Celestijnenlaan 200e - box 2408, 3001 Heverlee, Belgium*

The study area is located at the frontal part of the NE-SW striking Variscan fold-and-thrust belt, which is truncated by Mesozoic to Cenozoic NE-SW normal faults. Multiple quarries expose Variscan Carboniferous dolo- and limestones, one of them truncated by the seismically active Sandgewand normal fault. In this study, we present results from a quarry located in the footwall of the Sandgewand normal fault. The rocks were affected by several fluid pulses, as displayed by multiple generations of veins. We aim to better constrain the joint sets and up-scale the distribution of joints and faults from cm- to regional scale. Results will be integrated with the fluid history as displaced by vein to better constrain the structural diagenesis in carbonate rocks.

Major joint sets strike NE-SW (parallel to the folds of the Variscan orogeny), NW-SE (parallel to the recent stress direction and the normal faults), E-W and ESE-WNW (both associated to the recent maximum dextral shear-stress). ENE-WSW striking sets are associated with transfer faults. NNW-SSE striking sets only appear near the Sandgewand-fault and are associated with the equal orientated subvertical veins in the quarry.

Joints appear to rotate towards the Sandgewand-fault, suggesting a strike slip component on that fault. Major faults have been observed in the Hastenrath quarry by integrating virtual planes in our laser scans. Their direction continuously changes towards the Sandgewand fault. To prove the accuracy of the joint orientations derived from terrestrial laser scans (LIDAR), we compared such data with traditional geological compass measurements and smartphone measurements (using the app Rock-Logger on Motorola Defy). Data derived with the mobile app have been shown to match well with traditional techniques.

Large >10 cm wide veins cut vertically through the quarry wall over several meters and are filled with calcite, galena, dolomite and sphalerite. Fluid inclusion measurements have homogenization temperatures of 45-84°C. This indicates a depth of 1.5 to 2.25 km for the generation of the veins. The fluid composition shows a NaCl-$CaCl_2$ brine. Large veins are only found in the vicinity (<30m) and strike parallel to the main Sandgewand-fault. Multiple sealing events were dated in a single vein at 170±4Ma, followed by a second sealing event at 134±2Ma (Schneider et al. 2007).

# Erkundungsmaßnahmen zum tiefengeothermischen Potential der Leinetalgrabenstruktur

Bernd Leiss[1], David C. Tanner[2], Axel Vollbrecht[1], Till Heinrichs[1], Gernot Arp[1] und GGG[1*]

*[1]Geowissenschaftliches Zentrum der Universität Göttingen, D-37077 Göttingen, [2]Leibniz-Institut für Angewandte Geophysik, D-30655 Hannover, [*]GeothermieGruppeGöttingen*

Im Rahmen regionaler energiepolitischer Ziele, die Anteile erneuerbarer Energien in den nächsten 30 Jahren auf bis zu 100% zu erhöhen, spielt die Frage nach tiefengeothermischen Potentialen eine zunehmende Rolle. Die Stadt Göttingen liegt im Bereich des östlichen Hauptstörungssystems der generell N-S-streichenden Leinetalgrabenstruktur, so dass für den Stadtbereich bzw. die Region insbesondere die Frage nach dem störungsgebundenen tiefengeothermischen Potential im Fokus steht (Leiss et al. 2011a).

Kenntnisse zur Raumlage, Geometrie und Reichweite der Störungssysteme des Leinetalgrabens basieren bislang nahezu ausschließlich auf Kartierungen, da es in der Region nur wenige tiefe Bohrungen (max. 1500 m) gibt und keine verwertbare Seismik vorliegt. Aufgrund des Stockwerkbaus aus (a) variszischem Grundgebirge, (b) Zechsteinlager (in ca. 800 bis 1000 m Teufe Graben-Ostschulter) und (c) mesozoischem Deckgebirge, ergibt sich die Frage, ob die Störungssysteme des Deckgebirges im Zechsteinsalinar mechanisch entkoppelt sind oder sich bis in geothermische Zielhorizonte des Grundgebirges fortsetzen. Die im Deckgebirge beobachtete Verknüpfung von Dehnungs- und Kompressionsstrukturen kann durch unterschiedliche kinematische Entwicklungsmodelle erklärt werden, z. B. durch eine zweiphasige inversionsüberprägte Dehnung (Tanner et al. 2010) oder durch ein einphasiges ‚Pull-Apart'-Modell (Vollbrecht und Tanner 2011). Aktuelle Arbeiten z. B. zur Rekonstruktion von Paläospannungssystemen (Nikolajew et al 2012) und zur strukturellen 3D-Modellierung (Großmann et al. 2012, Werner et al. 2012) dienen u.a. der Prüfung dieser Modelle (s.a. Leiss et al. 2011b).

Um die strukturellen Beziehungen zwischen den o.g. tektonischen Stockwerken zu klären und damit das tiefengeothermische Potential besser quantifizieren zu können, sollen zwei senkrecht zueinander stehende reflexionsseismische Profile mit einem Tiefgang bis zum anvisierten geothermischen Zielhorizont im variszischen Grundgebirge, d.h. bis in eine Tiefe von ca. 5000 m realisiert werden. Der Verlauf der beiden NW-SE bzw. NE-SW Profile ist dabei so gewählt, dass idealerweise die Raumlage sowohl der variszisch streichenden Strukturen, als auch der Tiefenverlauf der jüngeren NNE-SSW-streichenden Haupt- und WNW-ESE-streichenden Querstörungssysteme im Deckgebirge abgeleitet werden kann.

**Referenzen**

Großmann, J., Leiss, B., Tanner, T. (2012). Abstracts TSK 14 Kiel, S. 45.

Leiss, B., Tanner, D., Vollbrecht, A. und Wemmer, K. (2011a). In Leiss, B., Tanner, D., Vollbrecht, A. und Arp, G. (Hrsg.). Universitätsdrucke Göttingen 2012, 163-170.

Leiss, B., Tanner, D., Vollbrecht, A. und Arp, G. (Hrsg., 2012b). Universitätsdrucke Göttingen 2012, 170 S.

Tanner, D.C, Leiss, B., Vollbrecht, A. und die GGG (2010). ZDGG, 161/4, 369-377.

Nikolajew, Ch., Vollbrecht, A., Leiss, B. und Kerkhof, A. v. (2012). Abstracts TSK 14 Kiel, S. 77.

Vollbrecht, A. und Tanner, D.C. (2011). In Leiss, B., Tanner, D., Vollbrecht, A. und Arp, G. (Hrsg.). Universitätsdrucke Göttingen 2012, 9-15.

Werner, H., Leiss, B., Heinrichs, T., Tanner, D.C. (2012). Abstracts TSK 14 Kiel, S. 110.

# Numerical investigation of stresses in sinking carbonate stringer in salt body

Shiyuan Li, Steffen Abe and Janos Urai

*Structural Geology, Tectonics & Geomechanics, RWTH Aachen University, Lochnerstr. 4-20, 52056 Aachen, Germany*

A large number of salt bodies contain layers of carbonate material, often called 'stringers'. These stringers have stresses inside them due to the bending deformation caused by gravitational loading and viscous drag due to the salt flow around the stringer. Detailed knowledge of the internal stresses in the stringers could have significant implications for example, for structural interpretation and the assessment of drilling risks. An important question which remains to be investigated is how those stresses depend on the depth location of the stringer in salt body.

In this work, we set up a numerical model using the Finite Element Modeling (FEM) package ABAQUS to simulate a stringer sinking in a block of salt. The model consists of a stringer passively sinking inside a large (6000m high and 10000m wide) salt body due to density contrast between salt and carbonate. Using this model, the stresses inside the stringer are observed for different depth location of the stringer.

Results show that the distribution of horizontal stresses in the sinking stringer is strongly dependent on its depth location. If the stringer is in a deep position (near the bottom of the salt body), the horizontal stress near the top of the central part of the stringer is less compressive than the vertical stress and the reversed situation occurs near the bottom of the central part. However, in the shallow position (near the middle part of the salt body), the horizontal stress near the bottom of the central part of the stringer is less compressive than the vertical stress and the reversed situation occurs near the top of the central part. Using the numerical models the difference between vertical and horizontal stress in the stringer is calculated quantitatively and the depth location where the horizontal and vertical stress generally are equal inside the stringer can be determined.

# Mechanical behaviour of anhydrite rocks: results of field investigations and mineralogical-geochemical studies

Michael Mertineit[1,2], Joachim Behlau[1], Jörg Hammer[1], Michael Schramm[1] and Gernold Zulauf[2]

*[1]Bundesanstalt für Geowissenschaften und Rohstoffe, Stilleweg 2, D-30655 Hannover, [2]Goethe-Universität Frankfurt/Main, Altenhöferallee 2, D-60438 Frankfurt/Main*

Understanding deformation behaviour of salt rocks is important for several purposes, e.g. rocksalt mining, cavern industry, or construction of a radioactive waste repository. In Germany Permian rocksalt, particularly the z2 sequence of the Stassfurt unit, is regarded as an appropriate host rock for highly active nuclear waste. The composition of different units, particularly the z3 sequence of the Leine unit, is characterized by stratigraphically and locally changing amount and number of anhydrite layers. For long-term safety considerations, the mechanical behaviour of these anhydrite layers and their capacity to store and transmit saline solutions in fissures and faults should receive attention.

The studied anhydrite samples were collected from the Morsleben salt structure and from the Gorleben salt dome, both in Northern Germany. In Morsleben, anhydrite rocks from the Anhydritmittelsalz (z3AM) were analysed. The Anhydritmittelsalz is characterized by a rhythmic stratification of rocksalt and anhydrite layers. The anhydrite layers are up to 2.5 m thick (Behlau & Mingerzahn 2001). In Gorleben the so-called Gorleben-Bank of the middle Orangesalz (z3OSM) has been studied. The Gorleben-Bank is an anhydrite bearing bed with an overall thickness of 3.5 to 70 cm (Bäuerle 2000).

The anhydrite rocks of both localities are strongly deformed by folding, boudinage, thrusting, fracturing, and formation of shear bands. Fissures and boudin necks are filled with salt, basically halite and carnallite containing high amounts of fluid inclusions. The bromide content of halite in boudin necks differs clearly from the bromide content in the surrounding rocksalt (difference ca. 40 µgBr/g halite). The reason is that metamorphic intrasalinare brines are involved in the rocksalt flow resulting in changes in the bromide content.

In fold hinges veil-like opaque phases occur. In these areas granular anhydrite crystals are very small (grain size < 50 µm). Similar features can be recognized close to the boundary anhydrite boudin – rocksalt. The grain size is also very small, and high amounts of opaque phases are present. Compared to folds, shear bands are common and clearly pronounced. The small grain size and the development of the opaque seams probably result from pressure solution, while the slightly soluble opaque phases remain at place, and the soluble components (halite, anhydrite) are removed. Another important deformation mechanism is grain boundary migration, indicated by lobate grain boundaries.

Towards the central part of a boudin, the grain size increases. Additionally, different generations and types of anhydrite crystals like fan-shaped and acicular crystals can be distinguished. The grain size reaches up to 3.5 mm. Large anhydrite crystals show undulose extinction, twinning planes and subgrains. A grain-shape fabric and, close to shear bands, a texture (LPO) result from recrystallization.

All these macro- and microstructures suggest the studied anhydrite rocks to have been deformed in the brittle-ductile deformation regime, which is compatible with literature data (e.g. Müller et al. 1981).

**References**

Bäuerle, G. (2000). Geochemisch-mineralogische Untersuchungen zur Genese, Lösungs- und Gasführung der Gorleben-Bank (Zechstein 3) des Salzstocks Gorleben. Dissertation, Technische Universität Clausthal, 147 pp. (unpublished)

Behlau, J. & Mingerzahn, G. (2001). Geological and tectonic investigations in the former Morsleben salt mine (Germany) as a basis for the safety assessment of a radioactive waste repository. Engineering Geology 61, 83-97

Müller, W. H., Schmidt, S. M. & Briegel, U (1981). Deformation experiments on anhydrite rocks of different grain sizes: Rheology and microfabric. Tectonophysics 78, 527-543

# (U)HP metamorphism in the Makbal Complex, Tianshan Mountains (Kazakhstan & Kyrgyzstan): Different P-T evolutions of intimately interlayered ultra high- and high-pressure rocks

Melanie Meyer[1] and Reiner Klemd[1]

[1]*GeoZentrum Nordbayern, Universität Erlangen-Nürnberg, D-91054 Erlangen*

Occurrences of UHP (ultra high-pressure) metamorphic rocks in orogenic belts provide a unique opportunity to obtain insight into subduction zone processes at great depth (> ca. 80 km) since they are the only natural, direct witness of such processes.

The Makbal (U)HP Complex is exposed on both sides of the Kazakh-Kyrgyz border. It is part of the Tianshan orogen which is located in the south-west of the Central Asian Orogenic Belt (CAOB), the biggest Palaeozoic orogen on Earth. The Tianshan orogen extends for approx. 2500 km from north-western China over Kyrgyzstan and Kazakhstan to Tajikistan. This mountain range contains several HP-UHP locations, but in contrast to the well studied Chinese Tianshan occurrence so far only a few petrological studies have been undertaken on the Makbal Complex.

Former studies on the Makbal Complex focused on UHP metasedimentary rocks (garnet-chloritoid-talc schist) and HP eclogites, which normally occur as boudins in the metasediments. This study, however, comprises a detailed petrographic and petrologic investigation of the different rock types constituting the Makbal Complex. Besides garnet-chloritoid-talc schists (host rocks) and eclogites, both of which have already been subject of previous studies (e.g. Tagiri et al., 2010), a blueschist-facies rock was also investigated.

Until now, only conventional geothermobarometric calculations, which revealed strongly variable peak pressures conditions ranging between 28 and 13 kbar at temperatures $\leq$ 560 °C, have been undertaken for the (U)HP rocks of the Makbal Complex (Tagiri et al., 2010). In the present study P-T pseudosection modelling of the different rock types was conducted for the first time. This approach is used to determine the P-T conditions and metamorphic evolution of the different (U)HP rocks. The peak metamorphic event was interpreted to have occurred between 510-500 Ma according to recent SHRIMP U-Pb zircon dating of eclogites and garnet-chloritoid-talc schist of the Makbal Complex (Konopelko et al., 2011).

The strongly variable peak metamorphic conditions including the intimate interlayering of high- and ultra high-pressure rocks were also reported from other localities of the Tianshan. The intimate occurrences of these rocks suggest that they were derived from different depths of the subduction zone and subsequently juxtaposed during exhumation within the subduction channel.

**References**

Konopelko, D., Kullerud, K., Apayarov, F., Sakiev, K., Baruleva, O., Ravna, E., Lepekhina, E. (2011). Gondwana Research, in press.

Tagiri, M., Takiguchi, C., Ishida, C., Noguchi, T., Kimura, M., Bakirov, Ap., Sakiev, K., Takahashi, M., Takasu, A., Bakirov, Az., Togonbaeva, A., Suzuki, A. (2010). Journal of Mineralogical and Petrological Sciences 105, 233-250.

# Isobaric evolution of staurolite-andalusite-cordierite-sillimanite schist in the Central Pyrenees – Early Variscan metamorphism of the Aston-Hospitalet domes

Jochen E. Mezger[1] and Jean-Luc Régnier[2]

*[1]Institut für Geowissenschaften und Geographie, Martin-Luther-Universität Halle-Wittenberg, D-06120 Halle, [2]ACR Mimarlik Ltd. Sti., Antalya, Turkey*

Staurolite- and cordierite-bearing rocks are generally considered to be the result of polymetamorphism, e.g. medium to high pressure regional metamorphism followed by a low pressure-high temperature thermal event (Pattison et al. 1999; Mezger et al. 2004). Staurolite-andalusite-cordierite schist are common in the Aston and Hospitalet domes of the Axial Zone of the Central Pyrenees. Textural evidence, i.e. preserved crenulation inclusion trails in all phases, suggest that nucleation of staurolite, andalusite and cordierite occurred within a narrow time frame during the development of the main schistosity, and thus can be interpreted as paragenetic.

Pressure-temperature conditions during peak-metamorphism were obtained from 18 samples using conventional thermobarometry (Holdaway 2000, 2001; Holland & Powell, 2009). In addition, pseudosections from three samples were constructed in the KFMASH and MnNCKFMASH systems with THERMOCALC 3.33 using the data set tcds55 (Holland & Powell, 2009). Both methods yield similar results, peak pressures between 3–4 kbar throughout both dome structures, and temperatures ranging from 525–625 °C. The P-T space and succession of stable assemblages (st-cd-bi-and, cd-bi-and, cd-bi-sill, cd-bi-sill-mu) produced by the pseudosections is in very good agreement with observations from thin sections, and corresponds to a prograde isobaric P-T path.

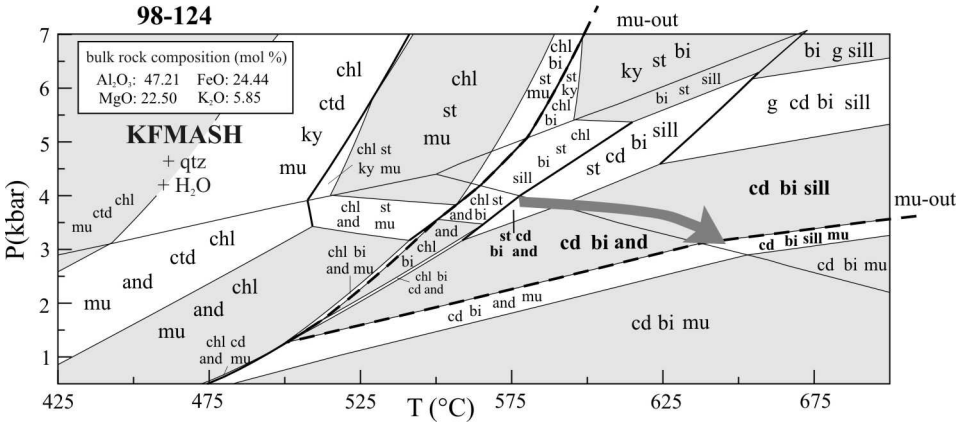


Pseudosection in the KFMASH system of a schist from the western Aston dome with observed parageneses outlined in bold. Arrow indicates possible isobaric P-T path.
and = andalusite, bi = biotite, cd = cordierite, mu = muscovite, sill = sillimanite, st = staurolite.

In the field, mineral isograds are flat-lying and related to early Variscan (Visean) magmatism that affected the Aston and Hospitalet metapelites and orthogneisses during the main phase Variscan deformation. The present shape of the isograds reflects the younger, late Variscan development of the Aston and Hospitalet gneiss domes.

**References**

Holdaway, M.J. (2000). Am. Mineral. 85, 881-892.
Holdaway, M.J. (2001). Am. Mineral. 86, 1117-1129.
Holland, H.D. and Powell, R. (2009). THERMOCALC 3.33.
Mezger, J.M., Passchier, C.W. and Régnier, J.-L. (2004). C. R. Geoscience 336, 827-837.
Pattison, D.R.M., Spear, F.S. and Cheney, J.T. (1999). J. Metamorph. Geol. 17, 685-703.

# Rifted structures of conjugated margins in the Tyrrhenian Sea

Moeller, S[1]., Berndt, C.[1], Grevemeyer, I.[1], Klaeschen, D.[1] Ranero, C.R.[2], Sallares, V.[2] and Zittelini, N.[3]

*[1]GEOMAR | Helmholtz Centre for Ocean Research Kiel, [2]Instituto de Ciencias del Mar, CSIS, Barcelona, Spain, [3]Instituto di Scienze Marine, ISMAR Bologna*

Stretching and thinning of the continental lithosphere leads to rifting and the formation of passive continental margins. However, there are still open questions regarding the development of rift basins, e.g. the relationship between horizontal extension by faulting and vertical crustal thinning. The Tyrrhenian Sea is a young rift basin of Neogene age located in the Western Mediterranean. Here, it is assumed that rifting and opening of the basin commenced in the context of slab rollback during the subduction of the Ionian lithosphere. The advantages of studying rift processes here are the conjugated margins which are very close to each other. We present results of a seismic reflection profile (MCS) crossing the North Tyrrhenian Sea along 41° N. The data of the 240 km long geophysical profile were acquired in April and May of 2010 during the MEDOC-Cruise in a two-ship operation with the Spanish and Italian vessels *Sarmiento de Gamboa* and *Urania*. The basin is characterized by N-S striking horst and graben structures indicating that the rifting occured in W-E direction. The MCS section shows a detailed image of the infill of these grabens, reveals normal faults and structures within the brittle upper crust to a depth of 5-6 km. Integrating drilling information of ODP leg 107, we identified Messinian syn-rift and Plio/Pleistocene post-rift sediments. The deep and thick Messinian evaporites near the Sardinian continental margin support the idea that this area marks the origin of rifting, subsidence and initial flooding. A comparison of crustal structures between the Sardinian and Campanian margins reveals significant differences in block size and in sedimentary thickness, which decrease from west to east. The horizontal extension in the West was accommodated by the formation of large horst and graben structures while extension in the East was generated by a series of smaller blocks and faults. These fault-bounded blocks dip at angles between 20° and 35°. A still open question is whether these faults were created at higher angles (~60°) and rotated to ~30° or were initially formed at these low angles.

# Texturanalyse des Steinsalzgefügetyps ‚Kristallbrocken'

Hans-Heinrich Müller[1], Bernd Leiss[1] und Michael Schramm[2]

*[1]Geowissenschaftliches Zentrum der Universität Göttingen, D-37077 Göttingen, [2]Bundesanstalt für Geowissenschaften und Rohstoffe, D-30655 Hannover*

Kristallbrocken sind charakteristische cm- bis dm-lange, laminierte Steinsalzgefügetypen, die vor allem in der Stassfurt-Formation des Zechsteins im Zentraleuropäischen Becken vorkommen. Die Kristallbrocken können gebrochen, boudiniert oder gebogen bzw. gefaltet sein. Mit Hilfe von Röntgentexturanalysen konnten Küster et al. (2010) nachweisen, dass es sich bei den Kristallbrocken um Einkristalle handelt, die Relikte ursprünglich größerer Einkristallstrukturen repräsentieren. Die schichtparallele Internlamination ist auf unterschiedlich hohe Anteile fester und stellenweise vorkommender fluider Einschlüsse zurückzuführen (Küster et al. 2011). Unklar ist bislang der Mechanismus der Gefügeentwicklung. Die Einkristallstrukturen können bereits vor der Deformation bei der Ausfällung aus der Salzlauge oder bei der Diagenese durch Sammelkristallisation entstanden sein. Unwahrscheinlich erscheint eine postdeformative Sammelkristallisation eines feinkörnigen Gefüges, da dabei die Lamination sicherlich nicht erhalten geblieben wäre.

Ziel der vorliegenden Studie ist es, die kristallographische Orientierung einer größeren Anzahl von Kristallbrocken in Bezug zur Foliation zu messen, um (a) Aussagen zum Gefügeentwicklungsmechanismus und (b) zum Deformationsverhalten über die Ableitung von aktivierten Gleitsystemen machen zu können. Röntgentexturanalysen wurden an 8 Kristallbrocken aus einem Probenblock aus dem ehemaligen Kalisalzbergwerk Asse sowie an 7 Proben aus den Bergwerken Gorleben und Teutschenthal durchgeführt.

Die Ergebnisse zeigen keine klare kristallographische Vorzugsorientierung der Kristallbrocken in Bezug zur Foliation. Anhand der gebogenen Kristallbrocken können unterschiedliche Gleitsysteme abgeleitet werden. Am häufigsten tritt das am leichtesten aktivierbare Gleitsystem {110}<011> auf. Es lassen sich aber auch die Gleitsysteme {100}<110> und {111}<110> nachweisen. Damit scheint das rheologische Verhalten der Salzbrocken, d.h. ob sie während der Deformation bruchhaft oder duktil reagieren von der kristallographischen Ausgangsorientierung unabhängig zu sein. Ein einheitliches Kristallwachstumsmodell bzgl. Präzipitation konnte, wie schon bei Küster et al. 2010, ebenfalls nicht nachgewiesen werden. Aufgrund der uneinheitlichen Ergebnissen bei der bislang geringen Anzahl untersuchter Kristallbrocken sind weitere statistische Aussagen nicht möglich.

**Literatur**

Küster, Y., Leiss, B. und Schramm, M. (2010). Int J Earth Sci (Geol Rundsch) 99: 505-526.
Küster, Y., Schramm, M. und Leiss, B. (2011). ZDGG 162: 276 – 293.

# Extremely rapid exhumation from eclogite-facies conditions to the surface in the Rhodope mountains, Bulgaria

Thorsten Nagel[1], Nikolaus Froitzheim[1], Silke Jahn-Awe[1], Maria Kirchenbaur[1] and Neven Georgiev[2]

[1]*Steinmann-Institut, Universität Bonn, Poppelsdorfer Schloss, 53115 Bonn, Germany;*
[2]*Department of Geology and Paleontology, University St. Kliment Ohridski, 15 Tzar Osvoboditel Blv., 1000, Sofia, Bulgaria*

In the Central Rhodopes, the deepest exposed tectonic level is represented by metamorphic continental basement-cover thrust sheets which are toped by a lithologically divers unit to which we refer as middle Allochthon. The middle Allochthon represents a mixture of various continental and oceanic rocks with different, partly Mesozoic protolith ages. Oddly, it contains ky-spl-crn-spr-bearing eclogites of Middle Eocene age as well as foliated granitic intrusions of Lower Eocene age suggesting major internal tectonic boundaries yet to be explored. This compound unit was placed on top of the pre-Mesozoic basement which we attribute to the Adriatic continental margin and the entire nappe pile was then subject to dramatic Late Eocene extension associated with the formation of sedimentary basins and core complexes. The metamorphic basement containing Middle Eocene kyanite-eclogites is covered with unmetamorphic Upper Eocene sediments and volcanoclastics. So far, there is no evidence for post-Eocene tectonic boundaries between eclogites and sediments in this area suggesting exhumation from >60 kilometers depth to the surface in less than 6 Ma. Regional extension was immediately followed by a pronounced pulse of granitic magmatism. The same Late Eocene to Early Oligocene magmatic event is found in Serbia external of the ophiolitc Vardar suture to west of the Rhodopes. Like other authors for the situation in Serbia, we attribute extension and magmatism in the Rhodopes to an event of slab rollback and associated upwelling of astenospheric mantle following delamination of continental crust from the down-going Adriatic slab after closure of the Vardar Domain. Accordingly, the lower portion of the nappe pile in the Rhodopes would represent a tectonic window into structural levels external, i.e. structurally beneath the Vardar Suture.

# A slap for eoarchean slab melting

Thorsten J. Nagel[1], J. Elis Hoffmann[1] and Carsten Münker[2]

[1]*Steinmann-Institut, Universität Bonn, Poppelsdorfer Schloss, 53115 Bonn, Germany;*
[2] *Universität zu Köln, Institut für Geologie und Mineralogie, Zülpicher Strasse 49b, 50674 Köln, Germany*

Earth's first continental crust is largely composed of magmatic rocks with tonalitic-trondhjemitic-granodioritic composition (TTGs). There is a vivid discussion whether TTGs o form by melting of hydrated MORB-like oceanic crust in subduction zones or alternatively by melting within thickened mafic arc crust or oceanic plateaus. In order to test different melting scenarios, we combine thermodynamic calculation of partial melting in different mafic host rocks and at different pressures with subsequent modeling of trace element partitioning between residual assemblages and coexisting tonalitic melt. The resulting modeled trace-element compositions are than compared with observed ones. We consider water-absent partial melting of modern N-MORB and of a typical Eoarchean arc tholeiite from the Isua Supracrustal Belt. The latter represents the country rock of World's oldest and arguably best-preserved TTGs, the Itsaq Gneiss Complex of SW Greenland. Isua tholeiites contain less Al and Na and more Fe and Mg as compared to present day MORB and thus form amphibole-rich and plagioclase-free residues even at low pressures. At 10 kbar, modeled tonalitic partial melt of MORB displays a trace element composition very different from the ones observed in TTGs. At higher pressures (14 and 18 kbar), with an eclogite as residue, the modeled trace element compositions become more similar to natural ones, but several parameters are still amiss. Also, producing tonalitic melt from an essentially dry residue requires enormously high temperatures. Perfectly-fitting trace element patterns at reasonable temperatures are achieved by using Isua tholeiite as host rock and melting pressures of 10 and 14 kbar. Some key observations in TTGs can only be reproduced using Isua tholeiite as protolith. These are, for instance, the pronounced negative Ti anomalies, the positive anomalies of Zr and Hf relative to Sm and Nd, and the variation in the Nb/Ta ratio. For some elements, e.g., Th and Ti, the better fit for the tholeiite protolith is partly inherited from the host rock, yet an appropriate fractionation by the residual phase assemblage is paramount. Formation of the Earth's oldest continental crust is therefore best explained by melting within tectonically thickened mafic island-arc crust.

# Mikrostrukturelle Charakterisierung von Karbonatgängen im Unteren Muschelkalk des Leinetalgrabens – erste Ergebnisse

Christian Nikolajew, Axel Vollbrecht, Bernd Leiss und Alfons v.d. Kerkhof

*Geowissenschaftliches Zentrum der Georg-August-Universität Göttingen, D-37077 Göttingen*

An Proben aus dem Unteren Muschelkalk wurden verschiedene Ganggenerationen anhand ihrer Orientierungen, Altersbeziehungen, Mikrostrukturen, Kathodolumineszenzfarben und Wachstumstexturen umfassend charakterisiert. Die Probenlokalität liegt am südlichen Ende des Ahlsburg-Lineaments, einer durch Halotektonik mitgeprägten Antiklinalstruktur innerhalb des nördlichen Teils des Leinetalgrabens ca. 15km nördlich von Göttingen (Abb.1). Karbonatgänge treten hier im Vergleich zur Umgebung besonders häufig auf. Es konnten fünf Hauptgangscharen unterschieden werden, deren Altersbeziehungen z.T. noch nicht eindeutig geklärt sind (Abb.1). Zusätzlich treten faserige kalzitische Lagenharnische auf, die etwa senkrecht zur Antiklinal-Achse ausgerichtet sind und daher auf Biegegleitung während der Aufwölbungsphase der Ahlsburg- Antiklinalstruktur zurückgeführt werden.

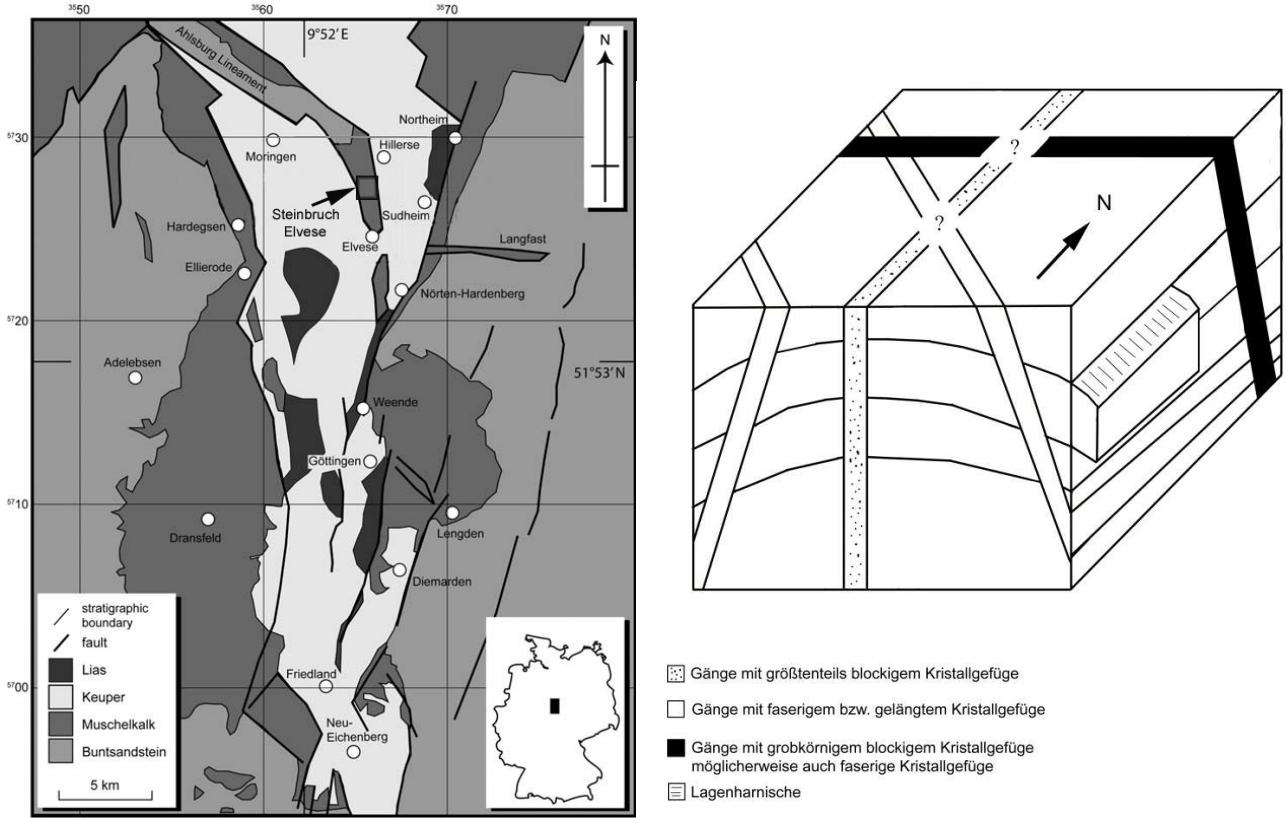


Abb.1: links: Vereinfachte Geologische Karte des Leinetalgrabens. Quartäre und Tertiäre Bedeckung sind nicht abgebildet. Der schwarze Rahmen markiert die Probenlokation. (Tanner et al. 2010, verändert); rechts: Schematisches Blockbild mit Raumlage der Karbonatgänge in Bezug zur Antiklinalstruktur im Steinbruch Elvese. Fragezeichen: bislang noch ungeklärte Altersbeziehungen.

Innerhalb der Gänge treten blockige, stengelige und faserige Kristallisationsgefüge auf, wobei i.d.R. jeweils eine Wachstumsform dominiert. Auch für makroskopisch homogene Domänen belegen die durch Kathodolumineszenzfarben abgebildeten Feinstrukturen eine z.T. komplexe Kristallisationsgeschichte. Wässrige hochsalinare Fluideinschlüsse (z.T. unterschiedliche Tochterkristalle) deuten darauf hin, dass die assoziierten hydrothermalen Lösungen mit tiefer liegenden Salzhorizonten in Verbindung standen (Röt, Zechstein). Spezielle Kathodolumineszenzfarben, die auf Mikrodomänen beschränkt sind, lassen auch auf meteorische Einflüsse schließen.

**References**

Tanner, D.C., Leiss, B., Vollbrecht, A. and The Göttingen Geothermal Group (2010). Z. Dt. Ges. Geowiss. 161: 369- 377.

# Polyphase deformation in NW Namibia – tools to reconstruct regional tectonics

Cees Passchier[1], Xavier Maeder[1] and Rudolph Trouw[2]

*[1]Institut für Geowissenschaften, Universität Mainz, [2]Institut für Geowissenschaften, Federal University of Rio de Janeiro, Brazil*

The Ugab-Goantagab Domain of NW-Namibia is a sequence of Neoproterozoic metaturbidites, deposited on basement at the edge of the Congo craton. In the western Ugab zone, the sequence was deformed under greenschist facies conditions into km-scale asymmetric NS- trending folds of apparently simple geometry with a single foliation, overprinted by EW trending younger folds. Detailed field mapping and analysis of vein systems has shown that the folds have a complex history, formed in non-coaxial flow and probably changed from an upright, symmetric to an asymmetric geometry during progressive deformation. Towards the east, in the Goantagab Domain, there is a gradual transition to another tectonic regime with more intense deformation and development of km-size sheath folds. Reconstructed flow patterns here show an orientation gradient of flow kinematic axes, and a change of these with time. In this area, north directed thrusting is dominant. On a large scale, the observed deformation patterns can be attributed to two orogenic events, the first a late Neoproterozoic oblique collision of the Rio de la Plata and Congo cratons along a NS trending mobile belt. The second event was a Cambrian collision along an EW trending mobile belt between the combined Congo-Rio de la Plata and Kalahari cratons, with partial reactivation of the older mobile belt. The western Ugab area is mostly affected by the first macrotectonic event, the eastern Goantagab area by the second event.

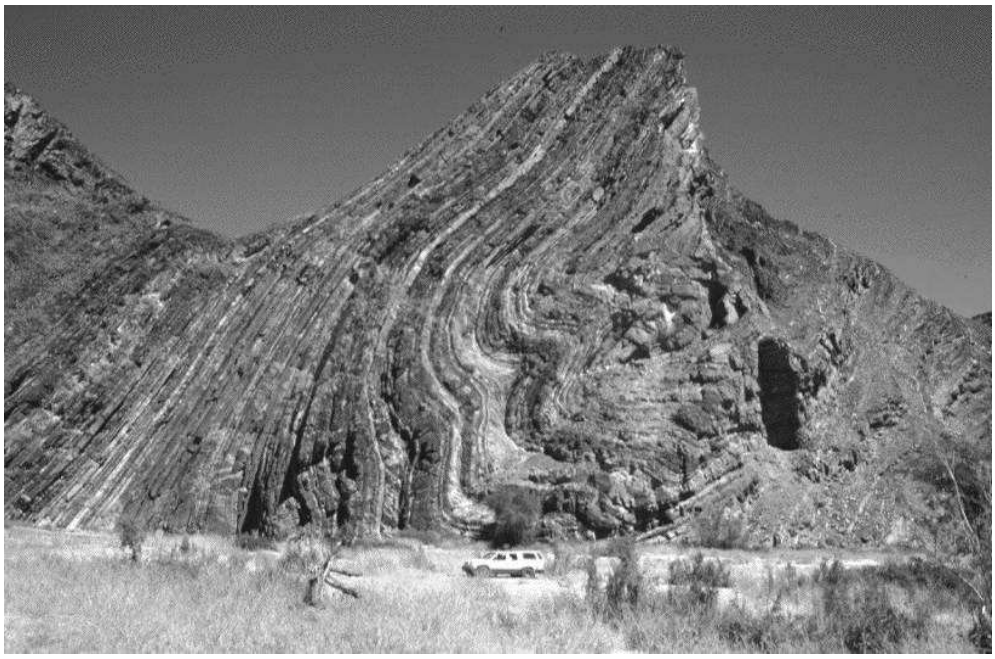

First generation fold in Neoproterozoic turbidites of the Ugab valley, NW Namibia.

It is possible to reconstruct the local sequence of events using classical overprinting criteria such as overprinting foliations, folds and veins. The complexity of local tectonics, however, and the macrotectonic evolution are hard to reconstruct with our static, classical structural geology tools. Key-ring structural gradients and other lateral changes in the style and geometry of structures reflect flow gradients due to the complex 3D rearrangement of three cratons. The area in NW Namibia shows these complexities because of nearly perfect exposure in a desert environment: similar complex structural gradients can be expected in other areas, but lack of outcrop obscures them and we may not be aware of their existence. One of the major challenges in tectonics is to try and develop tools to recognise this type of complexity in areas with poor outcrop, and develop methods to describe and interpret them.

# Spatial distribution of quartz recrystallization microstructures across the Aar massif

Max Peters[1] and Marco Herwegh[1]

[1]*Institut für Geologie, Universität Bern, Balzerstrasse 1+3, CH-3012 Bern*

In the Aar massif (Swiss Central Alps), main foliation and major deformation structures were developed during NW-SE compression associated with the Alpine orogeny (Steck, 1968). Shearing at the brittle to ductile transition may have initiated at different stages between 22-20 Ma and 14-12 Ma, followed by purely brittle deformation at around 10 Ma (Rolland et al., 2009). In light of the onset of dynamic recrystallization in quartz, Bambauer et al. (2009) defined a quartz recrystallization isograd in the northern part of the Aar massif. To the south, the grain size of recrystallized grains increases due to an increase of metamorphic temperatures from N to S. The aim of the current project is to carry out quantitative analysis on changes of the dynamic and static recrystallization behavior of quartz. A series of thin sections, covering an entire N-S transect from Guttannen to Gletsch, gives insights into the long lasting deformation and exhumation history of the crystalline rocks of the Aar massif. In addition, Titanium-in-quartz geothermometry was performed to learn more about the deformation temperatures and associated microstructural changes on the retrograde path.

In this N-S section, two general types of microstructures have to be discriminated: (i) weakly to moderately deformed host rocks and (ii) intensely deformed mylonites to ultramylonites out of high strain shear zones. (i) Volume fraction and size of recrystallized quartz grains increase towards the south showing grain size changes from around 5 µm up to ca. 230 µm. Microstructures are characterized by complete recrystallization in the S. In terms of recrystallization processes, a change from bulging recrystallization in the N to SGR recrystallization and the transition to grain boundary migration (GBM) recrystallization in the S occurs. Such a change in recrystallization processes, combined with grain size increase, points towards reduced differential stresses with increasing temperatures (Bambauer et al., 2009). This temperature gradient is also corroborated by a switch in the active glide systems in quartz from basal to rhomb dominated glide. (ii) In contrast to the granitic host rocks, the mylonites and ultramylonites show smaller recrystallized grain sizes compared to their host rocks, but they also reveal a general grain size increase from N to S. Here, enhanced strain rates compared to the host rocks result in overall smaller quartz grains.

In the south, microstructures from (i) and (ii) show equidimensional grains with 120° triple junctions and straight grain boundaries. Such microstructures are typical for static grain growth. For that reason, we suggest that towards the end of a deformation episode, strain discontinuously localized in narrow shear zones. In contrast to that, stress relaxation at the margin of such a zone of deformation would be a result of decelerated deformation rates or elevated temperatures. This stage of static grain growth might correlate with a fluid pulse between 12-10 Ma as suggested by Challandes et al. (2008) originating in post-tectonic annealing. Constraints on the grade of deformation based on grain size data and CPO analyses will be presented, supporting the hypothesis that various deformation stages are well preserved in statically recrystallized structures.

**References**

Bambauer, H.U., Herwegh, M., Kroll, H. 2009: Quartz as indicator mineral in the Central Swiss Alps: the quartz recrystallization isograd in the rock series of the northern Aar massif. Swiss Journal of Geosciences, 102, 345-351.

Rolland, Y., Cox, S.F., Corsini, M. 2009: Constraining deformation stages in brittle–ductile shear zones from combined field mapping and $^{40}Ar/^{39}Ar$ dating: The structural evolution of the Grimsel Pass area (Aar Massif, Swiss Alps). J. Struct. Geol., 31, 1377-1394.

Stipp, M. & Tullis, J. 2003: The recrystallized grain size piezometer for quartz. Geophysical Research Letters, 30 (21).

# Migration pathways in Upper Carboniferous unconventional reservoirs, Southern Ruhr Area, North Rhine-Westphalia, Germany

Stefan Pietralla[1], Martin Salamon[2] and Christoph Hilgers[1]

*[1]Energy- & Mineral Resources Group, Department of Reservoir-Petrology, RWTH Aachen University, Wüllnerstrasse 2, 52056 Aachen, Germany, [2]Geological Survey North Rhine-Westphalia, De-Greiff-Str. 195, 47803 Krefeld, Germany*

The study area is situated in the transition zone of the Variscan Rhenish Massif and the Ruhr foreland basin about 15 km north of Wuppertal. The geological units in the study area comprise strata of the so called “Flözleere” (coal-barren) in the south and the “Flözführendes” (coal-bearing) Upper Carboniferous in the north. The Weuste quarry has been examined in particular, where the oldest coal seams of the Ruhr basin (Sengsbänksgen and Sengsbank seam, Sprockhöveler Schichten, Namur C) crop out. A columnar section of this quarry has been logged at high resolution, in order to understand, illustrate and explain the depositional environment of this part of the Carboniferous Ruhr basin. Furthermore, rock and coal samples have been taken in the quarry, which have been examined by means of vitrinite reflectance (% $R_r$) measurements. These measurements have provided vitrinite reflectance values in a range between 1.471 and 1.588 (% $R_r$). By means of these measurements the Sengsbänksgen and Sengsbank coal is classified as medium to low volatile bituminous coal or according to German DIN as “Fettkohle”. In order to determine the major joint pattern in the study area, fracture measurements in the mapping area were carried out. Three major joint sets were found, striking NW-SE (~80-90°), ENE – WSW (~70-75°) and NE – SW (~25-35°). This joint pattern is in accordance with the large scale Variscan deformation pattern. Own mapping data were integrated with published surface and subsurface data towards a first 3d model using 3d Move.

Results are compared to core samples taken from an ongoing drilling site near Ratingen (Germany) (TVD= 74.5 m), which have been examined in terms of vitrinite reflectance (% $R_r$) and total organic carbon. Unfortunately, the drilling did not reach the expected Upper Alum Shale (Visé-Namur), which is considered a source rock for shale gas. However, the obtained vitrinite reflectance values from the Namur B formation have been compared to the samples taken from the Weuste quarry (Namur C). With a range of 3.024 – 3.174 (% $R_r$), these rocks have been buried deeper and have been exposed to far higher temperatures than the quarry samples. Based on vitrinite reflectance values a maximum rock temperature ($T_m$) in a range between 225 and 230 °C could be calculated. This temperature range can be correlated to a maximum burial depth for the rocks of around 7500 m.

Data were integrated in a 3D model of the study area, which helped to identify possible migration pathways for fluids in the reservoir rocks.

# The MEMIN research unit: hypervelocity impacts into geological materials

Michael H. Poelchau[1], Thomas Kenkmann[1], Klaus Thoma[2], Alex Deutsch[3], Tobias Hoerth[2] and Frank Schäfer[2]

*[1]Institut für Geowissenschaften-Geologie, Albert-Ludwigs-Universität Freiburg, Germany, [2]Fraunhofer-Institut für Kurzzeitdynamik, Ernst-Mach-Institut, Freiburg, Germany, [3]Institut für Planetologie, Westfälische Wilhelms-Universität Münster, Germany*

To date, the impact cratering process has seldom been observed "in-situ" on a planetary scale. While post-impact analysis of craters by remote sensing and field work gives many insights into the process, impact cratering experiments have several advantages for impact research: 1) excavation and ejection processes can be directly observed, 2) physical parameters of the experiment can be defined and varied, including projectile velocity, mass, density, and numerous target properties, and 3) cratered target material can be analyzed post-impact in an unaltered, uneroded state. Insights gained from impact cratering experiments can then be applied to planetary scale craters.

The MEMIN-Project (Multidisciplinary Experimental and Modeling Impact Research Network) is a delocalized DFG research unit (FOR 887) that focuses on impact experiments into geological materials to comprehensively understand details of the cratering process through real-time in-situ measurements, extensive post-impact analysis and numerical modeling (Schäfer et al. 2006, Kenkmann et al. 2011). Among several other aspects, MEMIN is also focused on the effects of porosity and pore space saturation on impact crater formation, and their implications for planetary-scale cratering.

Cratering experiments are carried out at the facilities of the Ernst-Mach-Institut, Freiburg, Germany, using two different two-stage light-gas guns. Smaller steel spheres weighing 67 mg were accelerated to ~5 km/s and impacted into dry and water-saturated sandstone cubes. Larger steel and iron meteorite (Campo del Cielo IAB) spheres weighing 4.1 and 7.3 g were accelerated to 2.5-5.3 km/s into dry and 50% saturated blocks. As target material, Seeberger sandstone was used, with an average porosity of 23.1±0.5%, and a uniaxial compressive strength (UCS) of 36.3±1.7 MPa.

In the experimental setup, high speed framing cameras with a frame rate of up to $5*10^5$ frames per second document the impact process. Ultrasound sensors attached to the target measure the passage of the shock wave and post-impact reverberations, and special witness plates, termed "ejecta catchers", positioned adjacent to the target surface capture sandstone particles and traces of the projectile ejected during cratering.

Impact crater dimensions were then measured with a 3D laser scanner. Our results confirm that crater size (measured as volume) is directly proportional to the kinetic energy of projectile. Interestingly, the effect of porosity becomes apparent when crater volumes of the sandstone and non-porous rocks are compared. For the same impact energy and roughly similar impact conditions (projectile mass, density and speed) the same crater volumes result, in spite of the fact that the target's strength strongly influences its size (e.g., UCS of impacted basalts used for comparison are one order of magnitude higher at 300±63 MPa). Apparently, porosity dampens the shock wave and reduces the amount of impact energy available to work against the target's strength to form a crater.

The details of how exactly pore space affects the shock wave are currently being examined, using results from numerical modeling and evaluation of high speed videos, ultrasound sensors and ejecta catchers. Microstructural analysis of deformation mechanisms and pore space reduction in the crater's subsurface is being performed, and will be presented by Buhl et al. at this conference.

**References**

Kenkmann, T., Wünnemann, K., Deutsch, A., Poelchau, M. H., Schäfer, F. and Thoma, K. (2011). Meteoritics & Planetary Science 46 (6), 890–902.

Schäfer, F., Thoma, K., Behner, T., Nau, S., Kenkmann, T., Wünnemann, K. et al. (Eds.) (2006). Proceedings of the 1st International Conference on Impact Cratering in the Solar System. Noordwijk, May 8-12, 2006. European Space Research and Technology Centre - ESA.

# The Giudicarie Fault System (Alps, Northern Italy): Evolution of a major Alpine fault system

Hannah Pomella[1], Michael Stipp[2] and Bernhard Fügenschuh[1]

*[1] Institute of Geology and Paleontology, University of Innsbruck, Innrain 52, 6020 Innsbruck, Austria, [2] Helmholtz-Zentrum für Ozeanforschung Kiel (GEOMAR), Kiel, Wischhofstr. 1-3, 24148 Kiel, Germany*

The Periadriatic fault system is the longest and most outstanding fault systems in the Alps, extending for some 700 km from north-western Italy to Slovenia. This fault system separates the Western-, Central- and Eastern Alps in the north from the Southern Alps to the south of it. The Giudicarie fault system represents the central, approximately NE-SW-trending segment of the Periadriatic fault system and can be subdivided into: (1) the Southern Giudicarie fault, (2) the Northern Giudicarie fault, and (3) the Meran-Mauls fault. In spite of numerous studies on the Periadriatic fault system during the last 100 years, the role of the Giudicarie fault system is still controversial. One end-member model assumes an originally straight Periadriatic line, sinistrally offset by the Giudicarie fault system in the Miocene due to the NNW-ward advancing Southalpine indenter. The other end-member model argues for an originally curved Periadriatic line, overprinted by Neogene compressional inversions on an inherited Early Permian to Lower Liassic NE-SW trending horst and graben structure. Based on a multidisciplinary approach, we present further data in order to decide which model is more likely.

Along the Giudicarie fault system detailed mapping and structural analyses have been carried out and the units forming the foot- and hanging wall have been analysed with respect to their structural evolution and time-temperature history. On Paleogene Periadriatic intrusions, termed “tonalitic lamellae”, which crop out along the Northern Giudicarie fault and the Meran-Mauls fault, geochronological, geochemical, and paleomagnetic analyses have been performed in order to investigate under which conditions they intruded and how they have been deformed.

The results of this multidisciplinary study lead to the following evolution-model of the Giudicarie fault system:

a) Oligocene: Intrusion of the northeastern units of the Adamello batholith adjacent to the straight, dextral strike-slip Periadriatic line. The northern rim of the batholith is dextrally sheared.
b) Late Oligocene / earliest Miocene: The NNW-ward movement of the Southalpine indenter leads to a bending of the fault.
c) Early Miocene: The brittle Passeier fault, Northern and Southern Giudicarie fault sinistrally offset the bent segment of the Periadriatic line. Along the northern part of the bent segment (Meran-Mauls fault) a nearly continuous tonalitic body persists, whereas along the Northern Giudicarie fault only small boudinaged bodies rotated during the later brittle faulting are present.

# Disequilibrium textures in lower crustal rocks: Magmatic fabrics in the Eastern Segment, SW Sweden

Bettina Richter and Uwe Altenberger

*Institute of Earth and Environmental Science, Potsdam University, Karl-Liebknecht-Str. 24, 14476 Potsdam, Germany*

The Southern part of the Eastern Segment in SW Sweden is dominated by a complex metamorphic and magmatic evolution. Magmatic series are overprinted by multiple high-temperature and high-pressure events. However, relict magmatic fabrics and minerals are still preserved. Typical examples of local disequilibrium crop out in Getterön and around lake Skårjö. In Getterön metagabbros still show magmatic large-scale cross-bedding, although the mineralogy is completely metamorphosed. While the metagabbros of Skårjö still contain primary magmatic phases. The garnet-bearing mafic rocks contain magmatic olivine ($Fa_{53}Fo_{47}$) and plagioclase ($An_{11-19}$), which is metamorphic reequilibrated. Metamorphic reactions led to the formation of corona textures between the primary magmatic minerals.

There are two different coronas developed around the magmatic phases. At first, magmatic plagioclase is surrounded by small, newly formed garnet grains. Secondly, a small rim of plagioclase is often formed around olivine and magmatic orthopyroxene. Besides, there is symplectitic intergrowth of olivine and plagioclase as well as plagioclase and garnet. In addition, biotite and hornblende form pronounced rims around iron-rich opaques (illmenite and magnetite).

Fortunately, magmatic as well as metamorphic orthopyroxenes coexist and afford the determination of the metamorphic origin of the corona structures. Some orthopyroxene grains are encrusted by garnet, hornblende and metamorphic plagioclase whereas other grains are overgrowing magmatic olivine.

Based on the minerals and structures several reactions and stages of the prograde rock evolution can be reconstructed.

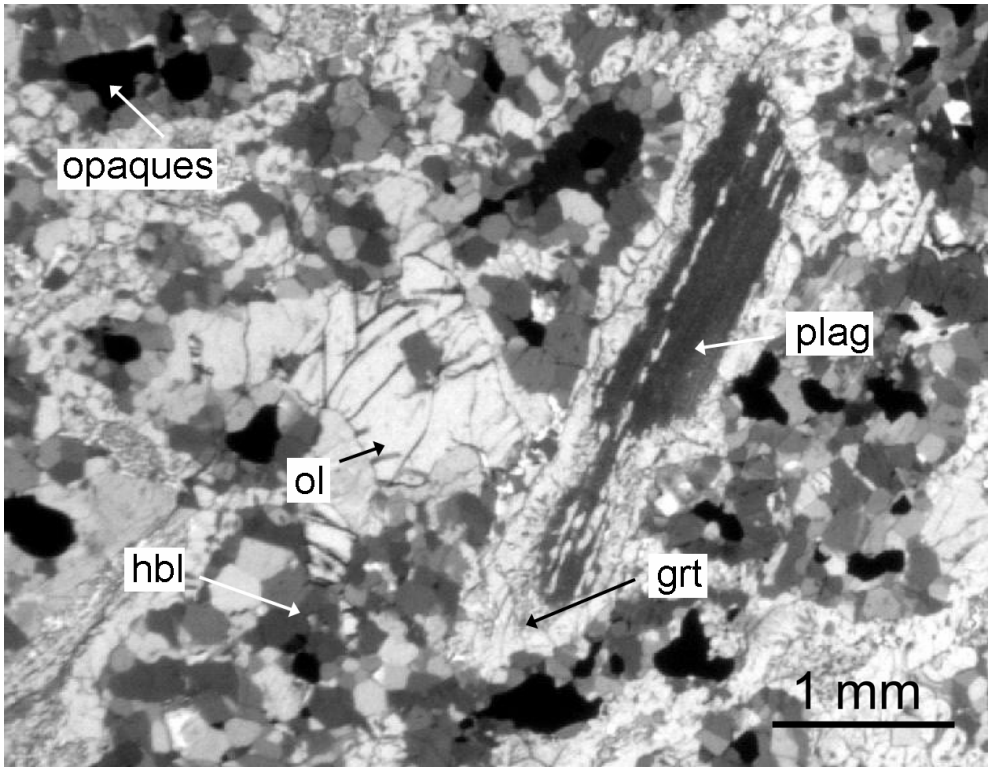


Fig. 1: Thin section of the magmatic fabrics and corona structures in the metagabbros of lake Skårjö. Magmatic, strongly altered plagioclase is surrounded by garnet (centre). Furthermore, opaques are surrounded by biotite and hornblende.

# Quantifying vertical surface motion on different time-scales, example of Crete, Greece

Stefanie Rieger[1], Nico Adam[2] and Anke M. Friedrich[1]

*[1]Department für Geo- und Umweltwissenschaften, Geologie, LMU München, Luisenstraße 35, 80335 München, [2]Deutsches Zentrum für Luft- und Raumfahrt e.V. (DLR), Institut für Methodik der Fernerkundung (IMF), Oberpfaffenhofen, 82234 Weßling*

Large earthquakes at subduction zones require the accumulation and sudden release of large amounts of elastically stored energy, which builds up when the plate interface is locked. This leads to elastic bending and in turn to transient vertical surface displacement of both, the down-going and the upper plate during the seismic cycle. Quantification of this transient vertical deformation behaviour, therefore, provides important constraints on models of the "earthquake cycle". We collected vertical displacement data on the island of Crete using radar interferometry.

Crete is an ideal test case to observe the interseismic vertical surface motion due to its proximity to the Hellenic subduction zone. The island was affected by large earthquakes in the past, e.g., in 365 AD a $M_S$ > 8 earthquake occurred along a reverse fault ~70 km SW of Crete, and induced sudden vertical uplift of the SW part of Crete of up to 9 m. The Persistent Scatterer Interferometry (PSI) approach provides a tool to quantify vertical motion of the Earth's surface with millimeter accuracy and a wide spatial coverage of hundreds of kilometers. We used the observational PSI system for wide areas (PSI-WAP), developed at the German Aerospace Center (DLR). Data of the ERS-1 & -2 satellites were used for the PSI analysis.

The results of the PSI WAP analysis for W-Crete indicate uplift of the SW corner of W-Crete of up to 5 mm/yr in the line-of-sight (LOS). The middle part of W-Crete appears more or less stable, whereas the eastern part of W-Crete is subsiding with up to 5 mm/yr (LOS). Therefore, the vertical motion of SW-Crete shows the same sense during the interseismic period as for the coseismic event of 365 A.D. These results are inconsistent with predicted vertical motion during the earthquake cycle of the subduction interface model of Hyndman and Wang (1993). We therefore suggest that the 365 A.D. earthquake did not occur along the main plate interface. Our data are more consistent with elastic strain accumulation along a fault in the overriding plate. Therefore it is likely that the 365 A.D. earthquake may occurred along the Hellenic Trench, a major reverse fault in the Aegean microplate located 25 km away from the SW corner of Crete. Detecting a geodetic signal during the interseismic period suggests strain accumulation for a possible earthquake in the future, either along the plate interface or along a fault in the overriding plate.

**References**

Hyndman R.D. & Wang K. (1993): Thermal constraints on the zone of major thrust earthquake failure – The Cascadia subduction zone. JGR, Vol. 98, Issue: B2, pages: 2039-2060. DOI: 10.1029/92JB02279

# Interpretative model of shearband boudins internal evolution in HT ductile shear zones

Benedito C. Rodrigues[1], Mark Peternell[2], António Moura[1], Martin Schwindinger[2] and Jorge Pamplona[3]

[1] *Centro de Geologia da Universidade do Porto (CGUP), Rua do Campo Alegre, 687, 4169-007 Porto, Portugal,*
[2] *Tektonophysik, Johannes-Gutenberg Universität Mainz, 55099 Mainz, Germany,*
[3] *Centro de Investigação Geológica, Ordenamento e Valorização de Recursos, Universidade do Minho (CIG-R), Campus de Gualtar, 4710-057 Braga, Portugal*

The internal structure of a shearband boudin resulting from an original igneous, hydrothermal or metamorphic segregation tabular rigid body is a subject of scientific interest. It allows understanding the deformation mechanisms acting on homogeneous quartz aggregate activated during simple shear progressive deformation.

This work is focused on the characterization of the internal evolution of shearband boudins, using microtextural analysis, fluid inclusions studies, fractal and OCP analysis. The proposed interpretative model shows the several structural stages that can be well established during the process of the internal evolution of shearband boudin.

In the first stage a quartz-rich layered body was submitted to the boudinage process. This layer has most likely a segregation or igneous and hydrothermal texture, in equilibrium with Lcw or Lwc fluids, catched in isolated fluid inclusions (FI). The quartz fabric is supposed to be random or controlled by a nucleation/growth process. In continuity, with major or minor time gap, were preserved vapor-carbonic fluids (Vc) in intracrystaline trails.

The boudinage process starts when the original layer achieved enough viscosity contrast relatively to the surrounding matrix, caused by a differential stress field. Two main transformations occur simultaneously: i) a change in the external shape with continuous evolution from tabular rigid body to sigmoidal assymetric morphology (shearband boudin) and, ii) localized dynamic recrystallization in the sharp-tips (parameter defined by Pamplona and Rodrigues, 2011) and, along the boudin's margin and grain boundaries. The smaller recrystallized grains, particularly in the sharp-tip domains (StD) accommodate most of the external strain and preserve the larger, relict grains in the centre.

The dynamic recrystallization was one single process, indicated by grain boundary fractal dimension analysis that results in a single mean fractal dimension $D_{EDM}$ = 1.13. Most strain is accommodated in the StD and the c´type structures. As a consequence of this strain partitioning the small recristallized quartz grains in the StD define c-axis patterns indicating an inferred anthithetical shear sense. Nevertheless, the recrystallization process is very complex, implying two internal rotations around kinematics axis Z and Y in amphibolitic facies conditions.

Two sub-stages inside the deformation stage are only recorded by textural analysis and fluid inclusion studies. The first of these sub-stages is characterized by the formation of the heterogeneous domain (HtD). The external envelope of the boudin is locally permeable to the penetration of external aluminous fluids with crystallization of a paragenesis dominated by andalusite. This episode is recorded by a new set of transgranular and intracrystaline trails of fluid inclusions within andalusite grains and quartz grains in the whole body of the boudin.

The last deformation episode shows the final formation of blunt-tip domain and secondary shear planes (c' type-I and c'type-II structures – shearband boudin parameters defined by Pamplona and Rodrigues, 2011), sometimes marked by sillimanite crystallization.

**References**

Pamplona, J. and Rodrigues, B.C. (2011). Kinematic interpretation of shearband boudins: New parameters and ratios useful in HT simple shear zones. Journal of Structural Geology 33, 38-50.

# HP-metamorphism in the Adula Nappe, Central Alps

Sascha Sandmann[1] and Thorsten J. Nagel[1]

[1]*Steinmann-Institut, Universität Bonn, Poppelsdorfer Schloss, D-53115 Bonn, Germany*

The Adula Nappe in the Lepontine Dome (Central Alps, Switzerland and Italy) is derived from the former distal continental margin of the European Plate that was subducted beneath the Adriatic margin in Eocene times. It mainly consists of various gneisses with layers of garnet-micaschist, marble, and bodies of mafic and locally of ultramafic rocks. High-pressure and ultra-high-pressure conditions are preserved in eclogite and ultramafic rocks but are virtually absent in gneisses and thus in the bulk of the nappe. It is unclear whether the Adula Nappe is assembled from rocks of different age and metamorphic grade during intense mixing in a subduction channel or represents a more or less coherent basement block which was exhumed in a single tectonic event.

We present major element distribution patterns in garnet from eclogite and garnet-micaschist and new Lu-Hf garnet age data. In the southern Adula Nappe garnet in eclogite does not reveal any growth zonation and consistently shows Eocene Lu-Hf ages. The central Adula Nappe is characterised by the presence of two populations of garnet. A first generation shows Variscan Lu-Hf ages, a second one an Alpine (Late Eocene) age (Herwartz et al., 2011; this study). Alpine garnet reveals perfectly preserved growth zonation without any diffusive reequilibration. In the northern Adula Nappe garnet is exclusively of Variscan age. Also garnet in micaschist shows grain size distributions and zonation patterns very similar to garnet from adjacent eclogite suggesting that they share the same metamorphic history.

We propose that the Adula Nappe represents a coherent piece of old European basement with Mesozoic synclines that was subducted towards the south in late Eocene times. Alpine metamorphic conditions completely reequilibrated Variscan assemblages in the southern part of the Adula Nappe. The Alpine metamorphic overprint decreases towards the northern part of the unit, where Variscan garnet was almost unaffected by Alpine metamorphism. The entire unit underwent the Alpine metamorphic cycle as a coherent block.

**References**

Herwartz, D., Nagel, T.J., Münker, C., Scherer, E.E. & Froitzheim, N. (2011). Tracing two orogenic cycles in one eclogite sample by Lu-Hf garnet chronometry. Nature Geoscience, 4, 178-183.

# The granulite facies Ongole domain of the Eastern Ghats Belt, India – A Proterozoic island arc?

Tapabrato Sarkar[1] and Volker Schenk[1]

[1] *Institute for Geosciences, University Kiel, 24098 Kiel, Germany*

The Eastern Ghats Belt is an assembly of several granulite terrains with different metamorphic ages on the eastern coast of India. It is bounded by the Singhbhum craton in the north and the Bhandara craton and Eastern Dharwar craton in the west. Shear zones along which the granulites are thrusted over the cratonic units, mark the western margin of the EGB.

Recent work has established four major crustal units separated by tectonic boundaries (Dobmeier and Raith, 2003): the Late Archean Jeypore and Rengali province (northwest and north), the Mesoproterozoic Eastern Ghats Province (east), and the late Palaeoproterozoic Ongole domain (southwest). The Ongole domain is mainly composed of a suite of felsic granulites (charnockites and enderbites) within which migmatitic metapelitic granulites and basic granulites occur as enclaves and rafts. The charnockites and the enderbites are of different generations showing complex cross cutting relationship in outcrop, indicating that the later Ongole domain grew through many felsic to mafic intrusions. The metapelitic granulites are Fe-Al rich hercynite-quartz bearing rocks showing beautiful reaction textures, helpful in deducing prograde and retrograde mineral reactions. Geothermobarometric data from previous workers and the considerations from the deduced mineral reactions in the petrogenetic grid show that the hercynite-quartz bearing granulites evolved through an anticlockwise P-T trajectory reaching peak metamorphic conditions of about 10kbar and 1000°C, followed by a near isobaric cooling at depth.

The best tectonic model (Waters, 1991) that supports UHT metamorphism of a hercynite-quartz bearing granulite, evolving through an anticlockwise P-T trajectory is a magmatic arc at a continental margin, where voluminous mantle derived magmas were transferred to higher levels causing medium P, ultrahigh T metamorphism, accompanied and followed by crustal thickening and then slow cooling at mid crustal levels.

In the Ongole domain the monazite apparent age population shows that the history of the high temperature metamorphism ended between 1600-1550 Ma. Though monazite does not record pre-intrusion tectonothermal events, the apparent ages indicate that the tectonothermal events in the Ongole domain are older than the formation of Rodinia, but younger than Columbia formation. Thus, the accretion of the possible Ongole island arc accreted in between the two supercontinent forming events.

LA-ICPMS zircon dating and trace element analysis of the intrusive rocks are aimed to decipher the formation history and the magmatic processes that formed the island arc of the later Ongole domain.

**References**

Dobmeier, C. and Raith, M.M. (2003). Geol. Soc. London. Spec. Publ. 206, 145-168.
Waters, D.J. (1991). European Journal of Mineralogy 3, 367-386.

# On the distribution and morphology of grain boundary fluids in natural rock salt

Joyce Schmatz, Marc Sadler, Guillaume Desbois and Janos L.Urai

*Structural Geology, Tectonics and Geomechanics, Geological Institute, RWTH Aachen University, D-52056 Aachen*

Solution-precipitation creep and dislocation creep play a significant role in the rheology of salt bodies (Urai and Spiers, 2007). These deformation mechanisms are strongly controlled by inter-granular fluid phases and grain boundary structures.

Grain boundary-fluid morphologies occur in a continuum ranging from semi-continuous fluid films to arrays of tube shaped inclusions or isolated near-spherical inclusions. Up to now, there is no quantitative description of the distribution and morphology, neither related to the nature of the adjacent grains, nor to the pT-conditions inside the salt body. Such information, however, is needed to fully reconstruct the deformation behavior of a wet salt rock.

We present a detailed study on the distribution and morphology of fluid inclusions in grain boundaries of domal salt with special emphasis on the relation to the dominant deformation mechanism in the respective grains, in order contribute to our understanding of the interplay of these two features. Herewith, we use a special designed U-stage that allows the investigation of fluid inclusions in the plane of the grain boundary using thick sections with a thickness of up to 100 µm. Grain boundary fluids also occur in the range of a few nm. Therefore we present an accompanying study using the same samples in which we investigate the grain boundary morphology and fluid inclusion trails with high-resolution SEM by matching surface pairs of grains.

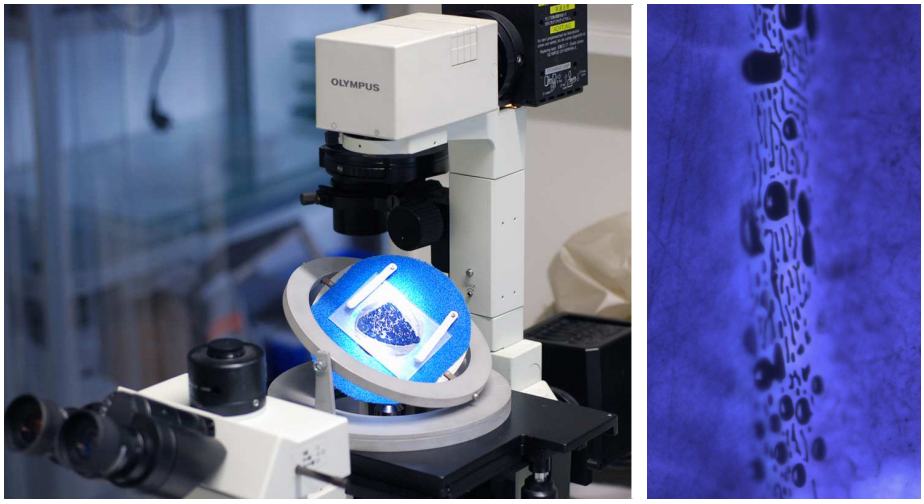


Left: Olympus Invertoscope equipped with an U-stage that allows investigation of grain boundaries in a plane. Right: Array of different shaped and sized fluid inclusions in Asse salt. Image width is 100 µm.

**References**

Urai, J.L. and Spiers, C.J. (2007). The effect of grain boundary water on deformation mechanisms and rheology of rocksalt during long-term deformation In: Wallner, M.,Lux, K.,Minkley, W.,Jr., H. Hardy (Eds.), The Mechanical Behavior of Salt – Understanding of THMC Processes in Salt Hannover.

# Investigation of Nb-Ta-enriched Pegmatites in the Eastern Alps

Tobias Schneider[1], Jürgen Konzett[1], Bernhard Fügenschuh[2] and Frank Melcher[3]

[1]*Institut für Mineralogie und Petrographie, Universität Innsbruck, Innrain 52 f, A-6020 Innsbruck, Österreich.*
[2]*Institut für Geologie und Paläontologie, Universität Innsbruck, Innrain 52f, A-6020 Innsbruck, Österreich.*
[3]*Bundesanstalt für Geowissenschaften und Rohstoffe, Stilleweg 2, 30655 Hannover, Deutschland.*

Permian lithospheric thinning led to T-dominated metamorphism in the Alps accompanied by numerous magmatic activities (Schuster & Stüwe, 2008). In the Eastern Alps the highest degrees of this Permian event are largely constrained to an E-W striking belt that was overprinted by high-P metamorphism during the Eoalpine cycle (Eoalpine high pressure belt (EHP), Schmid et al., 2004). The Schneeberg and Texel complexes form the westernmost occurrences of the EHP.

From the eastern parts of the Koralpe-Wölz unit three Nb-Ta-enriched Permian pegmatites were already known, the most prominent being the Li enriched Spodumene-Pegmatite located at the Weinebene (Göd, 1989, Černý et al., 1989), Europe's largest Li deposit. The serendipitous find of a Nb-Ta-enriched pegmatite in the Texel unit (Konzett, 1990) has further strengthened the correlation with the Koralpe-Wölz unit.

This presentation focuses on the pegmatite deposit in the Texel complex which owes its existence to the complex interplay of rifting, subduction und exhumation (Flöss et al., 2012). A wide variety of structural, mineralogical and chemical methods is used to gain new insights into this pegmatite deposit. The data is furthermore correlated with the other alpine deposits offering the unique opportunity to study the genesis of Nb-Ta enriched pegmatites in the context of alpine tectonics.

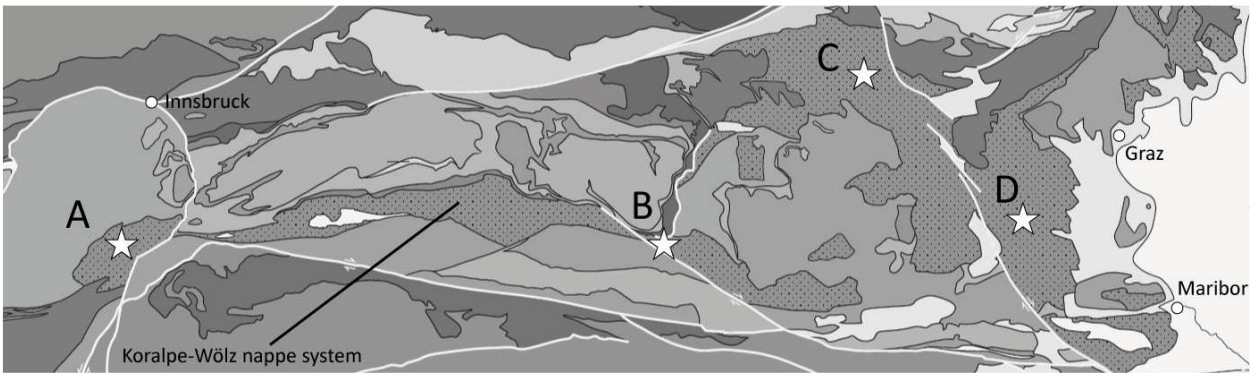


Tectonic map of the Alps showing Nb-Ta-phase bearing pegmatites: A – Texel Complex, B – Spittal an der Drau (Millstatt Complex), C – Pusterwald-Bretstein-Lachtal (Rappold Complex), D – Weinebene-Brandrücken (Koralpe Complex). All pegmatites lie within the Koralpe-Wölz nappe system. Based on the tectonic map of the Alps (Schmid et al., 2004).

**References**

Černý P., Chapman R., Göd R., Niedermayer G., Wise M. A. (1989). Exsolution Intergrowths of Titanian Ferrocolumbite and Niobian Rutile from the Weinebene Spodumene Pegmatites, Carinthia, Austria. Mineralogy and Petrology 40, 197 – 206.

Flöss, D., Pomella, H., Speckbacher, R., Fügenschuh, B., Tropper, P. (2012). Geometry and kinematics of the Eoalpine collision in the western Austroalpine basement units. (submitted)

Göd, R. (1989). The spodumene deposit at "Weinebene", Koralpe, Austria. Mineralium Deposita 24, 270 – 278.

Konzett, J. (1990). Petrologie des zentralen Schneeberger Zugs und des südlich angrenzenden Kristallins im Bereich der Hohen Kreuzspitze, Passeiertal, Südtirol. Unpublished Diploma Thesis, University of Innsbruck.

Schmid, S. M., Fügenschuh, B., Kissling, E., Schuster, R. (2004). Tectonic map and overall architecture of the Alpine orogen. Eclogae geol. Helv. 97, 93-117.

Schuster, R., Stüwe, K. (2008). Permian metamorphic event in the Alps. Geology 36, 603-606.

# Magnetic fabric studies in flood basalts – how to get information on magma flow direction

Stefan Schöbel[1] and Helga de Wall[1]

[1]*GeoZentrum Nordbayern, Universität Erlangen-Nürnberg, D-91054 Erlangen*

The determination of the flow direction in lava flows can be problematic, when macroscopic flow indicators are missing. The anisotropy of the magnetic susceptibility is a sensitive tool, which can provide useful information of the flow characteristics and gives insight into the mechanism of emplacement of massive, featureless lava flows like those forming flood basalt provinces.

Commonly, the principle axes of the AMS ellipsoid are oriented with respect to the flow fabric, whereby $k_{max}$ (magnetic lineation) is aligned parallel to the flow direction and $k_{min}$ normal to the flow boundaries. But this model is not always applicable. One major problem is the occurrence of abnormal fabrics (a phenomenon, where the magnetic axes seem to be transposed). Even samples inside the same flow, situated very close to each other can show a different adjustment of their magnetic axes. Various approaches were made to explain this behavior in the last years. It seems that the origin of these fabrics either lays in the physical-magnetic behavior of the ferromagnetic minerals or originates due to rheological and magmatic processes within the lava flow. Furthermore, in basalts with a high portion of Fe (Ti) Oxides the influence of the magnetic remanence on the magnetic susceptibility needs to be evaluated. The AMS of titanomagnetites with intermediate to high Ti substitution can be influenced by the field amplitude applied during the AMS measurements.

For this key study we sampled a N-S transect of 100 km in the northern part of the Deccan traps in India, the Malwa plateau. The flow thickness typically varies between ten and twenty meters, but much thicker flows also exist. A total of 202 samples have been analysed for the orientation of the AMS principle axes and the shape/ anisotropy of the AMS ellipsoids. The result show that AMS measurements in flood basalts need a thorough flow-evaluation before flow directions can be inferred.

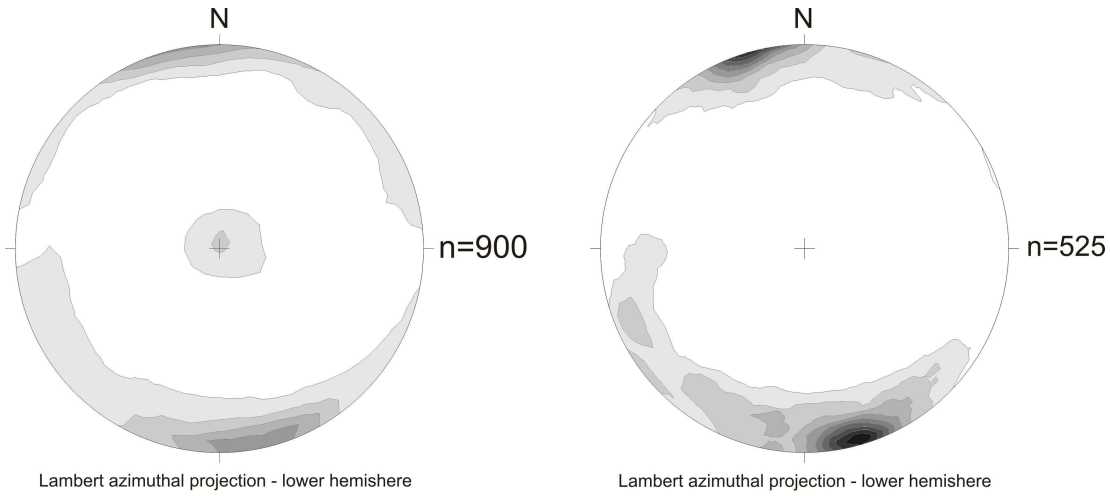


Figure shows density plots of the derivated flow directions for the Malwa plateau before (left) and after (right) flow evaluation.

# Ultrasonic wave velocities during experimental deformation of silty clays from the Nankai accretionary prism

Kai Schumann[1], Michael Stipp[1], Dirk Klaeschen[1] and Jan H. Behrmann[1]

[1] *GEOMAR, Helmholtz-Zentrum für Ozeanforschung Kiel, Wischhofstr. 1-3, D-24148 Kiel*

We have investigated 19 whole-round sediment cores from the shallow frontal thrusts, and the hanging wall to a major active splay fault in the Nankai accretionary prism offshore SW Japan. Cores were recovered during IODP Expeditions 315 and 316. Depth range of the cores is between 48 mbsf (meters below seafloor) and 128 mbsf. Quantitative X-ray diffraction analyses show a rather uniform composition of the silty clay samples. They consist of 16-25 % quartz, 13-34 % feldspar, up to 14 % calcite, and 30-60 % clay minerals. Clays are 16-33 % smectite, 33-45% illite, up to 10 % kaolinite, and 15-30 % chlorite (GUO and UNDERWOOD, 2012). Particle size distributions show 60-85% clay, 10-34% fine silt, 4-8% medium silt and < 0.3% of coarser fractions. The samples were deformed in a triaxial cell, using sample cylinders of 50 mm in diameter and up to 100 mm in length, under consolidated-undrained conditions, confining pressures of 400-1000 kPa, axial displacement rates of 0.01-9.0 mm/min, and up to ~50 % axial compressive strain. Three types of tests were conducted: (1) single step compression experiments at constant confining pressure and displacement rate, (2) pressure stepping compression experiments at constant displacement rate and three different confining pressures, and (3) displacement rate stepping experiments at constant confining pressure and increasing displacement rate.

Bender element velocity measurements were carried out during the triaxial shear tests. While increasing the confining pressure, p- and s-wave velocity measurements were conducted in 100 kPa steps. After reaching the final confining pressure, pore pressure relaxation was ensured by keeping the sample under static conditions overnight. During the deformation phase of the experiment, p- and s-wave velocities were measured in arbitrary time intervals. Incorrect first arrival detection using an automatic single trace algorithm, were identified by sorting the time series data into common shear test gathers. Primary, multiple, and converted phase were identified by seismic time series analysis. Manually picked travel times in the common shear test gathers were used to calculate propagation velocity variations for each experiment. A static correction removed mistakes in detecting the first arrival time. Based on velocity data refinements, systematic changes in the elastic properties can be determined and correlated to changes in bulk density and pore space as well as to compositional and microstructural differences between the samples. Ultrasonic p- and s-wave velocity measurements yielded 300 – 2400 m/s for the p-waves and 100 – 1000 m/s for the s-waves. Plots of $\sigma_{1eff}$ versus the p-wave velocity show two different developments during the experiments. The first group of samples (e.g., K018, displacement rate stepping) shows a strong increase of the p-wave velocity (around 350 m/s) during pressurization, which is attributed to the closure of microcracks. During the single steps, a Vp increase of 200 m/s (first step) and around 100 m/s during the second and third pressure step is observed. The second group, (e.g., K019, displacement rate stepping) shows a p-wave velocity increase of 800 m/s during pressurization and a relatively high velocity level of 1650 m/s thereafter. During the displacement rate steps, Vp is relatively constant and increases only slightly (20 m/s in maximum). Since Vp is an expression of the elastic moduli, which is strongly correlated to diagenetic compaction and tectonic strain, the high velocity level of sample K019 and the constant p-wave velocity during the single displacement rate steps points to an overconsolidation of this sample. Our observations suggest that acoustic velocity is correlated to sample stiffness, effective stress, and may be used as a proxy for the burial and consolidation history.

**Reference**

Guo, J. and Underwood, M. (2012). IODP Expedition 315 and 316, NanTroSEIZE Stage 1

# Synchrotron texture analysis of naturally and experimentally deformed water-rich sediments from the Nankai Trough offshore Japan

Kai Schumann[1], Michael Stipp[1], Bernd Leiss[2] and Jan H. Behrmann[1]

[1] *GEOMAR, Helmholtz-Zentrum für Ozeanforschung Kiel, Wischhofstr. 1-3, D-24148 Kiel;*
[2] *Geowissenschaftliches Zentrum der Universität Göttingen (GZG), Goldschmidtstr.3, D-37077 Göttingen*

Texture analysis of clays and clay rich sediments using standard X-ray goniometry is problematic due to artifacts from sample cutting, high water content and polishing, as well as from severe beam defocussing effects at small 2-theta angles. Because of the short wave lengths (in the range of 0.12 Å) and high energy, synchrotron radiation is a versatile tool for fast multi-mineral phase texture analysis. In contrast to X-ray goniometry, larger sample volumes can be measured, as the synchrotron beam has a penetration depth at mm- to cm-scale, depending on the material. This effectively reduces the surface effects. We have carried out synchrotron texture analysis on a set of mudstone samples from the Nankai trough and accretionary prism offshore Japan. The samples were recovered by IODP expeditions 315, 316 and 333 of the NanTroSEIZE project from a depth range between 25 mbsf (meters below seafloor) and 522 mbsf. Two different groups were analyzed: First, samples were taken as recovered from drilling; second, samples were additionally experimentally deformed in a triaxial deformation apparatus at Kiel University up to axial strains of 46%. Accompanying petrographic and fabric analysis yielded data on composition, grain size, microstructure, and strain. On average, the samples are uniform silty clays composed of approximately 40% clays, 25% quartz, 25% feldspar, and 10% calcite. Grain size fractions range from clay to fine sand, with the clay fraction making up 65-85% of the sample volumes.

Synchotron texture measurements were carried out at the DORIS W2 beam line of the "Deutsches Elektronen Synchrotron" (DESY) in Hamburg, Germany. In order to determine complete pole figures sample cylinders of 2 cm in diameter and 2 cm in length were measured in a phi angle-range from -90 to +90° in 5° steps. A MAR 345 image plate detector was installed at a distance of 1.30 m behind the samples. The detector data were analysed with the help of the MAUD software package (Lutterotti et al., 1997). To fit theoretical spectra to the measured data, background level, sample detector distance, wavelength as well as the necessary cell parameters were set. An E-WIMV algorithm (modified from the WIMV algorithm of Matthies and Vinel, 1982) was used for texture calculation.

Rietveld refinement results using MAUD show that the compositions of the Expedition 333 samples from the incoming plate differ from the relatively uniform Expedition 315 and 316 samples of the accretionary prism. The differences in composition are mirrored by differences in texture. For example specimen 333-C0012C-4H-5 (25 mbsf) is mainly composed of quartz and feldspar (68%) and 24% illite with the illite showing a weak preferred orientation. The accretionary prism samples display textures for illite, kaolinite and montmorillonite. In the depth range between 90 mbsf (sample 315-C0001E-11H-1) and 220 mbsf (sample 316-C0006E-30X-1) there is not a strong change in the degree of crystallographic preferred orientation. One important observation is that the textures relate to bedding parallel compaction rather than to tectonic deformation, as in zones of steep bedding (see Kinoshita et al., 2009) the maxima of poles to basal reflections of the sheet silicates remain at high angles to bedding The synchroton textures can be compared with the shape preferred orientations of sheet silicates seen in scanning electron micrographs (BSE images) of the Expedition 315 and 316 samples.

The results reflect a pioneering effort to use sychrotron radiation to analyze the textures of weakly deformed, highly porous, water-rich material in order to achieve quantitative full 3D texture characterization. Our data are a proof of concept, because the problem can be solved much easier in more compacted and stronger deformed material.

**References**

Lutterotti, L., Bortolotti, M., Ischia, G., Lonardelli, I. and Wenk, H.-R. (2007). Z. Kristallogr.,Suppl. 26, 125-130, 2007.
Matthies, S. and Vinel, G. (1982). Phys. Star. Sol. (b) 112, Klll-Kll4.
Kinoshita, M.; Tobin, H.; Ashi, J.; Kimura, G.; Lallemant, S.; Screaton, E.; Curewitz, D.; Masago, H.; Moe, K.; and the Expedition 314/315/316 Scientists (2009): Proceedings of the Integrated Ocean Drilling Program, Volume 314/315/316

# Metasomatic fault weakening at the Moresby Seamount detachment in the western Woodlark Basin (offshore Papua New Guinea)

Romed Speckbacher[1], Jan H. Behrmann[1], Michael Stipp[1], Thorsten Nagel[2], Julia Mahlke[1] and Colin W. Devey[1]

*[1]Helmholtz-Zentrum für Ozeanforschung Kiel (GEOMAR), D-24148 Kiel , [2]Steinmann-Institut, Universität Bonn, D-53115 Bonn*

The Woodlark Basin (east of Papua New Guinea) is among the most studied examples for an active transition from continental rifting to seafloor spreading. The submerged Moresby Seamount detachment (MSD) is arguably the best exposed active detachment fault in the world, and is the candidate structure for future crustal break and ocean floor spreading. Many experimental studies indicate that continental lithosphere is too strong to be parted by plate tectonic forces, if brittle rupture is to occur in typical crustal rocks. Yet geological evidence suggests that detachment faults in rifts are weak, and can thus operate under low differential stresses. However, nearly three decades of debate have failed to explain how initial crustal weakening and sustained operation of detachment faults occurs. While high fluid pressures assist in maintaining low strength of the faults in the brittle regime, other processes must be in operation to create ductile mylonites (today exhumed at the seafloor) capable of aseismic flow at greater depth. A fundamental process for this could be an enrichment of "weak" minerals, like calcite or quartz in the mylonites.

Using a dredged suite of 8 protoliths, 9 cataclasites and 11 mylonites we carried out whole rock compositional analysis to investigate mass transfer processes, fluid source and fluid flow along the MSD. The results demonstrate that deformation is indeed accompanied by important metasomatic changes, which are driven by a major active hydrothermal system connected to the fault zone. Immobile elements (essentially Zr, Hf, and P) of protoliths and fault rocks provide a reference frame for calculation of material gains and losses during syntectonic alteration. Si, Ca, and to a lesser extent K and Mn were syntectonically enriched throughout the MSD, while there is depletion in Fe, Ti, Mg, and Al. Mass balance calculations show that deformation is accompanied by mass increase whereby 100 g of protolith converts to 149 g of mylonitic fault rock due to the formation of numerous mesoscopic to microscopic quartz and calcite veins and ongoing cataclastic and plastic deformation. The enrichment in quartz and calcite causes the switch from dominant brittle to dominant plastic deformation at low differential stress. Continuous mylonitization is accompanied by continuous weakening of the fault rocks and widening of the fault zone. Maximum estimated flow stress is 72 MPa, inferred from the dynamically recrystallized quartz grain size. The time-integrated fluid flux couples fluid flow and chemical reactions and is calculated as $3x10^5 m^3 m^2$ – $1x10^6 m^3 m^2$, thus quantifying the MSD to be an important fluid conduit. The MSD with its intense metasomatic alteration represents a focused discharge zone of a hydrothermal flow system, likely present from the beginning of detachment operation, and still exhibiting active vents in the lowermost part of the outcropping MSD-surface.

We propose an important genetic link between fracturing, fluid flow, metasomatism, crustal weakening, and the development of the MSD. The release of crust-derived fluids appears to be a mechanism for the localization and long-lasting operation of low angle normal faults in the Woodlark Basin.

# Deformation fabrics of quartz- and calcite-rich mylonites from the Moresby Seamount detachment, Woodlark Basin (offshore Papua New Guinea)

Romed Speckbacher[1], Michael Stipp[1], Florian Heidelbach[2] and Jan H. Behrmann[1]

*[1]Helmholtz-Zentrum für Ozeanforschung Kiel (GEOMAR), D- 24148, [2]Bayrisches Geoinstitut, Universität Bayreuth, D-95440 Bayreuth*

The Woodlark Basin (east of Papua New Guinea) is a classic example of an active transition from continental rifting to seafloor spreading. The submerged Moresby Seamount detachment (MSD) is arguably the best exposed active detachment fault in the world. The fault rock protoliths are dominantly mafic (gabbros, dolerites). Yet we observed fault rocks derived from these protoliths, which are rich in quartz and calcite. We infer that the infiltration of calcite and quartz by hydrothermal fluids is deformation related and an important weakening process along the MSD.

To better understand the deformation switch from cataclasis to plastic flow and related weakening in the MSD we analyzed the deformation fabrics of the fault rocks by ligh-optical and crystallographic preferred orientation (CPO) measurements that were carried out based on automatically indexed electron backscatter diffraction patterns. The mylonitic fabric displays a small grain size and a polyphase composition comprising not only quartz and calcite, but also feldspar, chlorite, mica and minor phases. Chlorite forms either the foliation or represents a darkish, ultra-fine-grained chlorite matrix. Quartz displays subgrain rotation and bulging recrystallization microstructures. Calcite is arranged in layers (stretched aggregates) and/or disseminated in the mylonitic matrix.

The calcite porphyroclasts and recrystallized grains display c-axis pole figures with maxima close to Z. Related a-axis orientations are subparallel to the XY-plane. These CPOs are indicative of dominant slip on the basal plane. The quartz CPOs, however, are weaker and more difficult to interpret. C-axis pole figures display weak cross girdle fabrics which appear to be rotated about 30-60° around the Y-direction. Strongest CPOs are shown by the r- and z-rhomboeder planes. The weak CPOs suggest that the accommodated strain is low or that other deformation mechanism than dislocation creep considerably contribute to strain accommodation in quartz.

The results indicate that the strong stretching lineation of the fine-grained MSD mylonite samples is mainly formed by calcite, as the calcite pole figures correspond to the kinematic framework. The quartz pole figures are in an oblique orientation to foliation and stretching lineation suggesting a rotation or relocation of the fabric after plastic flow of quartz. The following rheological development is proposed for the MSD: The detachment originally operated by cataclasis accompanied by quartz and subsequent calcite veining. When the amount of quartz was high enough to cause a switch from dominant brittle to dominant plastic deformation, monophase quartz layers (former veins) deformed by dislocation creep, while fine-grained aggregates of quartz, feldspar, chlorite and mica deformed by diffusion creep. At least in the quartz layers, strain accommodation was low. As soon as the amount of precipitated calcite was high enough to form interconnected weak layers, plastic flow of calcite accommodates most of the deformation as indicated by a strong mylonitic fabric. Hence, the MSD is characterized by a continuous weakening during ongoing activity. From cataclasis to finally plastic flow of calcite shearing of the detachment required less and less differential stress.

# Triaxial deformation experiments indicate strong sediments at the deformation front, and weak sediments at the rear of the Nankai accretionary prism

Michael Stipp [1], Malte Rolfs [2], Yujin Kitamura [3] and Jan H. Behrmann [1]

*[1]Helmholtz-Zentrum für Ozeanforschung Kiel (GEOMAR, Germany), [2] TU Hamburg-Harburg (Germany), [3] JAMSTEC, Yokusuka (Japan)*

The NanTroSEIZE (Nankai Trough Seismogenic Zone Experiment) drilling project of IODP in the SW Japan forearc is the first-ever attempt to core and instrument the updip end of the seismogenic part of a subduction zone. For the tsunamigenic potential of the active frontal thrust system in the Nankai accretionary prism it is important to know if the sediments are dominated by localized brittle deformation and related near-surface fault slip, or alternatively, by distributed deformation and strain weakening causing a strain-dissipative creep-like behavior. To answer this question, 17 core samples of IODP expeditions 315 and 316 (e.g., Kinoshita et al., 2009) from a depth range of 48-128 m below sea floor were experimentally deformed in a triaxial cell using sample cylinders (5 cm in diameter, up to 10 cm in length) under consolidated and undrained conditions at confining pressures of 400-1000 kPa, room temperature, axial displacement rates of 0.005-0.1 mm/min and up to axial compressive strains of ~48%.

After saturation and consolidation geotechnical deformation tests at constant confining pressure and displacement rate were performed in compression. Despite the consistent low depth range and the lithological similarity of the sample cores, the samples can be separated into two distinct 'rheological groups'. The first sample group shows deviatoric peak stress after only a few percent of compressional strain (<10%) and a continuous stress decrease after peak conditions. Simultaneous to this decrease there is a pore pressure increase indicating contractant behavior characteristic of structurally weak material (e.g. Sultan et al., 2004). The second sample group does not weaken at all, but displays strengthening characteristics until finite strain. These samples are structurally strong (e.g. Sultan et al., 2004), and they are characterized by a decreasing pore pressure with increasing compressional strain indicating dilatant behavior after a maximum pore pressure at <10% strain. A few exceptional samples with somewhat intermediate behavior weaken only moderately to a relatively high residual strength level or they show a steady-state like behavior at constant deviatioric stress. Their pore pressure/strain-relationships correspond more or less to what is commonly expected for structurally weak material with some slight variations.

The structurally strong samples tend to be overconsolidated and are all from the drill holes at the toe of the accretionary prism, while the weak and preferentially underconsolidated samples are from the hanging wall of the Megasplay fault. This geomechanical characterization corresponds to the tectonic disposition of more distributed deformation and folding at the prism toe and strong faulting and localized deformation in the Megasplay zone. Hence, we postulate that brittle faulting of the structurally weak sediments of the Megasplay zone in response to a large seismic event is capable of producing surface breaks generating tsunamis. In contrast, the structurally strong sediments from the accretionary prism toe are more amenable to slow, stable slip and distributed deformation (folding) within large volumes. The observed difference in rheological behavior is therefore a key for understanding strain concentration and brittle faulting within the rather uniform silty and clayey sedimentary sequence of the Nankai accretionary prism.

**References**

Kinoshita, M., Tobin, H., Ashi, J., Kimura, G., Lallemant, S., Screaton, E.J., Curewitz, D., Masago, H., Moe, K.T., and the Expedition 314/315/316 Scientists (2009). Proc. IODP, 314/315/316: Washington, DC (Integrated Ocean Drilling Program Management International, Inc.). doi:10.2204/iodp.proc.314315316.2009

Sultan, N., Cochonat, P., Canals, M., Cattaneo, A., Dennielou, B., Haflidason, H., Laberg, J.S., Long, D., Mienert, J., Trincardi, F., Urgeles, R., Vorren, T.O. & Wilson, C. (2004). In: COSTA, continental slope stability; a contribution to the Energy, Environment and Sustainable Development Programme FP5 of the European Commission, number EVK3-CT-1999-00006, Elsevier, Amsterdam, pp. 291-321.

# Experimental deformation of partially molten aplite in simple shear

Michael Stipp [1], Jan Tullis [2] and Alfons Berger [3]

*[1]Helmholtz-Zentrum für Ozeanforschung Kiel (GEOMAR), [2]Department of Geological Sciences, Brown University, Providence (USA), [3]Department of Geography and Geology, University of Copenhagen (Denmark)*

The strength of the intermediate and lower crust is significantly affected by partial melting depending mainly on rock composition and geothermal gradient. The tectonic processes which are important for melt distribution and transport and which result in crustal weakening are not yet well understood. Natural migmatites are usually overprinted by annealing and retrogression during uplift and exhumation, largely obliterating the deformation structures and microstructures of their partially molten history. Deformation experiments on partially molten crustal rocks have so far been conducted in pure shear geometry and mostly under low confining pressures in the brittle deformation field, both of which are not representative of nature. We carried out deformation experiments in simple shear that predominates in the crust and especially crustal shear zones. Undrained experiments were carried out on Enfield aplite at ~1.5 GPa, 900°-1000°C, and $\leq 5*10^{-6}$ $s^{-1}$, conditions which favor crystal plastic deformation of quartz and feldspar (Dell'Angelo and Tullis, 1988). Sample slices 1.0-1.5 mm thick were placed between the shear pistons with the shear plane at a 45°-angle to the compression direction. Maximum shear strain in the experiments is $\gamma \approx 2.8$. Despite difficulties in controlling the melt content by varying the amount of added water, we were able to achieve the full range of brittle to crystal plastic deformation mechanisms. With decreasing melt content Enfield aplite displays a transition from discrete fracturing at a high angle (~70-90°) to the shear plane (>20 vol.% melt), to cataclastic shearing (10 - 20 vol.% melt) and to crystal plastic deformation (<10 vol.% melt) with shear bands at a lower angle (~10-50°). Stress-strain records of the cataclastically and plastically sheared samples display significant weakening after yielding, while some of the fractured samples with high melt content were weak from the beginning of shearing. The strong dependence of deformation mechanism on melt content is primarily due to the undrained experimental conditions; drained conditions were technically not feasible in our high pressure/high temperature set-up. Similar transitions in deformation mechanisms have been observed with increasing temperature or decreasing strain rate (decreasing differential stress). Plastic deformation of the aplite is indicated by dynamic recrystallization microstructures of quartz and initially also of albitic plagioclase. Fine-grained polyphase shear band layers of plagioclase, quartz, K-feldspar and some mica and other minor mineral phases are suggestive of diffusion creep and grain boundary sliding. Melt is concentrated along shear bands. In the samples with dominantly cataclastic and brittle deformation, the segregation of the melt and the transport inside the fractures appears to be more effective as most of the melt occurs in the fractures and at the sample-piston interface and not distributed as it is the case in the plastically deformed samples. Melt concentration during plastic deformation causes weakening (e. g., Holtzman et al., 2003) that adds to the likely weakening by grain size reduction and by shear zone/shear band-formation in these samples. The combination of these processes might result in local weakening of the intermediate and lower crust.

**References**

Dell'Angelo L.N. and Tullis J. (1988). J. Metam. Geol. 6 (4), 495-515.

Holtzman, B. K., Groebner N. J., Zimmerman M. E., Ginsberg S. B. & Kohlstedt D. L. (2003). Geochem. Geophys. Geosys. 4, Art. No. 8607.

# Fluid-enabled inversion of half-grabens in unconsolidated Upper Pleistocene sands

David C. Tanner[1], Christian Brandes[2] and Jutta Winsemann[2]

[1]*Leibniz Institute for Applied Geophysics (LIAG), Stilleweg 2, 30655 Hannover, Germany*
[2]*Institut für Geologie, Leibniz Universität Hannover, Callinstr. 30, 30167 Hannover, Germany*

In an open sand pit near the Osning Thrust, an Upper Pleistocene alluvial-aeolian complex (the so-called Upper Senne) is exposed. These unconsolidated sediments contain a set of syn-sedimentary half-grabens that have been partly inverted (see figure). We connect the structural development with the lithospheric stresses caused by the Late Pleistocene ice sheet and related movement on the Osning Thrust (Brandes et al., in press).

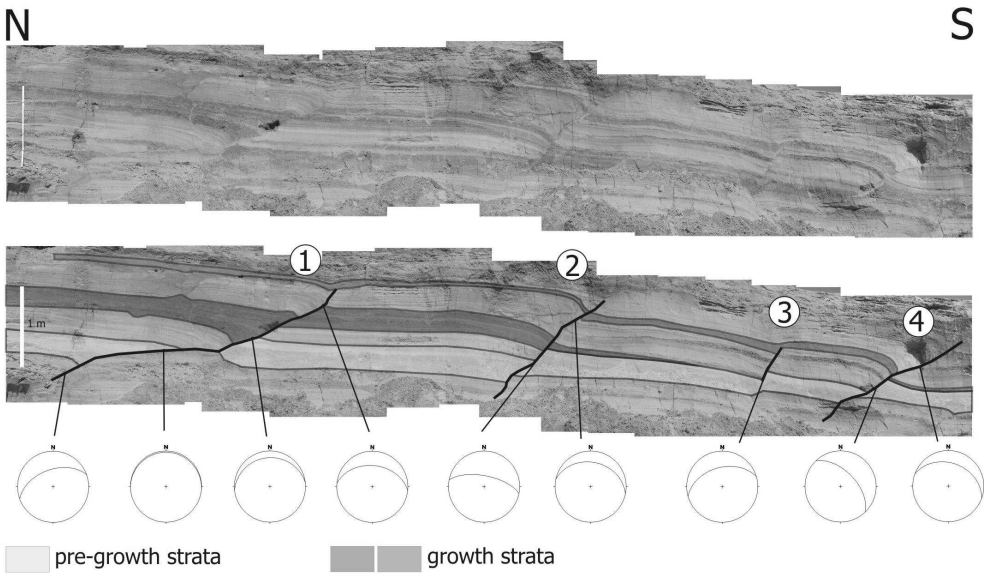


Fig. 1: Series of inverted half-graben structures exposed in the Oerlinghausen sand pit. Note the thickening of beds towards the fault, indicative of syn-sedimentary movement. The stereographic projections show the consistent northward dip of the faults. The panel shows the outcrop situation in May 2009. Scale bar 1m, (taken from Brandes et al., in press).

The "graben bounding faults" are only distinguishable by their (lighter) colouring (see figure). They are thin (1-3 cm thick) and, as can be seen, there was no shortcutting during inversion. Material in the fault zone is unconsolidated and partly consists of fluidized sand that was mobilized by overpressured porewater during earthquakes (Brandes & Winsemann, subm.). There is widespread evidence for excess pore pressure during seismic activity (i.e. sand-blows, Brandes & Winsemann, subm.). In some cases fluids from sand dykes can be seen to have migrated preferentially into the faults. We propose that the fault material was more porous than the surrounding material and used the resulting fluid capture during overpressuring to allow the inversion to take place.

**References**

Brandes, C., Winsemann, J., Meinsen, J., Roskosch, J., Tsukamoto, S., Frechen, M., Tanner, D.C., Steffen, H. & Wu, P. (in press): Activity along the Osning Thrust in Central Europe during the Late Glacial: ice-sheet and lithosphere interactions. Quaternary Science Reviews.

Brandes & Winsemann (subm.): Soft sediment deformation structures in NW Germany caused by Late Glacial seismicity.

# Scales of deformation within a compressional flower structure modelled by varying the amount of fault-zone complexity

David C. Tanner[1], Steffen Prüfer[2], Dirk Kuhn[2] and Charlotte M. Krawczyk[1]

[1]*Leibniz Institute for Applied Geophysics (LIAG), Stilleweg 2, 30655 Hannover, Germany*
[2]*Federal Institute for Geosciences and Natural Resources, Stilleweg 2, 30655 Hannover, Germany*

We analysed a 120m long and 20m high fault zone within Triassic limestones. It form part of a transpressive positive flower structure that outcrops in the Leine Valley in the central German state of Lower Saxony. The fault surface topography was determined with a LIDAR device with a spatial resolution of 4 cm. We ascertained 5 fabrics on the fault surface, they are, in order of decreasing size:

1. 20m long and 5m short segments, which are Riedel shear surfaces,
2. each long segments is helicoidal,
3. a strong relationship between fault angle and bedding stiffness,
4. ca. 4m wide zones of positive and negative Gaussian curvature, and
5. a dip-direction parallel fabric with amplitudes of ca. 5 cm.

Our analysis shows this was a sinistral strike-slip fault that was later reactivated as a dip-slip thrust.

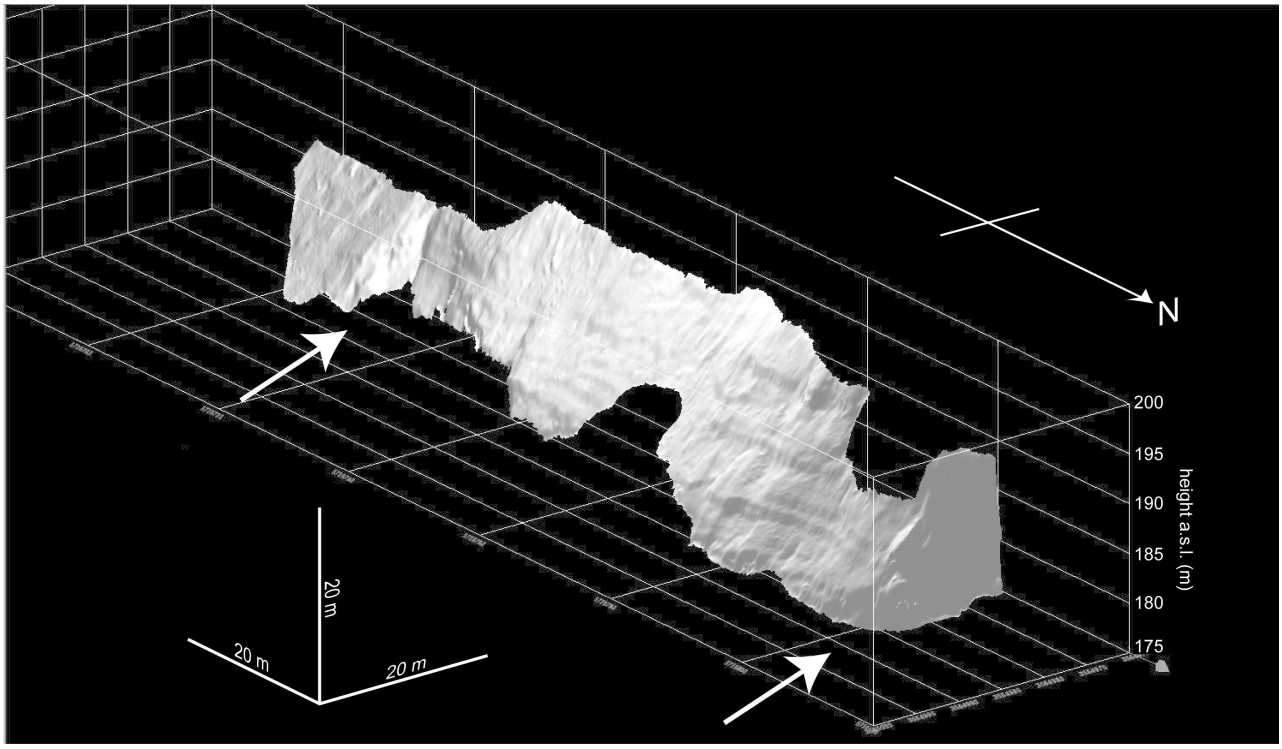


Oblique shaded-relief image of the fault as determined by LIDAR. Short segments are indicated by arrows. Fabrics 1-3, as mentioned in the text, can be seen in the relief.

Using the fault geometry reduced to the different scales of the fabrics, we show the resulting strain around the fault when the fault blocks are kinematically displaced. The strain distribution is determined by the kinematics and fault geometry, the strain quantities increases with the resolution of the model. We show how simplification of the fault geometry can lead to gross underestimation of the related strain in the fault near-field.

# Intra-oceanic subduction initiation caused by shear heating: What are the odds?

Marcel Thielmann[1] and Boris J.P. Kaus[2]

*[1]Institut für Geophysik, ETH Zürich, CH-8092 Zürich, [2] Institut für Geowissenschaften, Johannes Gutenberg-Universität Mainz, D-55128*

Subduction is one of the main features of plate tectonics, yet it remains unclear how subduction started on Earth. Shear heating has been proposed to play an important role in i) creating deep focus as well as intermediate-depth earthquakes (Ogawa, 1987) and ii) creating lithospheric-scale shear zones, thus creating a weak decoupling interface that enables subsequent subduction initiation.

To understand the physics of this mechanisms, Kaus & Podladchikov, 2006 conducted a scaling analysis for simplified viscoelastoplastic rheologies and found that the boundary between localization and no localization is quite sharp. Crameri & Kaus (2010) and Lu, Kaus, & Zhao (2011) extended this analysis to more realistic lithospheric setups and demonstrated that shear heating induced lithospheric-scale localization might occur for Earth-like parameters. It is however unclear if a lithospheric-scale shear zones on its own evolves into a subduction zone.

Here, we use numerical models to adress the question of shear heating induced subduction initiation. In the framework of our models, we can identify four different regimes, of which two show subduction initiation. We then develop scaling laws that are able to predict the behaviour of our models, thus providing means to better understand the physics of shear heating induced subduction initiation.

Our results suggest that shear heating induced subduction initiation is more likely to initate in a lithosphere consisting of dry olivine rather than wet olivine. A large plate age does not necessarily increase the potential for subduction initiation, as it increases the potential for convective instabilities to occur.

**References**

Crameri, F., & Kaus, B. (2010). Parameters that control lithospheric-scale thermal localization on terrestrial planets. *Geophysical Research Letters, 37, doi:10.1029/2010GL042921*

Kaus, B., & Podladchikov, Y. (2006). Initiation of localized shear zones in viscoelastoplastic rocks. *Journal of Geophysical Research, 111, doi:10.1029/2005JB003652*

Lu, G., Kaus, B., & Zhao, L. (2011). Thermal localization as a potential mechanism to rift cratons. *Physics of the Earth and Planetary Interiors, 111, doi:10.1029/2005JB003652*

Ogawa, M. (1987). Shear instability in a viscoelastic material as the cause of deep focus earthquakes. *Journal of Geophysical Research, 92, 13,801-13,810*

# Microfabrics and deformation mechanisms of hydrocarbon-bearing Gorleben rock salt

Nicolas Thiemeyer[1], Maximilian Pusch[2], Jörg Hammer[2] and Gernold Zulauf[1]

*[1]Institut für Geowissenschaften, Goethe-Universität Frankfurt, D-60438 Frankfurt, [2]Bundesanstalt für Geowissenschaften und Rohstoffe (BGR), D-30655 Hannover*

The Gorleben salt dome in northern Germany has been investigated for the last decades as a possible site for nuclear waste disposal. Rock salt is very suitable as host rock for waste disposal, because of the specific barrier properties of rock salt (low permeability, low porosity and low water content). Although the fluid-controlled deformation mechanisms of rock salt are well known (e. g. Schulze, 2007, Urai & Spiers, 2007), the behaviour and the pathways of fluids during diapiric emplacement of salt are not completely understood.

Hydrocarbons are assumed to migrate from subjacent Zechstein carbonates into the Gorleben salt dome (mostly autochthonous Zechstein products from thermal alteration of the organic matter of the Staßfurt-Karbonat, Gerling et al. 2002, Bornemann et al., 2008). They occur f.i. in the cross cut 1 west in the first exploration area (EB1) and play a significant role in the discussion about the suitability of the Gorleben salt dome as an adequate storage place for highly active nuclear waste. The distribution of these hydrocarbons within the salt dome is object of geological exploration restarted in November 2010. Our structural research is focused on the relation between strain and hydrocarbon distribution in the Gorleben Hauptsalz (z2HS).

Samples from 6 m long horizontal drill cores from cross cut 1 west (depth ca. 840 m) reveal presence of fluid inclusions (brines and hydrocarbons) at different sites: (1) halite grain boundaries, (2) anhydrite clusters or inclusions, (3) artificial cracks in EDZ samples or caused by sample preparation. Fluid inclusions occur in various shapes. Bubbles, stripes, branching networks, vermicular lines and fluid films display a manifold inventory of different types of fluid inclusions. Especially intracrystalline anhydrite inclusions are covered by stripes and bubbles of fluids. Fluorescence microscopy shows that artificial cracks may contain thin films of hydrocarbons, the latter entering immediately after cracking. For this reason, brittle fractures (originating during intensive diapiric uprise or from EDZ and sample preparation) seem to be the main pathways for fluid migration across salt structures (see Zulauf et al., 2010). Additionally, clusters of anhydrite crystals have trapped hydrocarbons due to their enhanced porosity.

The halite grains reveal strong subgrain fabrics. Average subgrain sizes are ranging from 113 to 231 µm and indicate low stress differences (0.9 – 1.8 MPa). The differential stress does not show a correlation with the amount of hydrocarbons. EBSD analyses of halite suggest that subgrain rotation recrystallization (SGR) played a minor role as is shown by the majority of the misorientation angles of the subgrains.

**References**

Bornemann, O., Behlau, J., Fischbeck, R., Hammer, J., Jaritz, W., Keller, S., Mingerzahn, G. and Schramm, M. (2008). Standortbeschreibung Gorleben, Teil III: Ergebnisse der über- und untertägigen Erkundung des Salinars. Geol. Jahrbuch, Reihe C, 73 (2008), 211 S.

Gerling, P., Faber, E. & Wehner, H. (2002): Interpretation der chemischen Analysen von gasförmigen und flüssigen Kohlenwasserstoffen, BGR-Bericht, Tagebuch-Nr. 12243/02, 82 S.

Schulze, O. (2007): Investigations on damage and healing of rock salt.- In Wallner, M., Lux, K.-H., Minkley, W. and Hardy Jr, H.R. (Eds.), The Mechanical Behavior of Salt – Understanding of THMC Processes in Salt. Taylor & Francis Group, London, pp. 33-43.

Urai, J.L. and Spiers, C.J., 2007. The effect of grain boundary water on deformation mechanisms and the rheology of rocksalt during long-term deformation. In Wallner, M., Lux, K.-H., Minkley, W. and Hardy Jr., H.R. (Eds.), The Mechanical Behavior of Salt – Understanding of THMC Processes in Salt. Taylor & Francis Group, London, pp. 149–158.

Zulauf, G., Zulauf, J., Bornemann, O., Brenker, F. E., Höfer, H. E., Peinl, M., Woodland, A. B., 2009. Experimental deformation of a single-layer anhydrite in halite matrix under bulk constriction. Part 2: Deformation mechanisms and the role of fluids. J. Struct. Geol. 31, pp. 460-474.

# Deformation mechanisms active during catastrophic rock failure: preliminary results.

Trullenque, G., Kenkmann, T. and Stein E.

*Institut für Geowissenschaften, Geologie, Albert-Ludwigs-Universität Freiburg, Albertstr. 23b, 79104 Freiburg im Breisgau*

A number of catastrophic geological scenarios such as earthquakes, landslides, or meteorite impacts are characterized by a sudden stress release following a period of short or long lasting loading. From the study of naturally deformed rocks we suggest that a considerable amount of deformation is occurring during this highly dynamic phase of unloading. To test this hypothesis deformation experiments under triaxial conditions ($\sigma1$, $\sigma2 = \sigma3$) have been performed on gabbro and granite samples from the Odenwald massif (Germany).

The starting material presents a homogeneous microstructure free from internal deformation. Cylindrical samples of 100 mm diameter and 200 mm length have been used for this study.

The experimental set up consists of an externally heated pressure vessel mounted on a frame able to produce uniaxial loads up to 3000 kN. The chosen experimental conditions are a sample confining pressure of 1500 bars and sample temperature of 200°C. This corresponds to a depth of 8 km assuming a geothermal gradient of 25°C/km.

Catastrophic rock failure is produced by a sudden release of confining pressure, according to a procedure tested by Weiss and Wenk (1983) on a modified Griggs apparatus. In our case, a complete release of confining pressure is achieved within 5 seconds due to the very low viscosity of the confining medium. Sample failure occurs within this time interval.

The produced deformation zone consists of a sharp diagonal fracture inclined about 60° from sample long axis.

The material present on the fracture walls consists of a pulverulent layer of about 1 mm thickness, white in color. SEM investigations reveal the presence of a very fine comminuted material, at sub-micrometer in size.

Further energy dispersive spectrometry and X-ray diffraction analyses are planned to characterize in more details the nature of this fault gauge.

**References**

Weiss and Wenk (1983): Experimentally produced pseudotachylite in Gabbro. Tectonophysics 96, 299-310.

# The long-term creep behavior of rock salt in nature *

Janos Urai[1], Frank Strozyk[2], Joyce Schmatz[1], Shiyuan Li[1], Guillaume Desbois[1] and Peter Kukla[2]

*[1]Structural Geology, Tectonics and Geomechanics, RWTH-Aachen University, Germany, [2]Geological Institute, RWTH Aachen University, Germany*

The rheology of rocksalt under low differential stress and very low strain rates is of fundamental importance for the predictions of long-term stability of nuclear waste repositories, and our understanding of the dynamics of salt-related sedimentary basins which host the majority of oil and gas accumulations on Earth, but estimates of this rheology vary over many orders of magnitude and are subject of much controversy.

Here we compare (i) in 3D seismic images of the Zechstein salt giant in NW-Europe the position, shape and density of isolated Anhydrite - Dolomite inclusions formed by tectonic disruption of initial sedimentary layer, and (ii) estimates of their gravitational sinking velocity over the Tertiary, with (iii) numerical simulation of the gravitational sinking of these inclusions through salt over geologic time using the competing rheologies (Newtonian and Power-law) corresponding to solution-precipitation creep and dislocation creep and conclude that the salt surrounding the inclusions can not have deformed by Newtonian solution-precipitation creep because the inclusions would have sunk to the bottom of the salt during the 60 Ma of tectonically quiet Tertiary.

This is in agreement with the ubiquitous structure of grain boundaries in Zechstein salt, in which the small but omnipresent brine phase is arranged in isolated fluid inclusions separated by water-free grain boundary which does not allow solution-precipitation processes so that the only possible deformation mechanism is dislocation creep. Recent results show that at the differential stress levels found around the stringers the grain boundary fluid films indeed evolve into such grain boundary inclusion arrays. Our results provide strong constraints for the long-term rheology of Zechstein salt, and point to a complex, as yet poorly understood constitutive behavior under conditions where these grain boundary films are activated and deactivated in a nuclear waste repository.

* Presented at the workshop *"Significance of long-term deformation and permeability of rock salt and clay for storage and waste disposal"*

# Evaluation of Crystallographic Preferred Orientations applying whole pattern deconvolution method

Roman Vasin[1] and Klaus Ullemeyer[2]

[1]*Frank Laboratory of Neutron Physics, 141980 Dubna, Russia,* [2]*Institut für Geowissenschaften, Universität Kiel, D-14098 Kiel*

Quantitative texture analysis (QTA; texture = crystallographic preferred orientation) of polycrystals is usually performed on a small number of diffraction pole figures. In Geosciences, this is practical for monophase samples and, from time to time, for samples consisting of only few high-symmetrical mineral phases. However, many rocks consist of low-symmetrical constituents and/or the number of constituents is large, leading to complex diffraction patterns with many peak overlaps. In such cases a different approach is recommended.

If diffraction patterns comprising a sufficiently wide *d*-range (*d*: lattice spacing) are recorded, the concept of RIETVELD structural refinement can be combined with the QTA. Rietveld (1969) introduced a method to evaluate the crystal structure from a powder sample diffraction pattern. Analytical functions were added later on to the basal algorithm, allowing for simple texture corrections (e.g., Dollase 1986). More recently, methods of modern texture analysis were included, leading to the possibility to determine crystal structure, texture and residual strain simultaneously (Von Dreele, 1997; Lutterotti et al., 1997). Particular algorithms are implemented in the GSAS and MAUD software packages (Larson and Von Dreele 2004; Wenk et al. 2010). In the following we use the MAUD software to evaluate the mineral textures of a retrograded eclogite sample* and to demonstrate the advantage of so-called 'Rietveld Texture Analysis' (RTA) over QTA from diffraction pole figures.

Diffraction spectra were recorded at the TOF neutron diffractometer SKAT in Dubna, Russia (Ullemeyer et al. 1998) using a 5x5° measuring grid (this infers, that in total 1368 spectra have been obtained from the sample). First, as many pole figures as possible were extracted from the diffraction spectra and QTA was performed applying the WIMV algorithm (Matthies and Vinel 1982). QTA was possible for two phases only (almandine, omphacite), for both phases peak overlaps with low-intensity reflections of the other rock constituents had to be accepted. Second, RTA was applied to the same set of diffraction spectra, revealing the textures of all rock constituents.

The random texture of almandine can be confirmed by both methods, whereas corresponding recalculated pole figures of omphacite show differences. The muscovite (001) pole figure obtained by means of RTA and the experimental muscovite (001) pole figure are different as well. All the observed discrepancies can be mainly attributed to the fact that the pole figure extraction from complex diffraction spectra is usually not free from peak overlaps, at least leading to erroneous texture determinations. This may be of particular importance for the prediction of the anisotropic physical rock properties from the mineral textures. Modelling the elastic moduli of bulk rock as an example shows that, in fact, differences are valid.

The results indicate that RTA offers advantages over standard QTA. In particular, the textures of all phases in polymineralic rocks can be determined due to an important property of applied method: the deconvolution of the recorded experimental spectrum into particular mineral spectra. Also, phase volume fraction could easily be obtained from the same set of data. Nevertheless, we want to point out that 'high quality' input data are essential and that the textures of phases with low volume fractions should be judged with care.

* consisting of almandine 23.8%, omphacite 37.5%, muscovite 19.3%, quartz 4.0%, albite 9.6%, hornblende 5.8%.

**References**

Dollase, W.A. (1986). J. Appl. Cryst. 19, 267-272.
Lutterotti, L., S. Matthies, H.-R. Wenk, A.J. Schultz and J. Richardson (1997). J. Appl. Phys. 81[2], 594-600.
Rietveld, H.M. (1969). J. Appl. Cryst. 2, 65-71.
Matthies, S. and Vinel, G.W. (1982). Phys. Status Solidi B 112, 111-120.
Ullemeyer, K., P. Spalthoff, J. Heinitz, N.N. Isakov, A.N. Nikitin and K. Weber (1998). Nucl. Instrum. Methods Phys. Res. 412, 80-88.
Von Dreele, R. (1997). J. Appl. Cryst. 30, 517-525.

# Heat flow in the Southern Chile Forearc controlled by large-scale tectonic processes

Lucia Villar-Muñoz[1], Juan Diaz-Naveas[2] and Jan H. Behrmann[1]

*[1]GEOMAR, Helmholtz-Zentrum für Ozeanforschung, Wischhofstr. 1-3, D-24148 Kiel, [2]Escuela de Ciencias del Mar, Pontificia Universidad Católica de Valparaíso, Av. Altamirano 1480, Valparaíso, Chile*

From north to south, the Southern Chile forearc is affected by the subduction of the aseismic Juan Fernandez Ridge, a number of major oceanic fracture zones on the downgoing Nazca Plate, the active Chile Ridge spreading center, and underthrusting of the Antarctic Plate. The tectonic structure is characterized by intense deformation of the lower continental slope within a variably wide accretionary wedge. In places the middle and upper slope is affected by out-of-sequence overthrusting and by normal faulting. In the area of the Chile Triple Junction at 46°S latitude most of the forearc is destroyed by subduction erosion, to be rebuilt further south by sediment offscraping and accretion from the Antarctic Plate.

The Southern Chile forearc has been intensively explored by reflection seismic surveys, and has been drilled by the Ocean Drilling Program during two expeditions (ODP Leg 141 - Behrmann et al., 1992; ODP Leg 202 – Mix et al., 2003). The widespread occurrence of gas hydrates has been known for some time. Regarding the analysis of reflection seismic sections we have used data of R/V SONNE Expeditions 101 and 161, R/V VIDAL GORMAZ Expeditions VG02 and VG06, and R/V ROBERT CONRAD Cruises RC2901 and RC2902. Using bottom water temperature data obtained from the World Ocean Data Base (NOAA) and an acoustic velocity model constrained from the seismic sections, and measurements of temperature, thermal conductivity and acoustic velocity from ODP boreholes, we use the position of the Bottom Simulating Reflector (BSR) in reflection seismic sections to estimate the heat flow through the forearc in an area between 32°S and 47°S latitude.

Heat flow in most of the upper and middle continental slope is on the order of 50-80 $mWm^{-2}$. This is normal for continental basement and overlying slope sediments, and is true also for those parts in the south of the area that are being underthrusted by hot, young oceanic crust. The middle and lower slopes, however, in some places display up to 50% increased heat flow. Here the sea floor is underlain by zones of active deformation and accretionary wedge building. This observation cannot be easily reconciled with models of conductive heat transfer, but is an indication that advecting pore fluids from deeper in the subduction zone may transport a substantial part of the heat there. The size of the anomalies indicates that fluid advection and outflow at the sea floor is diffuse rather than being restricted to individual fault structures, or mud volcanoes and mud mounds, as is the case in other convergent margins.

Two large areas with higher heat flow correlate in space with tectonic phenomena, however. Firstly, on the lower slope above the subducting Chile Ridge at 46°S, values of up to 280 $mWm^{-2}$ indicate that the overriding South American Plate is effectively heated by subjacent zero-age oceanic plate material on a regional scale. Secondly, offshore Valparaiso, the projection of the subducting Juan Fernandez Ridge defines a large area of scattered positive heat flow maxima located on the middle continental slope, and broadly connected to the Valparaiso Basin. We suspect that these could be connected to zones of increased hydraulic conductivity at depth in response to deformation and fracturing above the subducting Juan Fernandez Ridge.

**References**

Behrmann, J.H., Lewis, S.D., Musgrave R., et al. (1992) Proceedings of the Ocean Drilling Program, Initial Reports, 141. Ocean Drilling Program. College Station, TX

Mix, A.C., Tiedemann, R., Blum, P., et al. (2003) Proceedings of the Ocean Drilling Program Initial Reports, 202. Ocean Drilling Program, College Station, TX.

# Terrane accretion at active continental margins: Numerical Modelling

Katharina Vogt[1] and Taras V. Gerya[1,2]

*[1] Institute of Geophysics, Swiss Federal Institute of Technology (ETH-Zurich), CH-8092 Zurich, [2] Institute of Geology, Moscow State University, RUS-119899 Moscow*

The oceanic floor contains allochthonous terranes (extinct ridges and arcs, continental fragments and volcanic piles) that move with the oceanic crust and may collide with continental margins to form collisional orogens that are believed to have contributed to the growth of the continental crust (e.g. Ben-Avraham et al., 1981).

The dynamics of terrane accretion and its implication in relation to crustal growth were analyzed using a thermomechanical-pertological numerical model of an oceanic-continental subduction zone. The model is based on the i2vis code (Gerya and Yuen, 2003), that solves the governing equations of mass, momentum and energy for a viscous-plastic rheology.

Our results indicate that allochthonous terranes may subduct or accrete depending on their rheological strength and the negative buoyancy of the downgoing slab, which is imposed by its thermal structure.

Subduction of cold and dense oceanic lithosphere coupled with the collsion of rheologically strong terranes results in deep subdution. Crustal material may be subducted back into the mantle or be incorporated into active arcs that form above the overriding plate. Terranes with a weak crustal structure that are embedded in young oceanic lithosphere are less prone to subduction and may be accreted in form of collisional orogens and accreted terranes. Weak crustal material is scrapped off the downgoing plate and added to the continental margin, which leads to rapid growth of the continental crust and may result in plate failure associated with slab break off. In cases where slab break off occurs a new subduction zone is formed behind the accreted terrane.

**References**

Ben-Avraham, Z., Nur, A., Jones, D., and Cox, A. (1981). Science 213, 47-54.

Gerya, T. V. and Yuen, D. A. (2003). Physics of the Earth an Planetary Interiors 140 , 293–318.

# Tectonic control on submarine mass wasting off Central Chile

David Völker and Jacob Geersen

*GEOMAR | Helmholtz Centre for Ocean Research, Wischhofstr. 1-3D-24148 Kiel, Germany*

Submarine landslides are an important but underestimated geological hazard. They can destroy offshore installations like cables and oil platforms, and generate destructive tsunamis that can devastate populated shorelines regionally. Off Central and Southern Chile more than 60 submarine landslides were identified based on a unique bathymetric dataset that was continuously extended and refined over 16 years and 16 scientific cruises and that now covers ~ 90% of the continental margin. Despite of the good documentation, still little is known about the mechanisms that caused the individual slope failure events, about the frequency of such events and their relation to the powerful earthquakes that happen here each 50-100 years.

To investigate the preconditioning and triggering mechanisms for the landslides we combine the high resolution swath bathymetric data set with reflection seismic profiles and sediment-echosounder data. In particular we focus on how the tectonic regime, that significantly varies along-strike, impacts on the type, shape and frequency of slope failures. Furthermore, we investigate how the direct and instantaneous seismic loading generated by the magnitude 8.8 Maule Earthquake that ruptured parts of the study area on the 27 February of 2010 impacted on the slope stability. Such a comparison is possible as we mapped the rupture area bathymetrically before and shortly after the earthquake.

Our results indicate that the spatial occurrence of two groups of landslides - lower slope collapses and failures that affect the entire slope - are closely related to the tectonic segmentation of the forearc, and that the long-time tectonic stress regime is a major factor preconditioning slope failure. The seismic loading by the Maule earthquake, on the other hand had surprisingly little effect in triggering km-size submarine landslides, albeit steep slopes, ubiquiteous mass wasting of the past and extreme vertical acceleration in the rupture area.

# New Approaches in Rock Deformation and Recrystallisation Analysis at POWTEX Neutron Diffractometer, FRM II Germany

Jens M. Walter[1], Michael Stipp[2], Klaus Ullemeyer[3], Helmut Klein[1], Bernd Leiss[1], Bent T. Hansen[1] and Werner F. Kuhs[1]

*[1]Geowissenschaftliches Zentrum der Universität Göttingen (GZG), Goldschmidt Str. 3, D-37077 Göttingen, Germany, [2]Marine Geodynamik, GEOMAR, Helmholtz-Zentrum für Ozeanforschung Kiel, Wischhofstr. 1-3, D-24148 Kiel, [3]Institut für Geowissenschaften, Universität Kiel, Otto-Hahn-Platz 1, D-24118 Kiel, Germany*

For the quantitative analysis of crystallographic preferred orientations (CPOs) neutron diffraction has become a vital tool due to the high penetration capabilities of neutrons. Quantitative texture analysis is commonly used for the investigation of fabric development in mono- and polyphase rocks, their deformation histories and kinematics. Furthermore the quantitative characterization of anisotropic physical properties by bulk texture measurements can be achieved.

The new neutron diffractometer POWTEX (POWder and TEXture) is designed as a high-intensity diffractometer at the research reactor FRM II in Garching, Germany by groups from the RWTH Aachen, Forschungszentrum Jülich and the University of Göttingen. The design of POWTEX is complementary to existing neutron diffractometers (SKAT at Dubna, Russia; GEM at ISIS, UK; HIPPO at Los Alamos, USA; D20 at ILL, France; and the local STRESS-SPEC and SPODI at FRM II) as it is focused on fast (texture) measurements for either time-resolved experiments or the measurement of larger sample series as necessary for the study of large scale geological structures.

By utilizing a range of neutron wavelengths simultaneously (TOF-technique), a high flux ($\sim 10^7$ n $cm^{-2}$ $s^{-1}$) and a high detector coverage (9.8 sr) effective texture measurements without sample tilting and rotation are standard. Furthermore the instrument and the angular detector resolution is sufficient for strong recrystallisation textures as well as weak textures of polyphase rocks. Thereby large sample environments will be implemented at POWTEX allowing *in-situ* time-resolved texture measurements during deformation experiments on rocksalt, ice and other materials. In addition a furnace for 3D-recrystallisation analysis of single grains will be realized complementary to the furnace that already exists for fine grained materials at the synchrotron beamline BW5 at HASYLAB, Germany (Klein et al. 2009, and references therein).

The *in-situ* triaxial deformation apparatus is operated by an electromechanical spindle drive with a maximum axial load of 200 kN. The deformation apparatus will be redesigned to minimize shadowing effects on the detector. The HT experiments will be carried out in uniaxial compression or extension and an upgrade to triaxial deformation conditions is envisaged. The load frame can alternatively be used for ice deformation by inserting a cryostat cell for temperatures down to 77 K with a triaxial apparatus allowing also simple shear experiments on ice. Strain rates range between $10^{-8}$ and $10^{-3}$ $s^{-1}$ reaching to at least 50 % axial strain. The furnace for the recrystallization analysis will be a mirror furnace with temperatures up to 1500° C, which will be rotatable around a vertical axis to obtain the required stereologic orientation information.

**References**

Klein, H. (2009). Adv. Eng. Mat. 11, 452-458.

# Structural Evolution in the Aar Massif (Central Alps): First attempts of linking the micron- to the kilometer-scale

Philip Wehrens, Roland Baumberger and Marco Herwegh

*University of Bern, Institute of Geological Sciences, Baltzerstrasse 1+3, CH-3012 Bern*

The Aar massif belongs to the external massifs of the Alps and is mainly composed of granitoids and gneisses. Despite numerous detailed studies in the past decades, the overall exhumation history and the associated massif internal deformation (internal strain distribution and its evolution in time, kinematics etc.) are largely unknown at present. In this project, we aim to investigate the role of shear zones in the deformation history at a variety of scales. In this context it is important to understand their microstructural evolution, the involved deformation processes, kinematics and relative ages as well as the associated changes in rheology.

A GIS-based remote-sensing structural map, verified by fieldwork, (see Baumberger et al., this volume) served as base for our investigations. Lithological differences between the units (Central Aare granite, ZAGr; Grimsel granodiorte, GrGr and gneisses) cause strain to localize along these contacts. Furthermore, the initial magmatic differentiation in the granitoids locally controls the Alpine deformational overprint because of differences in effective viscosity during solid-state deformation. This behavior is illustrated by the increase of foliation intensity and the number of shear zones per rock volume from ZAGr to GrGr.

Preliminary results show that deformation at the N boundary of the Aar massif has to be distinguished from the central and the southern part. In the North steep NE-SW trending foliations and shear zones with subvertical lineations represent the major structures. The shear zones acted both as normal faults and as reverse faults, which mostly used pre-existing lithological boundaries between the different gneiss units. In a later stage, E-W trending shear zones and shear bands with moderate dipping angles cross cut the earlier structures. They always show a top to the North component and might be related to the late north directed movements of the Aar massif. Yet, no absolute age dating has been performed on such structures.

The central and southern part have NE-SW (dip azimuth 130°-180°) and NW-SE trending shear zones dissecting the Central Aar granite (ZAGr). The shear zones, mostly with steep lineations, are of ductile origin sometimes overprinted in a brittle manner. Again shear sense indicators of NE-SW structures show south block up and down movements for individual shear zones. In addition some of these strike-slip shear zones have both subhorizontal and subvertical lineations. They may represent a late strike-slip reactivation of earlier vertical movements.

Crosscutting relationships indicate that the NW-SE shear zones are younger than the NE-SW ones, and acted as dextral strike slip zones (subhorizontal lineations).

# Petrological and structural observations along the Nestos Shear Zone in southern Bulgaria with emphasis on grandite-cpx-bearing rocks

A. Katrin Wellnitz, Thorsten J. Nagel and Nikolaus Froitzheim

*Steinmann-Institut, University of Bonn, D-53115 Bonn*

We describe the Nestos Shear Zone in the area of Ilinden village, SW Bulgaria. This shear zone represents the base of an Eocene crustal wedge and separates two major tectonics units of the Rhodopes, the Lower Allochthon in the footwall from the structurally higher Middle Allochthon in the hanging wall. It is defined by an about 2 km thick mélange zone which consists of various high-metamorphic rocks including garnet-micaschists, amphibolites, orthogneises, marbles, and eclogites. From two localities in Greece, microdiamonds have been reported as inclusions in garnets from micaschists. In our study area, garnets in similar rocks from the same structural level display exsolution of rutile needles and inclusions of highly ordered graphite which have been described in UHP-metamorphic rocks elsewhere.

Amphibolites close to the protolith boundary contain lenses of spectacular calcsilicate rocks. These consist mainly of grandite garnet (10 - 30% andradite component) and diopside- hedenbergite clinopyroxene. Additionally, they contain epidote, quartz, plagioclase, and occasionally calcite. Irregularly-shaped lenses of these rocks measure 1 to 3 meters in diameter. The surrounding amphibolite is banded and consists mainly of hornblende, plagioclase and pyroxene. Element maps and back-scattered images reveal a patchy zonation in garnet which we interpret as growth zonation. In some samples, pyroxene shows an oscillatory zonation which suggests that fluid mobility and chemistry played an important role during formation. We present equilibrium assemblage diagrams calculated with THERAIK-DOMINO software and discuss the stability range of observed assemblages and the relevance of $CO_2$ content in coexisting fluids.

# Strukturgeologisches 3D-Modell des Nordcampusbereiches der Georg-August-Universität Göttingen – eine erste Näherung

Henrike Werner[1], Bernd Leiss[1], Till Heinrichs[1] and David C. Tanner[2]

*[1]Geowissenschaftliches Zentrum der Universität Göttingen, D-37077 Göttingen, [2]Leibniz-Institut für Angewandte Geophysik, D-30655 Hannover*

Der Nordcampus der Georg-August-Universität Göttingen liegt im Bereich des östlichen Hauptstörungssystems des NS-verlaufenden Leinetalgrabens. Im Bereich des Nordcampuses weist das NNE-SSW streichende Störungssystem einen Ost-West-streichenden sinistralen Versatz auf. Dieser komplexe Störungszonenbereich liegt in einem morphologischen Talbereich ist von teilweise mächtigen Quartärsedimenten bedeckt, so dass der Störungsverlauf bzw. –versatz der Gesteine des Keupers und Jura gegen die des Muschelkalkes nicht direkt kartiert werden kann. Die Kenntnis der strukturgeologischen Situation dieses Bereiches spielt aber sowohl in Hinblick auf das Verständnis der regionalen Entwicklung des Leinetalgrabensystems (vgl. z.B. Vollbrecht und Tanner 2012), als auch für die Erkundung des oberflächennahen und tiefengeothermischen Potentials (siehe Leiss et al., dieser Band) und die hydrogeologische Situation hinsichtlich der Göttinger Wasserversorgung eine Schlüsselrolle.

Im Zuge der Erkundung bzw. Erschließungsmaßnahmen zweier oberflächennaher geothermischer Sondenfelder (ein Feld bis zu 40 Sonden à 140m) wurden zunächst zwei Erkundungsbohrungen für Thermal Response Tests (Teufen 30m/150m) und zwei ca. 160m voneinander entfernte Bohrungen für Grundwassermessstellen (Teufen 140m/132m) niedergebracht. Die in dieser Arbeit durchgeführte Bohrkleinauswertung erlaubt eine stratigraphische Einordnung und in Kombination mit den Bohrkleinauswertungen sehr flacher Bohrungen (bis max. 12 m) eines älteren hydrogeologischen Gutachtens (Meischner 1980), der geologischen Kartengrundlage des Umfeldes und den strukturgeologischen Aufnahmen der südlich des Gebietes anschließenden Ebelhof-Überschiebungszone (Heinrichs 2012) eine erste Näherung an ein strukturgeologisches 3D-Modell.

In den Bohrprofilen wurden vor allem die Gesteine des Oberen Muschelkalks und des Unteren bis Mittleren Keupers angetroffen. Die Bohrprofile konnten lithologisch gut miteinander korreliert werden und belegen, dass sie sich alle noch im Grabeninneren befinden und die Hauptstörungszone folglich östlich verlaufen muss. In allen Bohrprofilen konnten die Ceratitenschichten (mo2) bestimmt werden, allerding ist in keiner der Bohrungen der Trochitenkalk (mo1) zu identifizieren, der aufgrund der Teufe der Bohrungen zu erwarten ist. Gründe dafür könnten eine Schichtverdoppelung der Ceratitenschichten oder ein Aussetzten des Trochitenkalks aufgrund von Störungen oder einer Antikline (Heinrichs 2011) sein. Anhand röntgendiffraktometrischer Analysen konnten in den Bohrungen auch dolomitische Bänke nachgewiesen werden, die ein Hinweis auf den Mittleren Muschelkalk sein könnten. Dies würde bedeuten, dass der mo1 nicht vorhanden, sehr geringmächtig oder, sehr untypisch, ohne Crinoidenstielglieder ausgebildet ist.

Auf der Basis aller genannten Daten wurden für das 3D-Modell die Basisflächen des Unteren Muschelkalks und des Keupers interpoliert und zusammen mit den bereits kartierten Störungen und Schichtgrenzen sowie mit Hilfe von bereits gemessenem Schichteinfallen modelliert und liefert einen wichtigen Beitrag für das in Entwicklung befindliche regionale Strukturmodell.

**Referenzen**

Heinrichs, T. (2011): In Leiss, B., Tanner, D., Vollbrecht, A. und Arp, G. (Hrsg.). Universitätsdrucke Göttingen 2012, 39-58.
Leiss, B., Tanner, D., Vollbrecht, A., Heinrichs, T., Arp, G. und GGG (2012). Abstracts TSK 14 Kiel, S. 68.
Meischner, D. (1980). Geologisches Gutachten für die Stadt Göttingen, 28 S.
Vollbrecht, A. und Tanner, D.C. (2011): In Leiss, B., Tanner, D., Vollbrecht, A. und Arp, G. (Hrsg.). Universitätsdrucke Göttingen 2012, 9-15.

# Experimental boudinage of anhydrite in rock-salt matrix: The impact of bulk finite strain geometry

Gernold Zulauf [1], Janet Zulauf [1], Michael Mertineit[1,2] and Jörg Hammer[2]

*[1]Goethe-Universität Frankfurt/Main, Altenhöferallee 2, D-60438 Frankfurt/Main, [2]Bundesanstalt für Geowissenschaften und Rohstoffe, Stilleweg 2, D-30655 Hannover*

In the present paper we are focusing on boudinage of a single layer of anhydrite (Gorleben deep borehole 1004) embedded artificially in weaker Asse rock salt (Speisesalz Na2SP). Coaxial deformation of the anhydrite layer results in boudins, which show different geometry depending on the bulk finite strain fields (plane, constrictional and flattening conditions). Parts of these studies have already been published (Zulauf et al., 2009, 2010, 2011). Here, we will show and discuss the impact of the bulk strain field on the geometry of the deformed anhydrite layer, the latter being oriented perpendicular to the principal shortening axis, *Z*. Deformation conditions were as follows: $T$ = 345 °C, $\dot{e}$ = ca. 1 * $10^{-7}$ $s^{-1}$, and $e_Z$ = ca. -30%. Under these conditions rock salt is deformed by non-linear viscous creep (subgrain rotation), whereas anhydrite deforms under brittle-viscous conditions (Zulauf et al., 2010, and references therein).

The deformed samples were analyzed using X-rax computer tomography (CT), microscopy and EBSD. In all experiments the thickness of the deformed layer, $H_f$, is almost the same like the initial layer thickness, $H_i$.The fracture spacing to layer thickness ratio (referred to as aspect ratio, $W_d$) was calculated by dividing the boudin width, $W_a$, through the finite layer thickness, $H_f$. Most of the necks between the boudins are entirely filled with halite. However, in a few cases where the layer is thick, halite was not able to fill the neck completely (for further details on microfabris and deformation mechanisms, see Zulauf et al., 2010).

In cases of *bulk constriction*, most of the boudins are trending oblique to the principal strain axes. There is an almost linear increase in boudin width (boudin wavelength) with layer thickness; the aspect ratio, $W_d$, is almost the same ranging from ca. 0.5 to 2.5. In sections cut perpendicular to the *X*-axis, the anhydrite layer shows weak folding (sensu Zulauf and Zulauf, 2005).

In samples undergoing *bulk flattening*, there is a clear pattern of radial and concentric necks. The direction of radial necks does not show a significant preferred orientation in plan-views. With increasing layer thickness, $H_i$, the mean diameter of the boudins in plan-views, $W_a$, increases almost linearly from ca. 1.5 to ca. 3.0 mm. The aspect ratio ($W_d$) is ranging from 0.8 to 1.8.

In cases of *bulk plane strain*, the sections cut parallel to the *X*-axis and perpendicular to the layer show striking boudinage of the anhydrite layer. The boudins are more continuous than the constrictional boudins. Similar to the other cases of boudinage, the width of boudins increases with layer thickness, and the aspect ratio is almost constant at ca. 1.2 ±0.6.

The results suggest that the shape of the boudins is significantly controlled by the finite strain geometry, whereas the boudin aspect ratio ($W_d$) is almost the same for all cases of bulk finite strain fields. The mean values of the aspect ratios range from 0.7 – 1.5 and thus are lower than those described from natural torn and drawn boudins (e.g. Goscombe et al., 2003). Boudinage of anhydrite by formation of extension fractures should be controlled by the transfer of stress from the viscous rock-salt matrix to the brittle anhydrite layer (Ramberg, 1955). The fracture spacing scales with layer thickness, which is referred to as fracture saturation (Bai et al., 2000). The concept of fracture saturation is based on frictional coupling between the competent layer (anhydrite boudins) and the incompetent rock-salt matrix. The modeling results of Bai et al. (2000) indicate that fracture saturation results from a domain of compressive layer-parallel stress that is attained at an aspect ratio of ca. 1. As this value is compatible with the aspect ratio of the anhydrite boudins, interfacial slip between anhydrite and rock salt was probably not significant.

**References**

Bai, T. et al., 2000. Nature, 403, 753-756.
Goscombe, B.D. et al., 2003.. J. Struct. Geol., 26, 739–763.
Ramberg, H., 1955. J. Geol., 63, 512-526.
Zulauf, G. et al., 2009. J. Struct. Geol., 31, 460-474, doi: 10.1016/j.jsg.2009.01.013.
Zulauf, G. et al., 2010. J. Struct. Geol. 32, 264-277, doi:10.1016/j.jsg.2009.12.001.
Zulauf, J. and Zulauf, G., 2005. J. Struct. Geol., 27: 1061-1068.
Zulauf, J. et al., 2011. J. Struct. Geol. 33, 1801-1815; doi: 10.1016/j.sg.2011.09.006.

# Microfabrics and deformation mechanisms of experimentally deformed and recompacted Asse rock salt: The impact of grain boundary brine

Janet Zulauf and Gernold Zulauf

*Goethe-Universität Frankfurt/Main, Altenhöferallee 2, D-60438 Frankfurt/Main*

The deformation mechanisms known to operate in rock salt at temperatures relevant for engineering and natural conditions (T = 20 – 200°C) are (1) fracturing and dislocation glide, (2) pressure solution and grain boundary sliding, and (3) dislocation creep (Urai and Speers, 2007, and references therein). Selection of these mechanisms is significantly controlled by the presence of humidity and brine. In dilatant salt, humidity from the environment or from fluid inclusions in the salt matrix can spread out through opened pathways influencing the mechanical behavior of salt (e.g. Hunsche and Schulze, 2002). Small amounts of saturated grain boundary brine may support solution precipitation creep (e.g. Spiers et al., 1990), fluid-assisted grain boundary migration (Schenk and Urai, 2004), or reduction in effective stress resulting in Coulomb fracture.

In the present paper we are focusing on the microfabrics and deformation mechanisms of Asse rock salt that was experimentally deformed and re-compacted under dry and wet conditions. Most of these grains are equidimensional with a grain size of ca. 1 mm. The largest grains are 10 mm in diameter. Two samples were deformed in a Kármán-type triaxial testing apparatus at BGR Hannover until maximum strength was attained. Deformation conditions were as follows: temperature, $T$ = 30°C, strain rate, $\dot{e}$ = 1.0E-05 1/s, confining pressure, $P_{conf}$ = 3 MPa. Subsequently the deformed samples were re-compacted at $P_{conf}$ = 30 MPa, first at $T$ = 60°C for 33 days, and then at room temperature for 23 days. Before re-compaction started, one sample was saturated with NaCl brine, whereas the other sample was left 'dry'.

To reveal the microstructure of the re-compacted samples, etched thick sections were investigated under transmitted and reflected light. The texture was analyzed using EBSD, and the three-dimensional network of open fractures was investigated using both a medical and a Micro-Computertomograph.

All of the samples show (1) a network of fluid inclusions along grain boundaries, (2) open microfractures with a mean length of 3 mm and with walls decorated by a film of opaque phase, (3) small inclusions of cataclastically deformed anhydrite. The open microfractures in halite are attributed to the deviatoric stress imposed by the triaxial apparatus. They occur as inter- and intragranular extension (mode I) fractures. Some of the intragranular types show an orthogonal pattern reflecting the cleavage of halite. The misorientation is small across intragranular open microfractures suggesting rotation did not play a significant role during microfracturing.

Striking differences between the 'dry' and 'wet' samples are shown by (1) the amount of open microfractures, (2) the degree and type of crystal plastic deformation, (3) the type of open and re-closed microfractures. The 'wet' salt displays almost half of the number of open fractures compared to the 'dry' sample. Moreover, in the 'wet' sample the number of subgrains and recrystallized grains is higher than in the 'dry' sample. Recrystallization seems to result from both subgrain rotation and grain boundary migration. The latter is indicated by lobate grain boundaries, which are particularly frequent and strong in the 'wet' sample. The number of re-closed microfractures is significantly higher in the 'wet' sample. There is also evidence for precipitation of a new phase in or adjacent to open fractures of the 'wet' sample which have not been analyzed yet.

From the results presented above, it is concluded that the degree of crystal plasticity in form of dislocation glide and climb is much higher in the 'wet' sample compared to the 'dry' sample. The viscous strain, accommodated by crystal plasticity, made the re-closure of previously opened microfractures possible. This observation is in line with previous observations that small amounts of brine could result in significant softening of rock salt (e.g. Talbot and Rogers, 1980; Urai et al., 1986; Hunsche and Schulze, 2002). In the present case of coarse-grained salt, the brine-induced softening was driven by enhanced subgrain formation/rotation and grain boundary migration. In cases where the grain size is much smaller than in the investigated Asse salt, pressure solution and re-precipitation of solved halite could act as an additional mechanism contributing to the softening of rock salt.

**References**

*We are grateful to O. Schulze (BGR) for delivering the samples.*

Hunsche, U. and Schulze, O., 2002. In: Cristescu, N.D. et al. (eds.), Basic and Applied Salt Mechanics, Proc. 5th Conference on the Mechanical Behavior of Salt (MECASALT 5) Bucharest, 1999, p. 73-87. Lisse: Swets & Zeitlinger (A.A. BalkemaPublisshers). Talbot and Rogers, 1980. Science, 208, 395-397. Urai, J.L. and Spiers, C.J., 2007. In: Wallner, M. et al. (eds.), The Mechanical Behavior of Salt – Understanding of THMC Processes in Salt. Taylor & Francis Group, London, p. 149-158. Urai et al., 1986. Nature, 324, 554-557. Spiers, C.J. et al., 1990. In: Knipe, R.J. and Rutter, E.H. (Eds.) Deformation Mechanisms, Rheology, and Tectonics. Geol. Soc. London, Special Publ., 54, 215-227. Schenk, O., Urai, J.L., 2004. Contrib. Mineral. Petrol 146, 671–682.

# MAILING LIST

**Altenberger, Uwe**
*altenber@rz.uni-potsdam.de*
Institute of Earth and Environmental Sciences
University of Potsdam
Karl-Liebknecht-Str. 24
14476 Potsdam-Golm, Germany

**Appel, Peter**
*pa@min.uni-kiel.de*
Institut für Geowissenschaften
Laborleiter Mikrosondenlabor und
Röntgenfluoreszenzlabor
Universität Kiel
24098 Kiel, Germany

**Baese, Rauno**
*rb@min.uni-kiel.de*
Institut für Geowissenschaften
Christian-Albrechts-Universität Kiel
Ludewig-Meyn-Str. 10
24118 Kiel, Germany

**Bartsch, Carolin**
*Carolin.Bartsch@bgr.de*
Federal Institute for Geosciences and Natural
Resources (BGR)
Stilleweg 2
30655 Hannover, Germany

**Baumberger, Roland**
*roland.baumberger@students.unibe.ch*
University of Bern
Institute of Geological Sciences
Baltzerstrasse 1+3
3012 Bern, Switzerland

**Behrmann, Jan H.**
*jbehrmann@geomar.de*
GEOMAR | Helmholtz Centre for Ocean
Research Kiel
Wischhofstr. 1-3
24148 Kiel, Germany

**Berger, Alfons**
*ab@geo.ku.dk*
University of Copenhagen
Institute for Geology and Geography
1350 Copenhagen, Denmark

**Berndt, Christian**
*cberndt@geomar.de*
GEOMAR | Helmholtz Centre for Ocean
Research Kiel
Wischhofstr. 1-3
24148 Kiel, Germany

**Bial, Julia**
*jb@min.uni-kiel.de*
Institut für Geowissenschaften
Christian-Albrechts-Universität Kiel
Ludewig-Meyn-Str. 10
24118 Kiel, Germany

**Blanke, Hartmut**
*blankeh@dbe.de*
DBE Endlager für radioaktive Abfälle
Morsleben (ERAM)
Schachtweg 3
39343 Ingersleben, Germany

**Bruijn, Rolf H.C.**
*rolf.bruijn@erdw.ethz.ch*
ETH Zürich
Geological Institute
Sonneggstr. 5
8092 Zürich, Switzerland

**Buhl, Elmar**
*e.buhl@gmx.de*
GFZ German Research Centre for Geosciences
Geomechanics and Rheology
14473 Potsdam, Germany

**Burchardt, Steffi**
*steffi.burchardt@geo.uu.se*
Department of Earth Sciences
Uppsala University
Villavägen 16
75236 Uppsala, Sweden

**Chakraborty, Sumit**
*sumit.chakraborty@ruhr-uni-bochum.de*
Institut für Geologie, Mineralogie und Geophysik
Ruhr Universität Bochum
44780 Bochum, Germany

**Crutchley, Gareth**
*gcrutchley@geomar.de*
GEOMAR | Helmholtz Centre for Ocean
Research Kiel
Wischhofstr. 1-3
24148 Kiel, Germany

**Dati, Francesco**
*francesco.dati@unina.it*
Department of Earth Sciences
Università degli Studi di Napoli 'Federico II'
Largo San Marcellino 10
80138 Napoli, Italy

**Dietl, Carlo**
*C.Dietl@em.uni-frankfurt.de*
Institut für Geowissenschaften
Goethe-Universität
Altenhöferallee 1
60438 Frankfurt am Main, Germany

**Fernandez, Naiara**
*fernande@uni-mainz.de*
Geophysics and Geodynamics
Institute of Geosciences
Johannes Gutenberg - University of Mainz
J.J. Becherweg 21
55128 Mainz, Germany

**Friedel, Carl-Heinz**
*Friedel@lagb.mw.sachsen-anhalt.de*
Landesamt für Geologie und Bergwesen
Sachsen-Anhalt
Geologie, D22
Postfach 156
06035 Halle/Saale, Germany

**Froitzheim, Nikolaus**
*niko.froitzheim@uni-bonn.de*
Steinmann-Institut
Universität Bonn
Poppelsdorfer Schloss
53115 Bonn, Germany

**Fügenschuh, Bernhard**
*bernhard.fuegenschuh@uibk.ac.at*
Institut für Geologie
Universität Innsbruck
6020 Innsbruck, Austria

**Geersen, Jacob**
*jgeersen@geomar.de*
GEOMAR | Helmholtz Centre for Ocean
Research Kiel
Wischhofstr. 1-3
24148 Kiel, Germany

**Gerya, Taras V.**
*taras.gerya@erdw.ethz.ch*
Institute of Geophysics
Department of Geosciences
ETH-Zurich
Sonneggstrasse 5
8092 Zurich, Switzerland

**Grevemeyer, Ingo**
*igrevemeyer@geomar.de*
GEOMAR | Helmholtz Centre for Ocean
Research Kiel
Wischhofstr. 1-3
24148 Kiel, Germany

**Grimmer, Jens**
*jens.grimmer@kit.edu*
Institut für Angewandte Geowissenschaften
Karlsruher Institut für Technologie (KIT)
76131 Karlsruhe, Germany

**Großmann, Johannes**
johannes-grossmann@stud.uni-goettingen.de
Geowissenschaftliches Zentrum der Universität
Göttingen
37077 Göttingen, Germany

**Gürer, Derya**
*derya.guerer@gmail.com*
Physics of Geological Processes
University of Oslo
P.O. Box 1048, Blindern, Oslo, Norway

**Halama, Ralf**
*rh@min.uni-kiel.de*
SFB 574 and Institut für Geowissenschaften
Ludewig-Meyn-Str. 10
Universität Kiel
24118 Kiel, Germany

**Herwegh, Marco**
*marco.herwegh@geo.unibe.ch*
University of Bern
Institute of Geological Sciences
Baltzerstrasse 1+3
3012 Bern, Switzerland

**Hetzel, Ralf**
*rahetzel@uni-muenster.de*
Institut für Geologie & Paläontologie
Westfälische Wilhelms-Universität Münster
Corrensstr. 24
48149 Münster, Germany

**Hilgers, Christoph**
*christoph.hilgers@emr.rwth-aachen.de*
Department of Reservoir Petrology
RWTH Aachen University
Wüllnerstr. 2
52062 Aachen, Germany

**Hindle, David**
*david.hindle@uni-jena.de*
Institut für Geowissenschaften
Friedrich Schiller Universität Jena
07749 Jena, Germany

**Hoffmann, Markus**
*ma.hoffmann@lmu.de*
Ludwig-Maximilians-Universität München
Luisenstr. 33
80333 München, Germany

**Holler, Hjördis**
*hjoerdismarisa.holler@gmx.de*
Federal Institute for Geosciences and Natural Resources (BGR)
Stilleweg 2
30655 Hannover, Germany

**Huismans, Ritske S.**
*ritske.huismans@geo.uib.no*
Department of Earth Sciences
Bergen University
Allegaten 41
5007 Bergen, Norway

**Iyer, Karthik**
*kiyer@geomar.de*
GEOMAR | Helmholtz Centre for Ocean Research Kiel
Wischhofstr. 1-3
24148 Kiel, Germany

**Karmakar, Shreya**
*sk@min.uni-kiel.de*
Institut für Geowissenschaften
Ludewig-Meyn-Str. 10
Universität Kiel
24118 Kiel, Germany

**Kenkmann, Thomas**
*thomas.kenkmann@geologie.uni-freiburg.de*
Institut für Geowissenschaften – Geologie
Albert-Ludwigs-Universität Freiburg
Albertstrasse 23-B
79104 Freiburg, Germany

**Keppler, Ruth**
*rkeppler@geomar.de*
Institut für Geowissenschaften
Otto-Hahn-Platz 1
Universität Kiel
24118 Kiel, Germany

**Kettermann, Michael**
*m.kettermann@ged.rwth-aachen.de*
Structural Geology, Tectonics and Geomechanics
RWTH-Aachen University
Wüllnerstr. 2
52062 Aachen, Germany

**Kilian, Rüdiger**
*ruediger.kilian@unibas.ch*
Geological Institute
Basel University
Bernoullistr. 32
4056 Basel, Switzerland

**Kirst, Frederik**
*fredster@uni-bonn.de*
Steinmann-Institut
Universität Bonn
Poppelsdorfer Schloss
53115 Bonn, Germany

**Kroner, Uwe**
*kroner@geo.tu-freiberg.de*
TU Bergakademie Freiberg
Department of Geology
B. v. Cotta Str. 2
09596 Freiberg, Germany

**Krumbholz, Michael**
*michael.krumbholz@geo.uu.se*
Department of Earth Sciences
Uppsala University
Villavägen 16
75236 Uppsala, Sweden

**Kübler, Simon**
*kuebler@iaag.geo.uni-muenchen.de*
Department für Geo- und Umweltwissenschaften
Geologie
LMU München
Luisenstraße 35
80335 München, Germany

**Kühn, Rebecca**
*rebecca.kuehn@stud.uni-goettingen.de*
Geowissenschaftliches Zentrum
Universität Göttingen
Goldschmidtstr. 3
37077 Göttingen, Germany

**Kühnlenz, Tatjana**
*tatjana.kuehnlenz@bgr.de*
Federal Institute for Geosciences and Natural Resources (BGR)
Stilleweg 2
30655 Hannover, Germany

**Kurzawski, Robert**
*robkurz@uni-bonn.de*
Steinmann-Institut
Universität Bonn
Poppelsdorfer Schloss
53115 Bonn, Germany

**Laux, Dennis**
*Dennis.Laux@rwth-aachen.de*
Department of Reservoir-Petrology
RWTH-Aachen University
Wüllnerstr. 2
52062 Aachen, Germany

**Leiss, Bernd**
*bleiss1@gwdg.de*
Geowissenschaftliches Zentrum
Universität Göttingen
Goldschmidtstr. 3
37077 Göttingen, Germany

**Li, Shiyuan**
*s.li@ged.rwth-aachen.de*
Structural geology-tectonics-geomechanics
RWTH-Aachen University
Lochnerstr. 4-20
52062 Aachen, Germany

**Mertineit, Michael**
*Michael.Mertineit@bgr.de*
Federal Institute for Geosciences and Natural Resources (BGR)
Stilleweg 2
30655 Hannover, Germany

**Meyer, Melanie**
*melanie.meyer@geol.uni-erlangen.de*
Universität Erlangen-Nürnberg
GeoZentrum Nordbayern
Schlossgarten 5a
91054 Erlangen, Germany

**Mezger, Jochen**
*jochen.mezger@geo.uni-halle.de*
Institut für Geowissenschaften und Geographie
Martin-Luther-Universität Halle-Wittenberg
06120 Halle, Germany

**Mizera, Marcel**
*marcel.mizera@gmx.de*
Institut für Geowissenschaften
Christian-Albrechts-Universität Kiel
Ludewig-Meyn-Str. 10
24118 Kiel, Germany

**Möller, Stefan**
*smoeller@geomar.de*
GEOMAR | Helmholtz Centre for Ocean Research Kiel
Wischhofstr. 1-3
24148 Kiel, Germany

**Müller, Hans-Heinrich**
*hansheinrichmueller@googlemail.com*
Geowissenschaftliches Zentrum
Universität Göttingen
Goldschmidtstr. 3
37077 Göttingen, Germany

**Nagel, Thorsten**
*tnagel@uni-bonn.de*
Steinmann-Institut
Universität Bonn
Poppelsdorfer Schloss
53115 Bonn, Germany

**Nikolajew, Christian**
*ChristianNikolajew@web.de*
Geowissenschaftliches Zentrum
Universität Göttingen
Goldschmidtstr. 3
37077 Göttingen, Germany

**Passchier, Cees**
*cpasschi@uni-mainz.de*
Institut für Geowissenschaften
Johannes Gutenberg Universität Mainz
Becherweg 21
55099 Mainz, Germany

**Patzschke, Mario**
*patzschke@dbe.de*
DBE Endlager für radioaktive Abfälle
Morsleben (ERAM)
Schachtweg 3
39343 Ingersleben, Germany

**Peters, Max**
*max-peters@gmx.de*
University of Bern
Institute of Geological Sciences
Baltzerstrasse 1+3
3012 Bern, Switzerland

**Pietralla, Stefan**
*stefan.pietralla@rwth-aachen.de*
Department of Reservoir-Petrology
RWTH-Aachen University
Wüllnerstr. 2
52062 Aachen, Germany

**Poelchau, Michael**
*michael.poelchau@geologie.uni-freiburg.de*
Institut für Geowissenschaften – Geologie
Albert-Ludwigs-Universität Freiburg
Albertstrasse 23-B
79104 Freiburg, Germany

**Pomella, Hannah**
*hannah.pomella@uibk.ac.at*
Institute of Geology and Paleontology
University of Innsbruck
Innrain 52
6020 Innsbruck, Austria

**Richter, Bettina**
*betti_richter@yahoo.de*
Institute of Earth and Environmental Science
Potsdam University
Karl-Liebknecht-Str. 24
14476 Potsdam, Germany

**Richter, Marianne**
*richmari@students.uni-mainz.de*
Institut für Geowissenschaften
Johannes Gutenberg Universität Mainz
Becherweg 21
55099 Mainz, Germany

**Rieger, Stefanie**
*stefanie.rieger@iaag.geo.uni-muenchen.de*
Department für Geo- und Umweltwissenschaften
Geologie
LMU München
Luisenstraße 35
80335 München, Germany

**Rodrigues, Benedito C.**
*bjcrodrigues@gmail.com*
Centro de Geologia da Universidade do Porto
(CGUP)
Rua do Campo Alegre, 687
4169-007 Porto, Portugal

**Rybacki, Erik**
*uddi@gfz-potsdam.de*
Helmholtz-Zentrum Potsdam
Deutsches GeoForschungsZentrum
Geomechanik und Rheologie
Telegrafenberg
14473 Potsdam, Germany

**Sadler, Marc**
*Marc.Sadler@rwth-aachen.de*
Geologie - Endogene Dynamik
RWTH-Aachen University
Lochnerstr. 4-20
52056 Aachen, Germany

**Sandmann, Sascha**
*s.sandmann@uni-bonn.de*
Steinmann-Institut
Universität Bonn
Poppelsdorfer Schloss
53115 Bonn, Germany

**Sarkar, Tapabrato**
*ts@min.uni-kiel.de*
Institut für Geowissenschaften
Ludewig-Meyn-Str. 10
Universität Kiel
24118 Kiel, Germany

**Schenk, Volker**
*vs@min.uni-kiel.de*
Institut für Geowissenschaften
Ludewig-Meyn-Str. 10
Universität Kiel
24118 Kiel, Germany

**Schmatz, Joyce**
*j.schmatz@ged.rwth-aachen.de*
Structural geology-tectonics-geomechanics
RWTH-Aachen University
Lochnerstr. 4-20
52062 Aachen, Germany

**Schnapperelle, Stephan**
*dem_stephan@web.de*
Universität Halle
Bornaische Str. 9
04277 Leipzig, Germany

**Schneider, Tobias**
*tobias47n9e@gmail.com*
Institut für Mineralogie und Petrographie
Universität Innsbruck
Innrain 52
6020 Innsbruck, Austria

**Schöbel, Stefan**
*stefan.schoebel@geol.uni-erlangen.de*
Universität Erlangen-Nürnberg
GeoZentrum Nordbayern
Schlossgarten 5
91054 Erlangen, Germany

**Schumann, Kai**
*kaschumann@geomar.de*
GEOMAR | Helmholtz Centre for Ocean
Research Kiel
Wischhofstr. 1-3
24148 Kiel, Germany

**Schwindinger, Martin**
*schwindi@students.uni-mainz.de*
Institute of Geosciences
Johannes Gutenberg - University of Mainz
J.J. Becherweg 21
55128 Mainz, Germany

**Speckbacher, Romed**
*rspeckbacher@geomar.de*
GEOMAR | Helmholtz Centre for Ocean
Research Kiel
Wischhofstr. 1-3
24148 Kiel, Germany

**Stipp, Michael**
*mstipp@geomar.de*
GEOMAR | Helmholtz Centre for Ocean Research Kiel
Wischhofstr. 1-3
24148 Kiel, Germany

**Stottmeister, Ljuba**
*Stottmeister@lagb.mw.sachsen-anhalt.de*
Landesamt für Geologie und Bergwesen Sachsen-Anhalt
Geologie, D22
Postfach 156
06035 Halle/Saale, Germany

**Strehlau, Jürgen**
*strehlau@email.uni-kiel.de*
Institut für Geowissenschaften
Otto-Hahn-Platz 1
Universität Kiel
24118 Kiel, Germany

**Tanner, David C.**
*DavidColin.Tanner@liag-hannover.de*
Leibniz Institute for Applied Geophysics (LIAG)
Stilleweg 2
30655 Hannover, Germany

**Thielmann, Marcel**
*marcel.thielmann@erdw.ethz.ch*
Institut für Geophysik
ETH Zürich
8092 Zürich, Switzerland

**Thiemeyer, Nicolas**
*nicthiem@stud.uni-frankfurt.de*
Institut für Geowissenschaften
Goethe-Universität Frankfurt/Main
Altenhöferallee 2
60438 Frankfurt/Main, Germany

**Trullenque, Ghislain**
*ghislain.trullenque@geologie.uni-freiburg.de*
Institut für Geowissenschaften – Geologie
Albert-Ludwigs-Universität Freiburg
Albertstrasse 23-B
79104 Freiburg, Germany

**Ullemeyer, Klaus**
*kullemeyer@geomar.de*
Institut für Geowissenschaften
Otto-Hahn-Platz 1
Universität Kiel
24118 Kiel, Germany

**Urai, Janos**
*j.urai@ged.rwth-aachen.de*
Structural geology-tectonics-geomechanics
RWTH-Aachen University
Lochnerstr. 4-20
52062 Aachen, Germany

**Villar-Muñoz, Lucia**
*lvillar@geomar.de*
GEOMAR | Helmholtz Centre for Ocean Research Kiel
Wischhofstr. 1-3
24148 Kiel, Germany

**Vogt, Katharina**
*katharina.vogt@erdw.ethz.ch*
Institute of Geophysics
ETH-Zürich
8092 Zürich, Switzerland

**Völker, David**
*dvoelker@geomar.de*
GEOMAR | Helmholtz Centre for Ocean Research Kiel
Wischhofstr. 1-3
24148 Kiel, Germany

**Walter, Jens M.**
*jwalter@gwdg.de*
Geowissenschaftliches Zentrum
Universität Göttingen
Goldschmidtstr. 3
37077 Göttingen, Germany

**Wehrens, Philip**
*philip.wehrens@geo.unibe.ch*
University of Bern
Institute of Geological Sciences
Baltzerstrasse 1+3
3012 Bern, Switzerland

**Wellnitz, Anne Katrin**
*a.k.wellnitz@web.de*
Steinmann-Institut
Universität Bonn
Poppelsdorfer Schloss
53115 Bonn, Germany

**Werner, Henrike**
*henrike.werner1@stud.uni-goettingen.de*
Geowissenschaftliches Zentrum
Universität Göttingen
Goldschmidtstr. 3
37077 Göttingen, Germany

**Wex, Sebastian**
*sebawex@students.uni-mainz.de*
Institute of Geosciences
Johannes Gutenberg - University of Mainz
J.J. Becherweg 21
55128 Mainz, Germany

**Zulauf, Gernold**
*g.zulauf@em.uni-frankfurt.de*
Institut für Geowissenschaften
Goethe-Universität Frankfurt/Main
Altenhöferallee 2
60438 Frankfurt/Main, Germany

**Zulauf, Janet**
*j.zulauf@em.uni-frankfurt.de*
Institut für Geowissenschaften
Goethe-Universität Frankfurt/Main
Altenhöferallee 2
60438 Frankfurt/Main, Germany